Ministry of Higher Education & Scientific Research
Ninevah University
College of Electronics Engineering
Communication Engineering Department

Cognitive Radio Solution For Ultra Dense 5G Radio Communications

By

Marwa Younes Abdallah

M.Sc. Thesis

In

Communication Engineering

Supervised by

Asst. Prof. Dr. Dia M. Ali

2022 A.D. **1443 A.H.**

Ministry of Higher Education & Scientific Research
Ninevah University
College of Electronics Engineering
Communication Engineering Department

Cognitive Radio Solution For Ultra Dense 5G Radio Communications

A thesis Submitted

By

Marwa Younes Abdallah

To

The Council of the College of Electronic Engineering

Ninevah University

As a Partial Fulfillment of the Requirements

for the Degree of Master of Science

In

Communication Engineering

Supervised by

Asst. Prof. Dr. Dia M. Ali

2022 A.D. **1443 A.H.**

يَرْفَعِ اللَّهُ الَّذِينَ آمَنُوا مِنْكُمْ وَالَّذِينَ أُوتُوا الْعِلْمَ دَرَجَاتٍ وَاللّهُ بِمَ ا تَعْمَلُونَ خَبِيرٌ

سورة المجادلة الاية 11

ACKNOWLEDGEMENTS

" Praise be to ALLAH, Lord of the whole creation"

I dedicate my humble effort with respect and appreciation ……

To the beacon of my path, my guidance, my support in life my dear father (may ALLAH have mercy on him)

To the symbol of tenderness, and sacrifice, to the light of my eyes and a piece of my heart, my dear mother (may ALLAH have mercy on her)

To my brothers and my sisters and all my family

To my supervisor, **Asst. Prof. Dr. Dia Mohamed Ali**, for his continuous guidance, helpful suggestions, and constant encouragement Throughout this work

To the former head and current and all members of the communication department

To my friends, classmates, and who accompanied me during my studies, I would single out (Zhraa Zuheir)

To all those who teach me in my academic career, my esteemed teachers

Marwa Younes

ABSTRACT

To meet the increase in wireless services and applications for the Fifth Generation (5G), the Ultra-Dense Network (UDN) has recently evolved as one of the key enabler technologies for future 5G systems.

In UDN, a large number of Small Cells (SCs) are deployed compared to the number of active users. The deployment density of SCs will increase the spectrum scarcity problem. Cognitive Radio (CR) has been suggested as a solution to the problem of limited spectrum resources by exploiting the unused spectrum that is allocated to the Primary Users (PUs). This approach enables the Secondary User (SU) to use the spectrum when the PU is not using it, and this should happen without interfering with the PU. Spectrum Sensing (SS) is one of the most important functions in CR.

In this work, a model of the SS system was proposed to perform the sensing process. The Energy Detection (ED) algorithm was relied upon, and to enhance the performance, three adaptive thresholds have been proposed utilizing Simulink LabVIEW NXG. To Represent the PU traffic Modes, two scenarios were adopted. The first scenario was in the form of the semi-deterministic traffic mode, and the second is the burst traffic mode.

Simulation results of the conventional energy detector (fixed threshold) have been compared with the first suggested method (which depends on the average of the total energy of the receiving signals) when the power of received signals is equal (special case). In comparison to the fixed threshold, the first suggested method improved detection performance compared with the fixed threshold in both scenarios. In the general case where the received power signals depend on the distance between the PUs, the second and third proposed adaptive thresholds have been applied. The second adaptive threshold depends on taking the average of the total energy of the receiving signal plus the average of the energy for the lowest two bands, while the third adaptive threshold depends on the average of the

lowest and highest energy bands. Simulation results showed that the second proposed method performed better than the third method in the first scenario, while the third proposed threshold outperformed the second proposed threshold in the second scenario.

To provide a reliable performance assessment of the SS system, the ED algorithm has been implemented using the Universal Software Radio Peripheral (USRP) X310, one of the Software Defined Radio (SDR) hardware technology products. By following the same simulation model of the SS system, the testbed was implemented for the first scenario. Practical results show that the ED achieved good performance and was closer to that of the simulation.

TABLE OF CONTENTS

LIST OF FIGURES

LIST OF TABLES

LIST OF ABBREVIATIONS

Abbreviation	Name
P_d	Probability of Detection
P_{fa}	Probability of False Alarm
P_m	Probability of Miss Detection
P_{te}	Probability of Total Error
1G	First Generation
2G	Second Generation
3G	Third Generation
4G	Fourth Generation

5G	Fifth Generation
8PSK	8 Phase Shift Keying
ADC	Analogue-to-Digital Converter
AM	Amplitude Modulation
ANN	Artificial Neural Network
ASK	Amplitude Shift Keying
AWGN	Additive White Gaussian Noise
BPF	Band Pass Filter
BS	Base Station
CAPEX	Capital Expenses
CAV	Covariance Absolute Value
CDMA	Code Division Multiple Access
CR	Cognitive Radio
CRN	Cognitive Radio Network
DAC	Digital-to-Analogue Converter
DARPA	Defense Advanced Research Projects Agency
DDC	Digital Down Converter
DSP	Digital Signal Processors
DUC	Digital Up Converter
ED	Energy Detection
EMBB	Enhance Mobile Broadband
EME	Energy with Minimum Eigenvalue
FCC	Federal Communications Commission
FFT	Fast Fourier Transform
FM	Frequency Modulation
FN	False Negatives
FNR	False negative rate
FP	False Positives
FPGA	Field-Programmable Gate Array
FPR	False positive rate
FSK	Frequency Shift Keying
Gig E	Gigabit Ethernet
GMSK	Gaussian Minimum Shift Keying
GSM	Global System for Mobile
HMFD	Hybrid Matched Filter Detection
IEEE	Electrical and Electronics Engineers
IF	Intermediate Frequency
IOT	Internet of Things
IQ	In-phase and Quadrature components
ISM	Industrial, Scientific, and Medical
KNN	K-Nearest Neighbors

LabVIEW NXG	Laboratory Virtual Instrument Engineering Workbench Next Generation
LNA	Low Noise Amplifier
LO	Local Oscillator
LOS	Line of Sight
LTE	Long Term Evolution
MED	Maximum Eigenvalue Detection
MF	Matched Filter
MFD	Matched Filter Detection
MIMO	Multiple-Input Multiple-Output
MME	Maximum-Minimum Eigenvalue
MMTC	Massive Machine Type Communication
NI	National Instruments
NLOS	Non-Line of Sight
OPEX	Operating Expenses
P2P	Point to Point
PC	Personal Computer
PCIe	Peripheral Component Interconnect Express
PSD	Power Spectral Density
PU	Primary User
QAM	Quadrature Amplitude Modulation
QOS	Quality of Service
RDM	Random Data Matrix
RF	Radio Frequency
RF	Radio Frequency
RJ 45	Registered Jack-45
ROC	Receiver Operating Characteristics
RRHs	Remote Radio Heads
RTL-SDR	RTL- Software Defined Radio
SC	Small Cell
SMA	Sub Miniature version A
SNR	Signal to Noise Ratio
SPCAF	the Symmetry Property of Cyclic Autocorrelation Function
SS	Spectrum Sensing
SU	Secondary User
SVM	Support Vector Machine
T	Threshold
TCO	Total Cost of Ownership
TE	Total Energy
TN	True Negatives
TP	True Positives

UDN	Ultra-Dense Networks
URLLC	Ultra Reliable and Low Latency Communications
USRP	Universal Software Radio Peripheral
VI	Virtual Instruments
VR/AR	Virtual and Augmented Reality
WCDMA	Wideband Code Division Multiple Access
WiMAX	Worldwide Interoperability for Microwave Access
WRAN	Wireless Regional Area Network

LIST OF SYMBOLS

Symbol	Name
H_0	Null hypothesis
H_1	Alternative hypothesis
λ	Threshold
E	Detection metrics
K	Sub-bands number
n	Sample number
N	Number of FFT samples.
T	Threshold

CHAPTER ONE
INTRODUCTION

1.1 Overview

The massive increase in the number and variety of connected devices, the significant increase in subscriber traffic volume and types, as well as the performance limitations of Fourth Generation (4G) networks, have compelled the industrial sector to continue to develop, deploy, and use Fifth-Generation (5G) technologies. The 5G mobile wireless networks have been designed to meet various and multiple system requirements. 5G is a secure, fast, and reliable connected ecosystem comprising machines and humans, which allows for effective communication, increased communication density, increased industrial production, etc. Comprehensive studies and research on 5G show a number of key techniques that have contributed to meeting the requirements of the system [1].

First, the massive Multiple-Input Multiple-Output (MIMO) technique was suggested to enhance the spectrum utilization of 5G cellular networks. Second, millimeter-wave technologies were introduced in order to increase the bandwidth efficiency of 5G cellular networks. Additionally, the Small Cell (SC) technique has emerged to increase throughput and improve the system while reducing energy usage in wireless applications. To provide perfect service, 5G cellular networks must use a greater number of SCs that are densely distributed. As a result, Ultra-Dense Networks (UDN) are seen as one of the key aspects of 5G cellular networks [2].

The evolution of cellular networks, i.e., from First Generation (1G) to 5G, can be seen as the procedure of network densification to some extent. The cell radius in 1G networks is approximately 10 miles, and cell division may occur, in which the radio range of one cell is divided into two or even more SCs to alleviate path loss and enable extra users. The average radius of a macrocell in a Second Generation (2G) network ranges from several

hundred meters to many kilometers. SCs, which are low-powered radio access points with a range of a few tens of meters to one or two kilometers, are used in 2G networks to offload capacity from macrocells in addition to cell dividing. SCs are becoming increasingly prevalent in Third Generation (3G) and 4G networks and are seen as an essential component of increasing system throughput and regulating network traffic. Because many SCs are deployed to service a particular geographic area, cell coverage areas become smaller and smaller, leading to cell split gain. Also, with the deployment of SCs, homogenous cellular networks become heterogeneous due to differences in power level and BS transmission range. So, to provide high data rates and seamless coverage, the number of SCs in 5G technology would be enhanced in comparison to 4G technology [3].

Many researchers and academics have focused their efforts on many issues that can be encountered with UDN implementation. At the same time, the reality of spectrum scarcity is a substantial impediment to achieving good radio resource utilization. This issue is projected to worsen because of the increasing density of 5G networks which are necessary to offer continuous connectivity between humans, systems, and devices. There are many new challenges with network access, communication, transfer, and handling of massive amounts of data sent by both devices and users. In addition to many problems that have a significant impact on dynamic communication scenarios, such as the shortage of communication resources, complex electromagnetic environments, interference, etc. The cognitive functions of Cognitive Radio (CR) devices allow for the effective use of unutilized spectrum and coexistence between several networks working in the same or contiguous wide frequency bands, thus providing solutions to the problems outlined above [4]. By dynamically reusing the frequency bands allotted to licensed users, CR technology can be an efficient method to deal with low spectrum use and shortages of the spectrum [5].

1.2 Literature Review

A number of researchers studied CR technology in terms of Spectrum Sensing (SS) techniques and have discussed this subject from diverse points of view.

- In 2013, R. Ujjinimatad and S. R. Patil presented an algorithm for SS based on Random Data Matrix (RDM) created from samples taken from received signals. Researchers used identically and independently distributed signals and wireless microphone signals. Simulation results show that the RDM algorithm performs much better than Maximum-Minimum Eigenvalue (MME), Energy with Minimum Eigenvalue (EME), Maximum Eigenvalue Detection (MED), Energy Detection (ED), and Covariance Absolute Value (CAV) at lower Signal-to-Noise Ratio (SNR) values. Furthermore, this proposed method is also considered efficient because it does not demand prior knowledge of noise, signal, and channel [6].
- In 2014, Y. Zhao et al. introduced an algorithm to sense the spectrum based on the wavelet transform called WATRAB. This idea depends on the fact that the Primary Users (PUs) signals carry a limited amount of information as opposed to the noise signals that contain a lot. Researchers have shown that this difference can be exploited to create different transform results. They proved that this algorithm performed well in terms of SS [7].
- In 2015, A. Nafkha et al. proposed three SS methods: The first two algorithms use the MME ratio and the sum of the EME ratio to make their decisions. However, the third algorithm depends on cyclostationary feature detection, and it utilizes the symmetry property of the cyclic autocorrelation function (SPCAF). Two Universal Software Radio Peripheral (USRP) platforms and the GNU-radio toolkit have been relied upon to use three types of modulation 8 Phase Shift Keying (8PSK),

Gaussian Minimum Shift Keying (GMSK), and Frequency Modulation (FM). This study demonstrated that a cyclostationary feature detector outperformed eigenvalue detection [8].

- In 2015, S. Lavanya, B. Sindhuja, and M. A. Bhagyaveni presented a comparison between the performance of Matched Filter (MF), ED, and Eigenvalue technology using MATLAB. When information is available about the PU signal, the MF technique is applied. If no information is available about the PU, the ED and Eigenvalue are applied. The study demonstrated that the performance of the ED does not work well when the SNR is reduced, so the ED is applied when the SNR is high and the eigenvalue when the SNR is low [9].
- In 2015, L. K. Mathew, S. Sharma, and P. Verma presented an algorithm for SS based on ED, Because the performance of conventional ED degrades in low SNR areas, an adaptive threshold-based ED technique is suggested in order to achieve a better tradeoff between the probability of miss detection (P_m) and false alarm (P_{fa}). The numerical results show that the proposed approach outperforms the conventional one [10].
- In 2017, M. Sardana and A. Vohra presented a study to overcome the fading problem facing channels in wireless environments. Because of this problem, there is an exponential decrease in the strength of the signal when it is sent in a wireless environment. The study relies on the performance analysis of the relay-based Cooperative SS. Researchers have shown that this method overcomes the problem of fading [11].
- In 2018, F. Wasonga, T. O. Olwal, and A. M. Abu-Mahfouz presented a literature review of single and two-stage SS methods to improve accuracy, sensor time, and efficiency. In this study, researchers concluded that the two-stage SS methods are of great computational complexity and that the sensor accuracy is not good. To improve performance, the researchers indicated that the ED method must be used in the coarse

sensing stage, followed by the feature detection method in the fine sensing stage [12].

- In 2018, V. S. Muradi and R. K. Paithane presented a CR system in the practical environment. The authors rely on a simple method of detecting the spectrum, which is not dependent on the characteristics of senders or channels. In this work, the presence of a principal user is recognized using a Laboratory Virtual Instrument Engineering Workbench (LabVIEW) code and the NI USRP-2943R transceiver. The USRP features two channels with a frequency range of 1.2 GHz to 6 GHz for both transmitter and receiver. The presence of PU was detected using the ED approach, as well as the ISM spectrum was also used as a free spectrum. The ED method compares the energy detector output to a threshold energy level based on the noise floor to detect the existence of PUs. Finally, the channel must be used by the secondary user (SU) depending on whether or not the PU is present [13].
- In 2019, R. M. Elshishtawy et al. Presented how the ED algorithm is applied to sensing the spectrum to detect the existence or absence of PUs. Two USRP-2942R transceivers were used to send and receive the signal. Simulation results showed different curves in multiple frequency tones for transmitter and receiver signals using Labview. Researchers explain that after a comparison with a threshold value, the presence or absence of signals is determined. As the number of samples grows, so does the value of the threshold, raising the SNR even further. As well as the P_{fa} diminishes when the threshold value is raised [14].
- In 2020, M. Saber et al. Proposed the SS method based on real signals created by smart embedded devices at wireless transmitters using Frequency Shift Kenig (FSK) and Amplitude Shift Keying (ASK) modulations. The receiving interface was built using the RTL- Software Defined Radio (RTL-SDR) dongle and linked to MATLAB software. The

signals were detected using four techniques: Support Vector Machine (SVM), K-Nearest Neighbors (KNN), the Artificial Neural Network (ANN), and Decision Trees. This study shows that the comparison between the performances of each technique has shown that the performance of SVM and ANN can be more accurate than TREE and KNN [15].

- In 2021, D. N. Reeday and Y. Ravinder suggested a method based on fuzzy logic to sense the spectrum and detect the existence of PU, assuming that noise follows a non-Gaussian distribution. The results show that the Laplacian noise leads to a marked deterioration in the performance of the ED. This study showed that through the appropriate selection of fuzzy rules and membership functions, fuzzy logic provides reliable detection [16].
- In 2021, A. Brito et al. proposed the Hybrid Matched Filter Detection (HMFD) method. It is a modern non-cooperative way of detecting the spectrum. Using MATLAB software, the simulation shows the effect of the variation of parameters such as SNR, the number of samples, and P_{fa} on the probability of misdetection (P_m). The performance of this technique has been compared to that of the ED and MF using the same parameters to show which one is more efficient. The study showed that the Matched Filter Detection (MFD) and HMFD techniques outperform the ED technique, HMFD techniques better than MFD techniques in terms of PU detection [17].

1.3 Problem Statement

To satisfy the demands of explosive data traffic in 5G wireless communication, UDN has been developed as one of the most important enabling pillars of 5G technologies. Through UDN, cells will be density spread, so this dense deployment results in many problems, such as an unavailable spectrum for all users. In other words, if there is a large number

of users, the available frequency spectrum will be very little. Through CR technology, available spectrum frequencies are sensed and exploited by unlicensed users to send information from one user to another.

1.4 Aims of the Thesis

This thesis is aimed at designing a real-time SS system that can improve the use of the spectrum. This can be divided into the following identified objectives:

1. Study CR technology as a solution to the problem of inefficient spectrum use in UDN.
2. Modeling and simulation of the proposed SS system using the LabVIEW Next Generation (LabVIEW NXG), in addition to evaluating the performance of the ED algorithm by three proposed methods for the adaptive threshold, through which the available spectrum can be determined.
3. Practical implementation of some scenarios using the SDR platform.

1.5 Thesis Outlines:

The thesis is organized in the following sequence:

Chapter one provides an overview of 5G and the use of UDN in it, a literature review, and Research Objectives.

Chapter two explains the concept of UDN, its components, and the main challenges it faces, as well as the CR technology and its most important functions, and finally, most of the techniques used to sense the spectrum.

Chapter three contains a simulation analysis and the results of the proposed work using LabVIEW NXG software simulators.

Chapter four describes the configuration of the SDR and the implementation of the energy detector on USRP X310 platforms. In addition to the practical results of the proposed methods.

Chapter five presents the conclusion and the future works.

CHAPTER TWO
COGNITIVE RADIO BASED ULTRA-DENSE NETWORKS

2.1 Introduction

To meet the expected 1000 times increase in wireless capacity needs in 5G, network operators will aggressively densify their network architecture in order to reuse spectrum as much as possible. From here, several techniques emerge, such as UDN and CR, both of which have been, in their own right, objects of scientific interest that have yielded many significant accomplishments. This chapter illustrates the concept of UDN, which is one of the leading technologies of 5G, in addition to illustrating the most important challenges facing this technology. The shortage of spectrum resources is also discussed and addressed using cognitive radio technology, which is one of the most important factors of empowerment in 5G.

2.2 5G Fundamentals

5G depends on previous generations of mobile communications, but it differs in several respects. It's designed for a broader range of applications than ever before: This includes not just consumer services such as data, video, and audio, but also industrial uses such as machine-type communications. To assist in satisfying such requirements, the network uses a number of technologies such as software-defined networking, network slicing, and network function virtualization to conserve flexible, basic resources that can be readily adjusted to satisfy new demands as they occur. In order to achieve better system capabilities and larger data speeds, the air interface uses many antennas and supports more Radio Frequencies (RFs) than before [18].

The 5G scope can be better understood by investigating the primary use models targeted by this trend, which are Massive Machine-Type

Communications (mMTC), Ultra-Reliable Low-Latency Communications (URLLC), and Enhanced Mobile Broadband (eMBB) [1]. Figure 2.1 depicts the various 5G use case classifications.

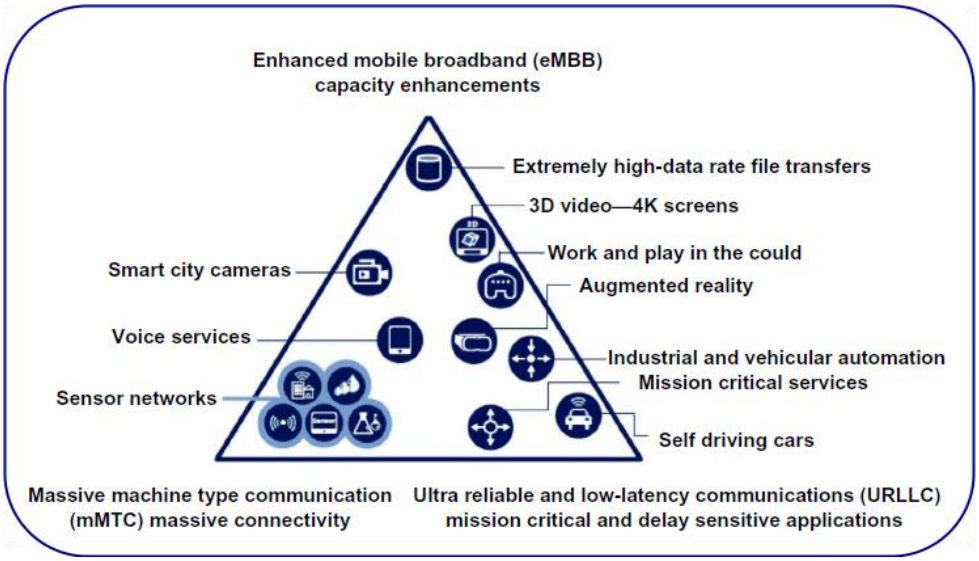

Figure 2.1. 5G use case categories [1]

1. Enhanced Mobile Broadband

The eMBB is the first step of the 5G system and can be viewed as an extension of existing 4G services. The eMBB set primarily addresses services requiring high data rates and high bandwidth, such as high-definition videos, mobile broadband, and Virtual and Augmented Reality (VR/AR). As a result, eMBB is centered on establishing a digital lifestyle.

2. Massive Machine-Type Communications

The mMTC is primarily concerned with services and applications related to vast and dense Internet of Things (IoT) devices. This involves the communication solutions for these devices to develop digital societies such as smart cities.

3. Ultra-Reliable and Low Latency Communications

The uRLLC set focuses on latency-sensitive and high-reliability applications like industrial control, automated driving, and the Tactile

Internet. As a result, the uRLLC set is focused on reaching the digital industry [19].

When compared to 4G networks, 5G networks are predicted to provide roughly 1000 times the system capacity, tenfold the data rates, 25 times the average cell throughput, 90% less energy use, and a fivefold decrease in latency. Three main research directions are needed to meet the goals outlined above: network densification, improved spectrum extension, and spectral efficiency. UDN is one of the enabling factors, and it is regarded as the basis for a 1000-fold increase in data traffic. The fundamental idea of UDN is to densify access nodes per unit area, bringing them closer to the User Equipments UEs. The following section discusses the concept of UDN in detail [20].

2.3 Ultra-Dense Networks (UDN) Principles

In 5G, The UDN is seen as a dense deployment of Base Stations (BS) that use heterogeneous radio access techniques to meet the data rate demands of users using both unlicensed and licensed spectrum [21].

UDNs are networks that have a high density of low-power radio access nodes with different levels of transmission power, data/signal processing capabilities, and radio frequency coverage areas [22]. The density of BSs in ultra-dense networks (UDNs) is highly anticipated to come up to 2,500 BSs per km^2, which reaches or even exceeds the UE density [23].

By previous definitions, the concept of UDNs in 5G is about the densification of SCs and the use of spatial reuse of spectrum to support a large number of customers, machines, and applications. UDNs increase capacity and coverage in 5G networks by utilizing power-efficient and low-cost infrastructure. 5G UDN deployments are expected to be dense and heterogeneous, with SCs like picocells and femtocells being used extensively. Examples of locations where 5G UDN is expected to be

installed are shopping malls, airports, campuses, apartments, open gatherings, and train stations [24].

Figure 2.2 shows a transition diagram from traditional networks to UDN. The expansion of dense networks has provided the requirements for subscriber data, user throughput, spectrum, and so on [25]. Comparing the features of UDN to those of the preceding networks is shown in Table 2.1. [24].

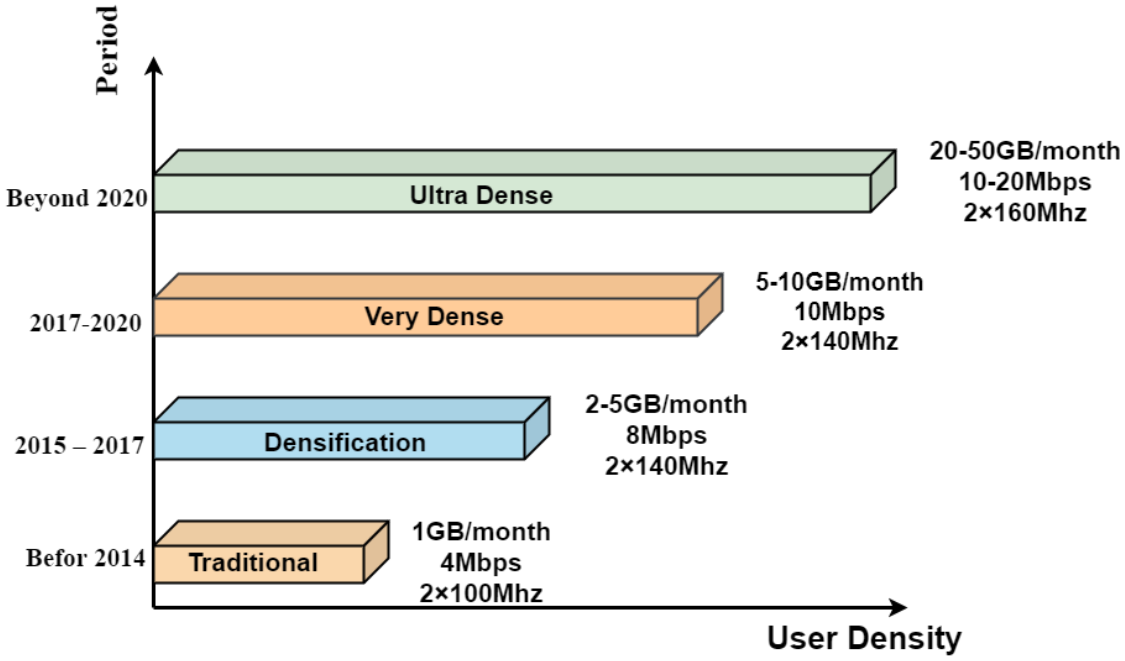

Figure 2.2. Evolution of dense networks [25]

Table (2.1). UDN properties in comparison to older networks [24]

	Traditional networks	Denser networks	Very dense networks	Ultra-dense Networks
Period	Before 2014	2015 – 2017	2017 – 2020	Beyond 2020
Subscriber data	1GB/ month	2 – 5 GB / month	5 – 10 GB / month	20 -50 GB / month
Min. user throughput	4 Mbps	8 Mbps	10 Mbps	10 – 20 Mbps
Spectrum	2 x 100 MHz	2 x 120 MHz	2 x 140 MHz	2 x 160 MHz
Site / Km2	7 sites	21 sites	26 sites	93 sites

2.3.1 Components of UDN

UDN is made up of several access technologies, each with its own set of potential and limits. These technologies enable effective reuse of the spectrum and are considered to be one of the fundamental options for increasing capacity in next-generation wireless networks. Generally, UDN cells can be divided into three categories:

1. High-power macrocells that are fully functional (legacy cells).
2. Fully functional SCs (femtocells and picocells) that can perform all macrocell functions while using less energy and covering a smaller area.

3. Access points for macrocell extension, like Remote Radio Heads (RRHs) and relays, improve macrocell signal coverage [20].

Table 2.2 illustrates the characteristics of the various types of cells mentioned above.

Table (2.2). Key features of different types of cells [20]

Type of SC	Deployment Scenario	Coverage	Transmit Power
Macrocell	outdoor	Few Km	43-46 dBm
Picocells	Indoor/outdoor	< 300 m	23-30 dBm
Femtocells	Indoor	10-50 m	< 23 dBm
Relays	Indoor/outdoor	300 m	30 dBm
RRHs	outdoor	300-500 m	≥ 30 dBm

To improve signal reception, SCs are deployed in houses, small business locations, lampposts, or street poles. The goal of SC deployment is to improve communication quality when a user is in a low-signal location, such as the BS coverage boundary or indoors [26]. Figure 2.3 shows the components of UDN.

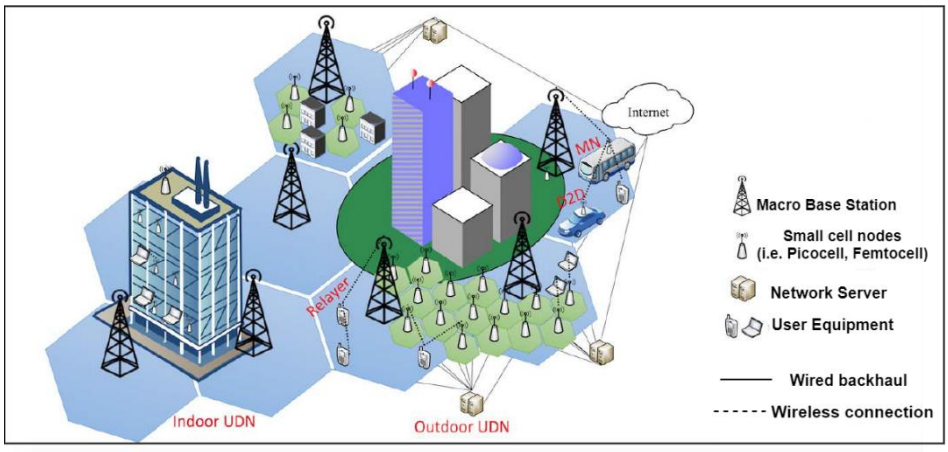

Figure 2.3 An example of UDN [27]

2.3.2 Benefits of UDN

The benefits of UDNs are mainly viewed from the three aspects below:

1. The UDNs significantly reduce the deployment cost because the SCs can be deployed by customers.
2. The deployment of UDNs is elastic, the interference can be reduced, and the energy efficiency can be enhanced by using intelligent usage regulations.
3. UDNs not only thoroughly eliminate the influence of blind spots but also achieve the requirement of load-balancing among the SCs [23].

2.3.3 Challenges of UDN

The challenges facing deploying SCs can be addressed as follows:

1. Interference management: Today's networks, which are primarily macro-based, will be replaced by SC networks containing a few macros. Operators require a long-term strategy for the deployment of SCs since interference levels can increase if cells are not planned from the beginning.
2. Mobility concerns: Throughput can be damaged by handovers due to mobility and the desire of participants to have the highest reliability in

communication and the highest possible throughput. Therefore, future networks will need to carefully balance mobility and throughput.

3. Total Cost of Ownership: The Total Cost of Ownership (TCO) for SCs is significant since the number of sites in a densified network multiplies exponentially. TCO includes both Capital and Operating Expenses (CAPEX and OPEX). There are many different components that make up the TCO for SCs. The largest cost component is often the construction and acquisition of sites.
4. Backhaul: The backhaul requirement will be determined by the SC use case and location. In general, there are three possibilities usable:

- When discussing future bandwidth requirements, fixed backhaul, primarily fiber, comes to mind.
- Point to Point (P2P): Non-Line of Sight (NLOS), Line of Sight (LOS) wireless transmission.
- Point to multipoint wireless transmission [28].

5. SC site planning: Deploying the right number of SCs requires identifying hotspots and categorizing their traffic. Misunderstanding of this information might result in an under-or over-estimation of the number of deployed cells, affecting both energy and efficiency [29].

2.4 Integrating Cognitive radio Functionalities in Ultra-Dense Networks

The scarcity of spectrum resources causes a jamming condition in network capacity improvement. To address this issue, cellular networks have been pushed to seek out a more efficient radio spectrum. As a result, the wireless sector has undergone a new metamorphosis through ultra-densification. UDNs, heterogeneous networks, device-to-device networks, CRNs, millimeter-wave networks, and cloud-radio access networks look to be the key technology for attaining the distinct capabilities that 5G and beyond networks are likely to provide for many years to come. As a result,

in terms of capacity, these technologies will be essential enablers for next-generation mobile communications. Because resources are scarce and must be shared by several users, resource allocation systems become increasingly appealing. As a result, resource allocation in cellular networks is intended to optimize resource utilization, such as power efficiency, spectrum efficiency, and so on [30].

Both the UDN and CR approaches have sparked strong scientific attention in their own right, yielding numerous notable successes. Integrating CR functions into UDN is a feasible solution to the issue of spectrum scarcity, which is becoming increasingly crucial, particularly in large-scale deployment states [4]. The following section illustrates the concept of CR and its main functions.

2.5 Cognitive Radio Fundamentals

The correct use of the radio frequency spectrum is the most important aspect of wireless communication networks. Due to the nonflexible assignment of its license for usage, the frequency spectrum is not exploited effectively. Government organizations manage these licenses, which are given to service providers for a long time and a large geographic region. The Defense Advanced Research Projects Agency (DARPA) conducted signal strength distribution measurements for the wireless communication frequency spectrum. They found that some bands are very crowded and that a lot of the spectrum isn't being used. Where only 6% of the frequency is used. On the other hand, the number of users in a wireless communication network is increasing very rapidly, and demand for high quality leads to spectrum scarcity. Because of this contradiction, it is important to manage the spectrum in a very flexible and intelligent way [31].

CRs are an emerging solution to the problem of spectrum overpopulation that takes advantage of the spectrum holes (spectrum holes are the unutilized frequencies in the RF range) that are not being used by

licensed users (also called PUs) [32]. The idea of CR was first introduced in 1998 by Joseph Mitola III. A CR is an intelligent wireless device that has cognitive, or unlicensed, or secondary users (SUs). These CRs sense the PU's licensed spectrum band in order to establish a communication link between radio nodes in real-time. A CR comes under the Institute of Electrical and Electronics Engineers (IEEE) 802.22 Wireless Regional Area Network (WRAN) standard and can detect channel usage, analyze the channel information, and make a decision on whether and how to access the channel.

The US Federal Communications Commission (FCC) gave a generalized definition: *"cognitive radio: a radio or system that senses its operational electromagnetic environment and can dynamically and autonomously adjust its radio operating parameters to modify system operation, such as maximizing throughput, mitigating interference, facilitating interoperability, and accessing secondary markets*" [33].

Figure 2.4 depicts the presence of spectrum holes in PU channels. The SU transmits across these spectrum holes. PU and SU cannot be transmitted at the same time. As soon as the PU emerges, the SU must leave the channel, which causes the forced termination of the SU connection. Figure 2.5depicts a SU connection being forcefully terminated and blocked. The SU's throughput is determined by the forced termination probability and blocking probability [34].

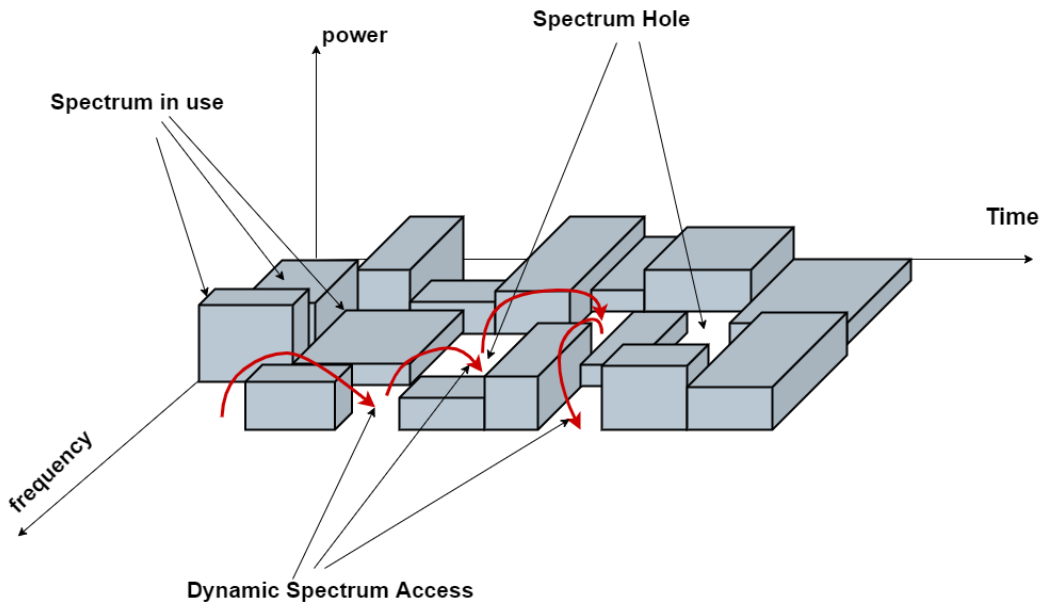

Figure 2.4 Conceptual illustration of spectrum hole [34]

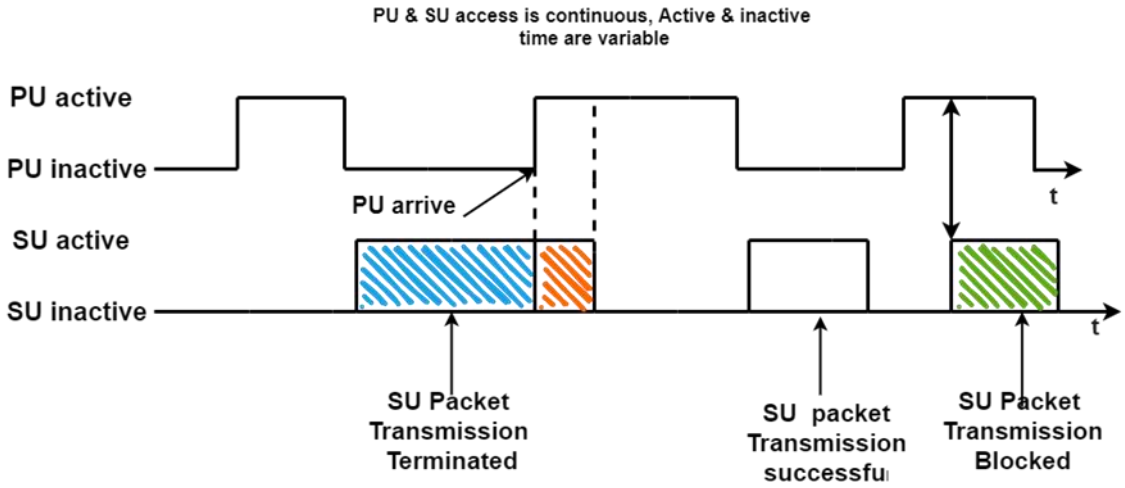

Figure 2.5 Illustration of forced termination and blocking [34]

A- Cognitive Radio Functions

The main roles of the CR are illustrated as follows:

1. SS: The purpose of SS is to determine the state of the spectrum and also to define the activity of PUs by periodically sensing the required spectrum band. In particular, users of CR detect the vacant spectrum and determine a method to reach this spectrum without interference with the licensed users [35].

2. Spectrum decision: Spectrum decision-making follows the detection of the vacant spectrum band (spectrum hole), where the CR user selects the best idle channel following the Quality of Service (QOS) requirements. The decision on the spectrum has three basic goals:

- Spectrum characterization.
- Spectrum selection.
- Reconfiguration of the CR.

3. Spectrum Sharing: The next section that follows the decision on the spectrum band is spectrum sharing among PUs and SUs and between existing SUs in order to optimally exploit resources [36]. Spectrum sharing is divided into three types:

1. Overlay mode: CR can transmit simultaneously with a non-cognitive user; the interference to the non-cognitive user can be balanced by using part of the cognitive user's power to relay the non-cognitive user's message.
2. Underlay mode: In the underlay mode, SUs can transmit simultaneously with the PUs, but in that case, to protect the PU, signals the power constraint is used with the adjustment, meaning, SUs cannot send above the interference limit allowed by the PUs receivers. Therefore, since PUs are not aware of the existence of SUs, the measurement of the interference is very necessary.
3. Interweave mode: in this mode, SUs can use the resource when the channel is vacant until the PUs return. Therefore, SUs must leave the resource directly to avoid interfering with PUs. In this manner, the SUs will use the resource opportunistically without impacting the PUs [37]. The three modes of spectrum sharing are illustrated in Figure 2.6

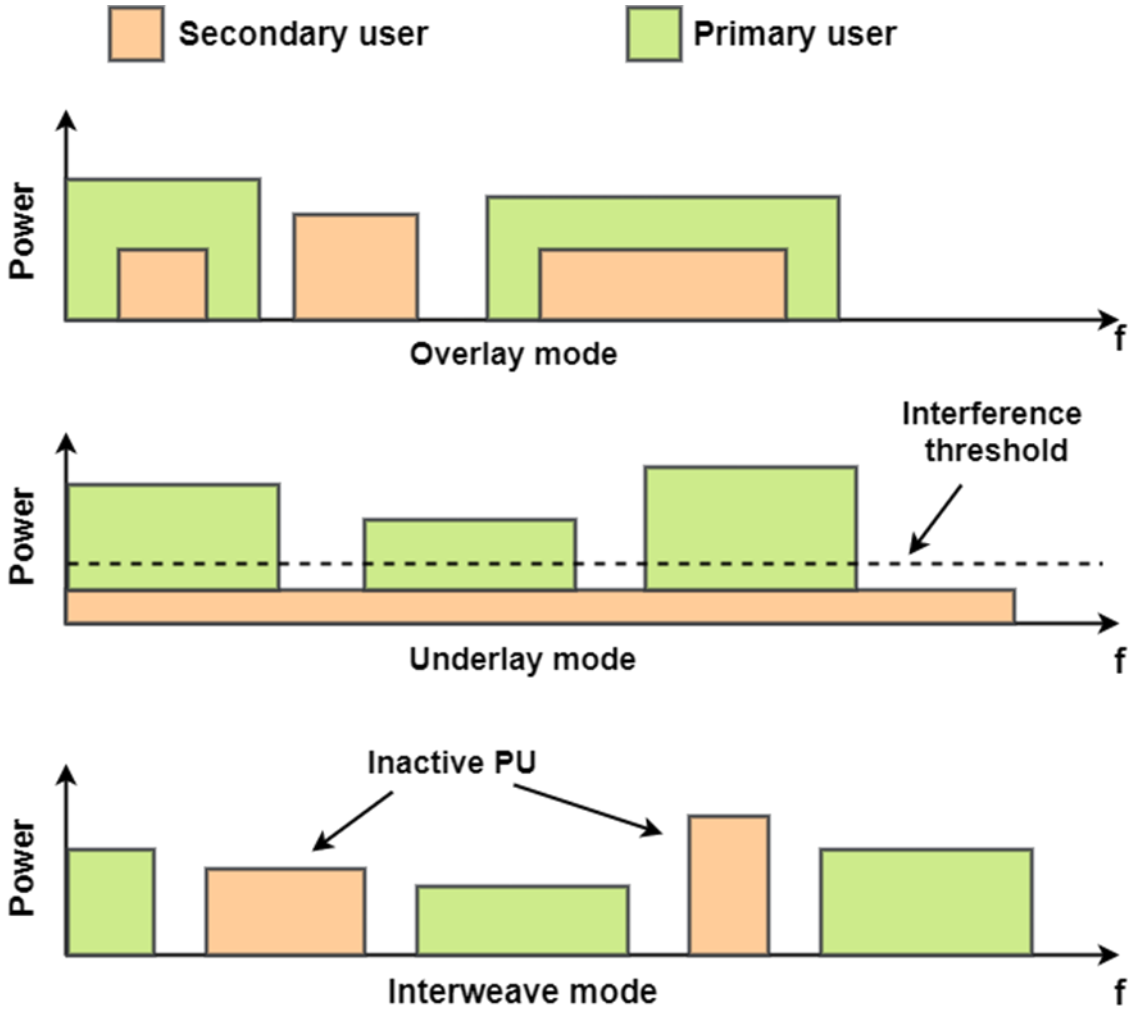

Figure 2.6 Spectrum sharing patterns [37]

4. Spectrum mobility

In CR (SU), the primary job of spectral mobility is to maintain communication continuity as the user goes from one idle channel to another while using the system.

After the SU detects the idle channel (spectrum hole), it continues to use it until the PU returns and transmits again. In this case, SU must leave the channel and transition to another idle channel [38]. The CR functions are illustrated in Figure 2.7.

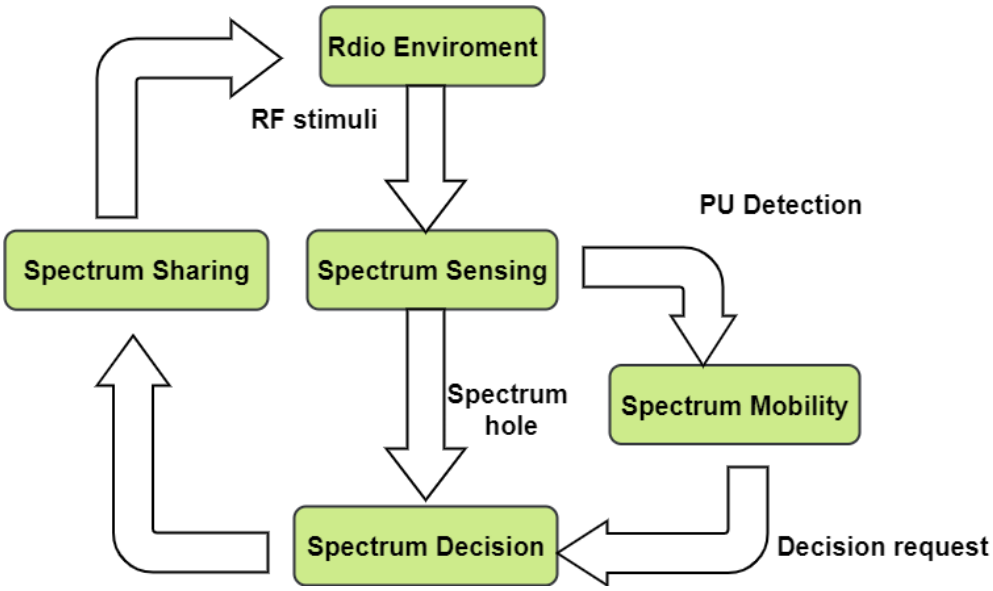

Figure 2.7 Basic functions of a cognitive radio

Based on the spectrum bands, there are two kinds of cognitive radio networks:

- Licensed bands: The spectrum is licensed into several applications, such as Long Term Evolution (LTE)-North America: 700 MHz, 800 MHz, 1.9 GHz, 1.7/2.1GHz, 2.6 GHz, AM radio: 535 kHz, and 1.605 MHz, and aeronautical and maritime communications: 300–535 kHz [39].
- Unlicensed bands: These unlicensed bands involve Industrial, Scientific, and Medical (ISM) bands like 902–928MHz, 5.725–5.875GHz, and 2.4–2.5GHz. Certain applications use the ISM band that is not related to ISM. For example, IEEE 802.11/WiFi: 2.45 and 5.8GHz bands; and IEEE 802.15.4, ZigBee and Bluetooth: (2.402–2.48GHz). [39].

B- Applications of Cognitive Radio Networks

With the capabilities of CRNs, the performance of many networks and communication systems can improve and coordinate with other nodes in the networks effectively. Several applications of CR in real-time are illustrated as follows:

1. CRNs as a Military Network: A military network operates under very similar conditions to a CRN: avoidance of interference between official users, sensing spectrum holes or vacant bands for better utilization of spectrum, localization of other neighboring devices, etc.
2. TV White Spaces Applications: Television white spaces are the main application of CRN. In the TV spectrum, the frequencies between the channels are either used or left unused. A CRN is one of the keys to adjusting the change in frequencies and improving the performance of such networks. This would lead to increased utilization of the TV spectrum efficiently.
3. Emergency Network: An emergency network is one of the most common applications supported by CRN. Such applications need CRN abilities that prominently include location determination, sensing spectrum use by nearby devices, and changing frequency.
4. Multimedia: Multimedia can also be considered a prospective application area for CRNs. CR features such as interference avoidance and spectrum mobility mainly attract the multimedia domain. [33].
5. Healthcare: The Internet of Things (IoT) is used in health care, where smart sensors are placed on and around a patient to track critical information like blood pressure, temperature, and glucose levels. A medical team regularly monitors the parameters through remote monitoring. Healthcare data can be communicated to medical personnel without the necessity for spectrum assignment. This may be accomplished using CR-based IoT frameworks without having to worry about spectrum availability [40].

2.6 Spectrum Sensing

SS is a necessary part of the development of a CRN. It is very important since it detects the current state of frequency band occupancy to allow for opportunistically re-utilizing it. In other words, the goal of SS is to provide knowledge of spectrum utilization. It offers knowledge of the presence of PUs at various points in time and space. As opposed to the traditional understanding of SS, which is defined as the measurement of the spectral content of a signal or measuring RF energy over a spectrum of frequencies, CR is a more public term that refers to getting the spectrum utilization characteristics over a wide range of dimensions, such as frequency, code, time, and space. Considering this concept, it is evident that SS can be considered an enabling technology for the interweaving of CRs [41].

2.7 Spectrum Sensing Techniques

Due to the dynamic properties of the radio environment and the differences between PUs, in addition to the unknown effect of interference, SS has become a challenging issue in CR. In general, SS approaches may be divided into three categories: transmitter detection, interference-based detection, and cooperative detection. In this thesis, the focus was on transmitter detection, which is often used in practical systems. The transmitter detection method relies on detecting a signal from a primary transmitter. To enable dynamic spectrum sharing, the CR transmitter must be able to discern whether a PU signal is available locally in a given spectrum or not. Three approaches exist for transmitter detection, which is shown in Figure 2.8 [42].

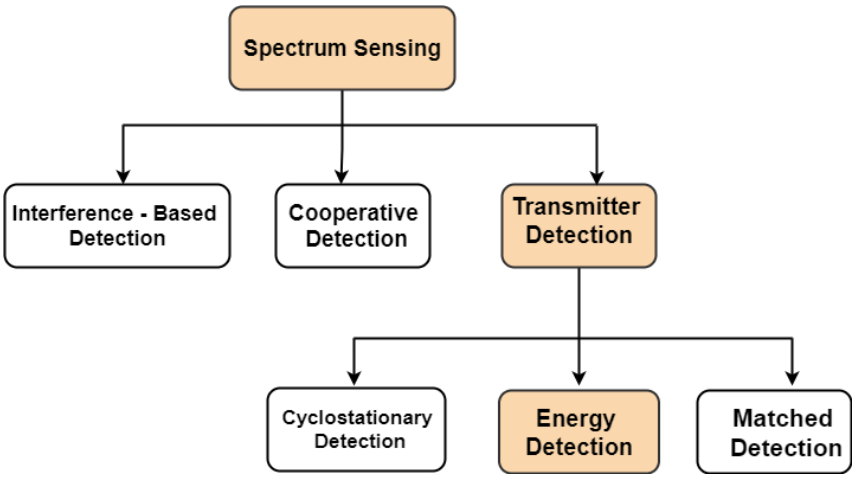

Figure 2.8. Spectrum sensing techniques [42]

2.7.1 Matched Filter Detection

This technique is also known as "coherent detection" and represents the best spectrum detection technique in the case of providing information about the PU signal like modulation type, packet format, pulse shape, transmitting power, pilots, synchronization words, operational frequency, preambles, spreading codes, and bandwidth. The feature of the Matched Filter (MF) is that it has a lower sensing time, but its main weakness is that it requires the PU's prior information, which is not a preferable solution to detect the licensed band in the real world. Also, the implementation is computationally complex [33].

2.7.2 Cyclostationary Feature Detection

A licensed user's sent signal has a periodic pattern in most cases. Cyclostationarity is a periodic pattern that can be used to detect the existence of a licensed user. A licensed user's transmitted signal can be differentiated from noise using this periodic pattern. In general, cyclostationary detection provides a more precise sensing result and is more resistant to noise power changes. On the other hand, detection is difficult and necessitates extensive observation time to achieve the sensing result [35].

2.7.3 Energy Detection

The ED method is the most commonly utilized SS method since it does not require any prior knowledge of the primary signal and it has a low calculation complexity. The cognitive user calculates the energy of the incoming signal and compares it to a threshold in ED. When the received signal's energy falls below the threshold, it means the primary transmitter is turned off. The cognitive user can then use the PU's frequency band [43]. Table 2.3 shows a brief comparison of the SS techniques described above [44].

Table (2.3). Comparison of spectrum sensing techniques [44]

Spectrum sensing technique	Advantages	Disadvantages
Matched filter detection	-Optimal efficiency. -Low computational cost.	Prior knowledge of the PU's signal is required.
Energy detection	-Low complexity. -No primary knowledge is required.	- Underperformance for low SNR. - Cannot distinguish between signal and noise.
Cyclostationary detection	- In the low SNR region, it is robust. - Strong in the face of interference.	- Requires some prior knowledge. - High computational cost.

CHAPTER THREE

SPECTRUM SENSING, PROPOSED SYSTEM, DESIGN, SIMULATION, AND RESULTS

3.1 Introduction

CR technology has provided solutions to some of the constraints in wireless sensing networks. Therefore it is important to seek to understand the key functions that constitute the cognitive cycle. This study focuses on the aspect of SS, which is the most important part of the CR cycle.

This chapter presents the design simulation and results for the proposed SS system using the LabVIEW NXG simulation. In addition to evaluating the performance of the energy detector technique, which is the most popular SS technique for detecting the presence of the PU signal.

3.2 Model Assumptions

In this work, several assumptions were adopted. The model assumptions are:

1. Nine transmitters will be built, which represent the PUs signals. The total bandwidth is 4 MHz, and the bandwidth for each sub-band is 200 KHz.
2. A 16 Quadrature Amplitude Modulation (QAM) will be adopted in each transmitter.
3. Two scenarios of traffic mode have been used for the primary users. The first scenario is the semi-deterministic traffic mode, and the second is the burst traffic mode.
4. The performance of the ED is evaluated over an Additive White Gaussian Noise **(**AWGN) channel.
5. The fixed threshold and the adaptive threshold (the first proposed method, which was determined by relying on the average of the total energy of the receiving signals), will be presented and their performances in both

scenarios will be compared. In this proposal, the power of received signals is assumed to be equal (special case).

6. Proposing two methods for the adaptive threshold (as the second and third proposed methods) and comparing their performances in both scenarios, in this proposal, the power of all received signals is unequal (general case).
7. The effect of different SNR values on the probability of detection (P_d), P_{fa}, P_m, and Probability of Total Error (P_{te}) will be evaluated. The range of SNR starts from -30 dB to 30dB. For each value of SNR, 1000 iterations are taken for the approved measurement.
8. The proposed system can be used as one of the IoT applications.

Table (3.1) illustrates a summary of the parameters used for the simulated SS system.

Table (3.1): Simulation Parameters

Parameters	**Description**
Number of the primary user	9
FFT size	16384
Modulation type	16-QAM
Channel noise	AWGN
Bandwidth for each sub-band	200KHZ
Signal-to-noise ratio	-30db to 30db
Number of iterations	1000

3.3 Performance Metrics for the Energy Detection Algorithm

The following are the most important performance parameters that must be taken into account when conducting sensing:

1- **Detection Probability**

P_d refers to the probability that the PU is detected when the PU actually existed or the probability of the SU detecting the PU's signal when it already exists. To prevent interference and protect the PU from it, the P_d must be high as possible.

2- **False Alarm Probability**

SU announces the presence of the PU in the case that the spectrum is actually vacant. To increase the efficiency of the utilized spectrum, the value of this probability must be low as possible because increasing this probability reduces the chances of the vacant spectrum.

3- **Missed Detection Probability**

The SU announces the absence of the PU in case the spectrum is already busy with the PU. This probability indicates that the SU interferes with the PU.

4- **SNR wall**

SNR wall is a minimum SNR below, which signal cannot be detected.

5- **Confusion Matrix**

A confusion matrix can be defined as a table that can be used to identify the performance values of a classifier's mode based on a group of analyzing data. Table (3.2) shows the confusion matrix [45].

Table (3.2): Confusion matrix.

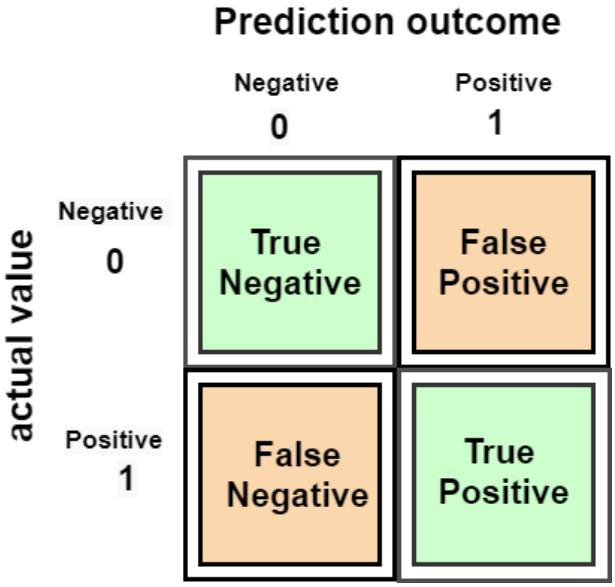

The entries in the confusion matrix are classified as follows: True Negatives (TN), True Positives (TP), False Negatives (FN), and False Positives (FP). The number of cases that a channel is correctly predicted as busy is expressed by TP, whereas the number of cases that a vacant channel is predicted to be busy, is expressed by FP. Conversely, TN represents the number of right predictions of a vacant channel, and FN denotes the number of times a busy channel is predicted as vacant.

From the confusion matrix, four different measurements can be calculated to measure the validity of the ED algorithm that was relied upon in this thesis.

1- Accuracy = (all correct/all)

$$Accuracy = (TP + TN)/(TP + TN + FP + FN) \quad \ldots (3.1)$$

2- Misclassification = (all incorrect/all)

$$Misclassification = (FP + FN)/(TP + TN + FP + FN) \quad \ldots (3.2)$$

3- False positive rate (FPR) is the proportion of true negatives that are incorrectly predicted positive.

$$(FPR) = FP/(FP + TN) \quad \ldots (3.3)$$

4- False negative rate (FNR) is the proportion of true positives that are incorrectly predicted negative.

$$(FNR) = FN/(FN + TP) \quad \ldots (3.4) [46]$$

3.4 Spectrum Sensing System Design

Wireless communication is a broad term that incorporates all procedures of communicating between two or more devices using wireless communication technologies. A typical wireless communication system can be divided into three elements: the transmitter, the channel, and the receiver.

This section explains the design of a system that senses the spectrum using LabVIEW NXG, which is a graphical programming environment used for test and measurement. NXG is the next generation of LabVIEW for communication from National Instruments. The new platform was developed in 2017 to enhance the user experience, and it is more advanced for designing wireless communication systems [47]. Figure (3.1) shows the block diagram of the SS system design.

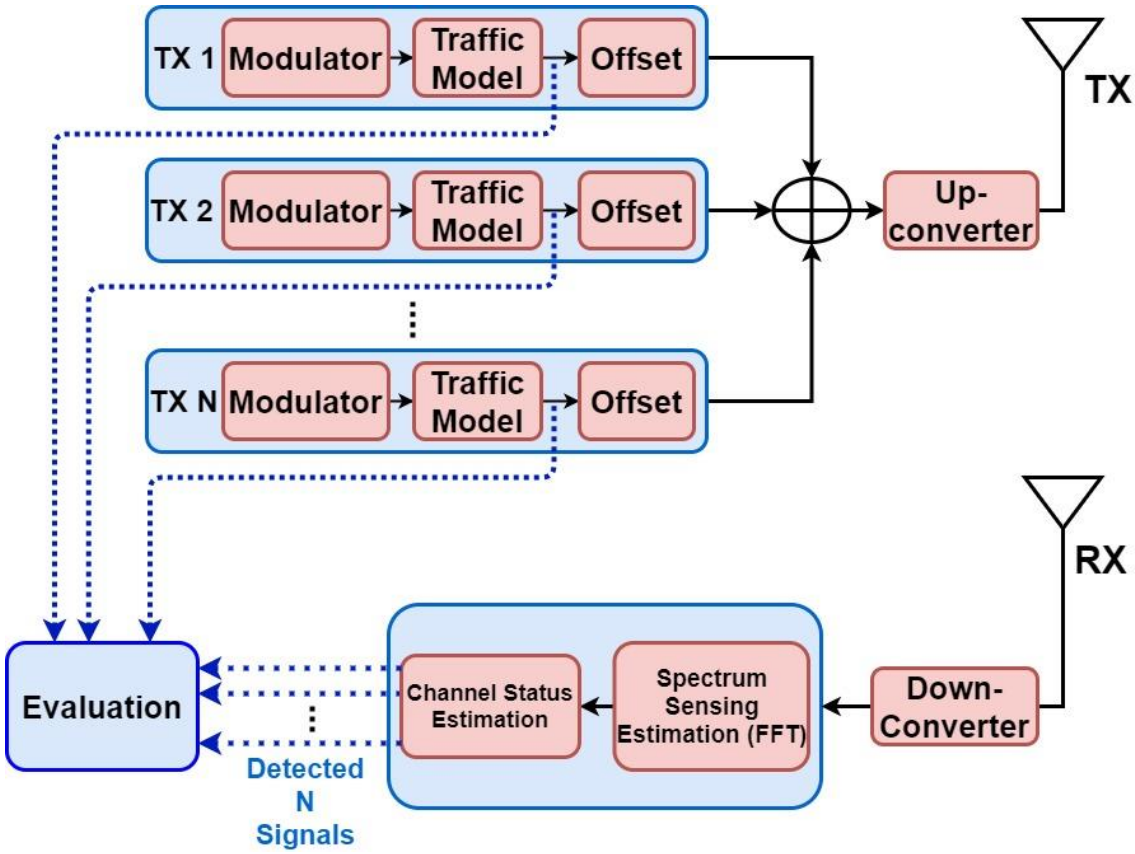

Figure (3.1) Block diagram of the SS system design

3.4.1 The Transmitters Side

In general, transmitters are devices that are used to send out data as radio waves in a specific band of the electromagnetic spectrum to fulfill a specific communication. In this work, the transmitter consists of:

A. The Modulator

In this study, a multi-band transmission system was designed and implemented. QAM has been used in the design of the nine transmitters, figure (3.2) illustrates one QAM transmitter scheme. The first step in designing QAM modulation is to generate a sequence of bits by the MT Generate Bits (Galois, PN Order) node.

MT Modulate QAM node receives this sequence as data bits, performs QAM modulation, and returns the modulated complex baseband waveform in the output complex waveform parameter. MT Modulate QAM node also depends on the MT Generate QAM System Parameters (M) node which

accepts an M-ary value that specifies a predefined symbol map with the number of distinct symbol map values to use as symbols.

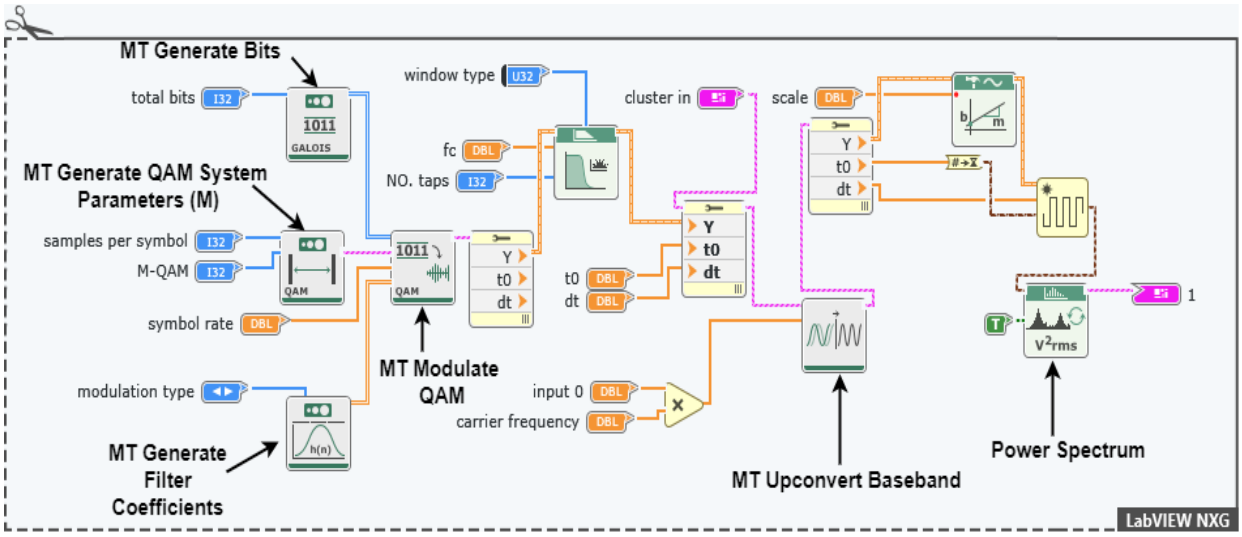

Figure (3.2) QAM Transmitter scheme

Table (3.2) shows the parameters relied upon in the design of the QAM transmitter scheme.

Table (3.3) QAM Transmitter design parameters

Parameters	values
Total bit	1024
Sample per Symbol	40
M-QAM	16
Symbol rate	100KHz

B. Traffic Mode

The traffic mode for PUs and other SUs is the process of describing their dynamic behavior. In this study, two types of traffic modes have been implemented: semi-deterministic and burst traffic modes. The aim is to understand and analyze the performance of the SS process with more realistic traffic modes of users. In this work, the spectrum usage mode depends on the ON/OFF random mode; if the spectrum is not busy by PU or SU, in this case, it is represented by OFF; if the spectrum is busy by PU or SU, in this case, it is represented by ON. The following is an explanation of the traffic modes of users used in this study:

1. First Scenario (Semi-Deterministic Traffic Mode)

As explained in the previous chapter, the PUs may not always use their assigned spectrum. Hence, SUs can opportunistically utilize the spectrum when it is not being occupied by PUs. The PU traffic mode has been assumed to be semi-deterministic in the first scenario. Semi-deterministic traffic can be observed, for example, in television transmission, where the periods can be long. Figure (3.3) shows an implementation of the semi-deterministic traffic mode of PU.

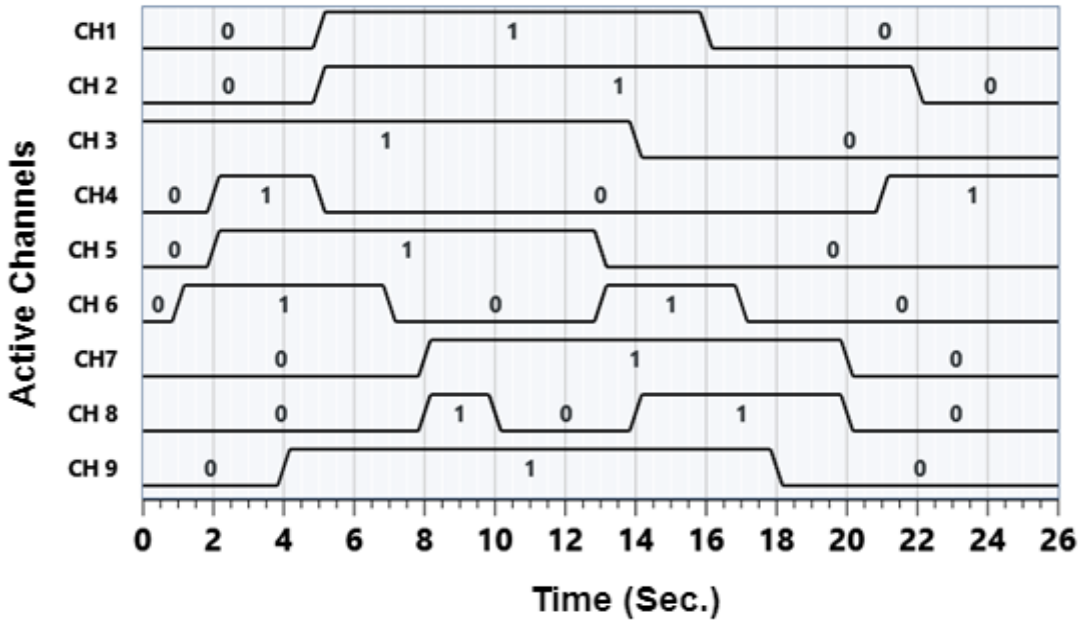

Figure (3.3) Semi-deterministic traffic mode of primary users

In this work, the traffic of PUs can be described in statistical terms where the test statistic is assumed to follow a Gaussian distribution under the hypotheses H_0 and H_1. The test statistic can be defined as the numerical summary of the received signal data set. Figure (3.4) shows the distribution of hypotheses H_0 and H_1 in the ideal case.

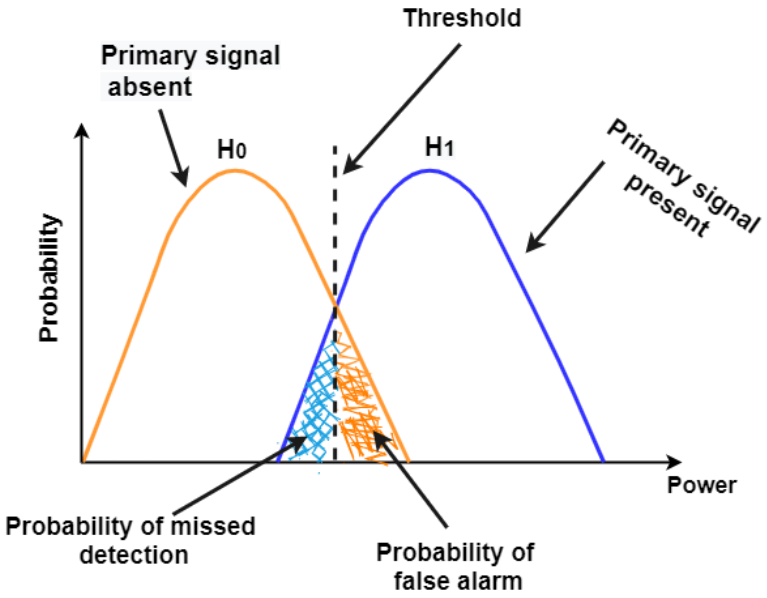

Figure (3.4) Distribution of hypotheses H_0, H_1

2. Second Scenario (Burst Traffic)

In this scenario, the burst traffic mode is introduced, which is another type of PU traffic mode that is implemented in this work. The burst represents data transmitted intermittently rather than as a continuous stream. At low data rates, some IoT applications follow a burst traffic mode, such as IoT applications connected to a sensor or actuator.

The (ON) case indicates that the spectrum is occupied by PU or SU, while the (OFF) case means that the spectrum is empty or unoccupied. Figure (3.5) illustrates the traffic pattern of PU (burst traffic).

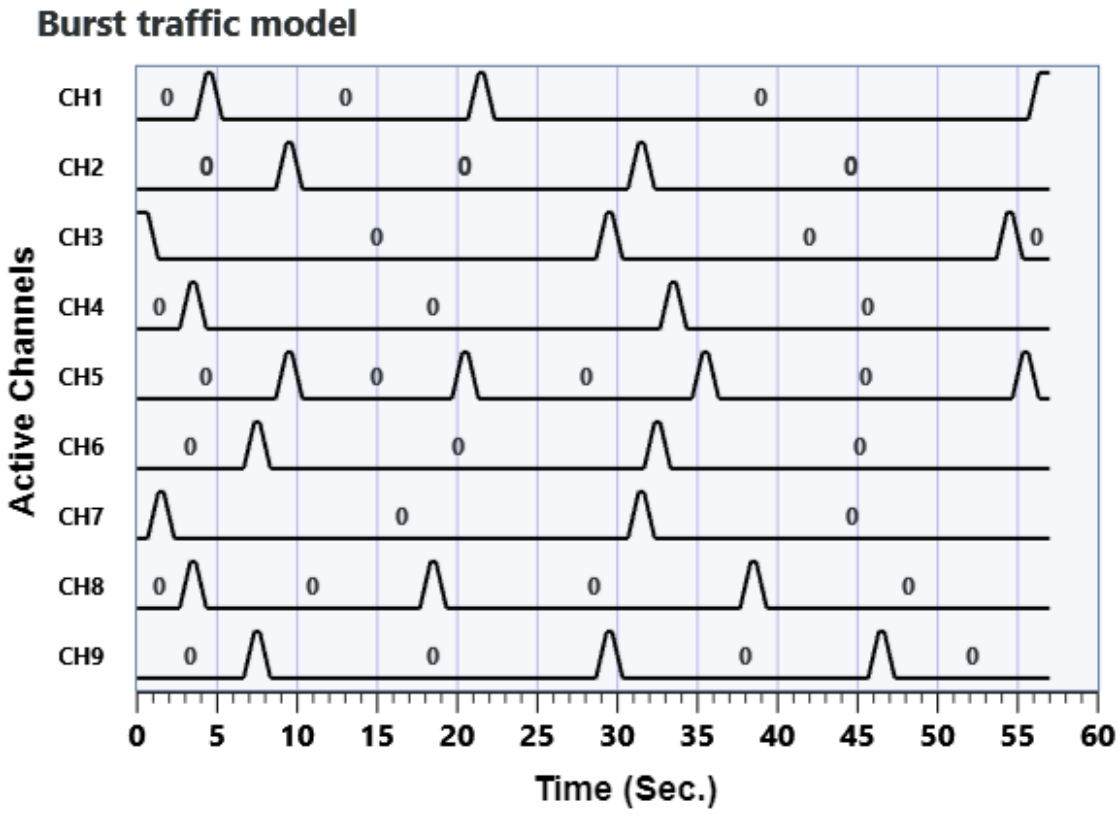

Figure (3.5) Burst traffic mode

One of the most widely used and oldest traffic modes is the Poisson Mode, where a Poisson distribution describes a discrete random variable representing the number of occurrences of an event over a specified interval of time or space [48].

A discrete random variable X is said to have a Poisson distribution with parameter λ > 0, if, for k = 0, 1, 2, . . . , the probability mass function of X is given by Eq. (3.5).

$$P(X = K) = \frac{\lambda^K e^{-\lambda}}{K!} \qquad \ldots (3.5)$$

Where k! is the factorial of k. The Poisson distribution probability function diagram is shown in Figure (3.6) [49].

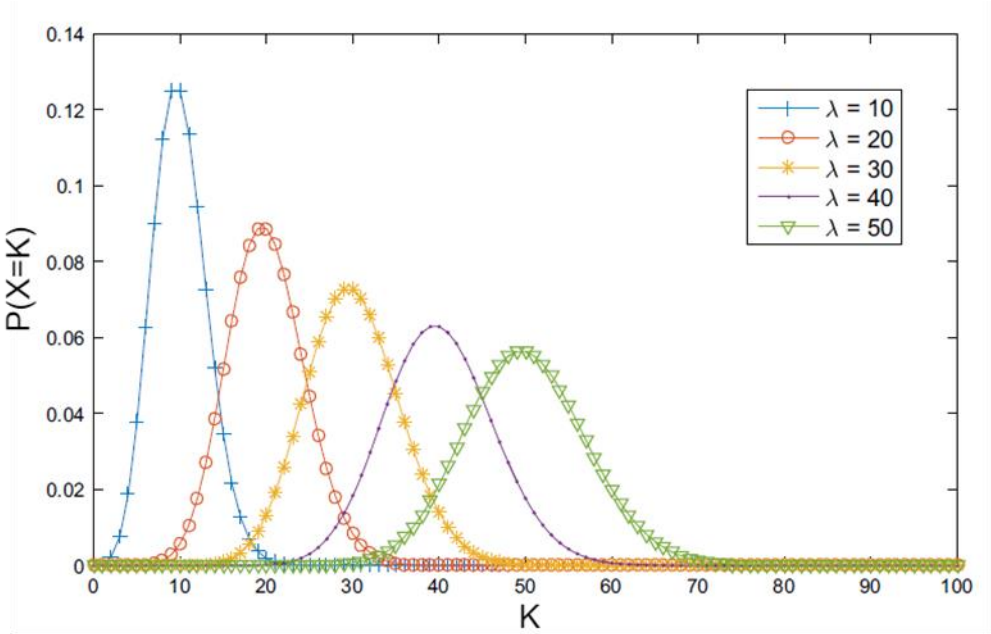

Figure (3.6) Poisson distribution

C. Frequency Offset

Nine transmitters were built using QAM, which in this work represents PUs signals with carrier frequencies set to 0.45 MHz, 0.9 MHz, 1.35 MHz, 1.8 MHz, 0 MHz, -0.45 MHz, -0.9 MHz, -1.35 MHz, -1.8 MHz, carrier signal frequencies were regularly spaced at frequency 450 KHz. The total bandwidth is 4 MHz, and the bandwidth for each sub-band is 200 KHz.

The power spectrum of all nine transmitters (when the power of all transmitted signals is equal) is depicted in figure (3.7).

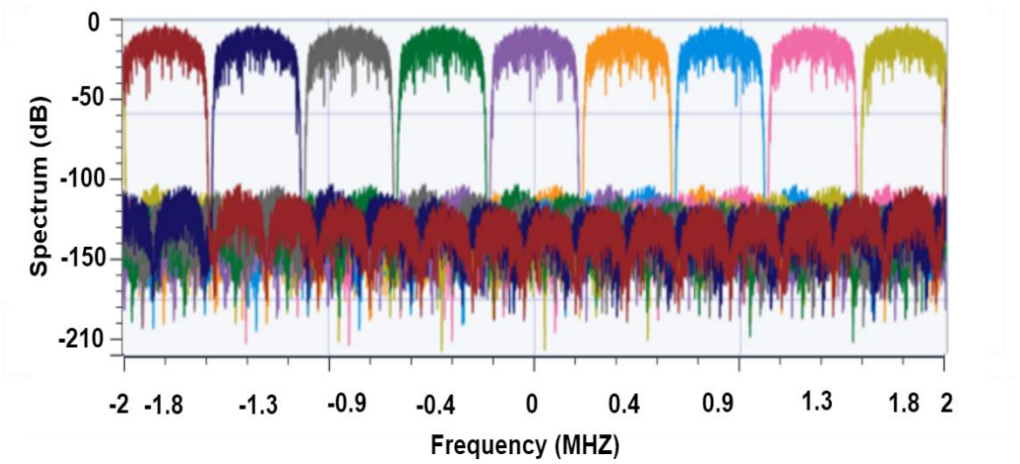

Figure (3.7) Power spectrum of the nine transmitters (equal power)

Figure (3.8) illustrates the power spectrum of all nine transmitters (when the power of all transmitted signals is unequal).

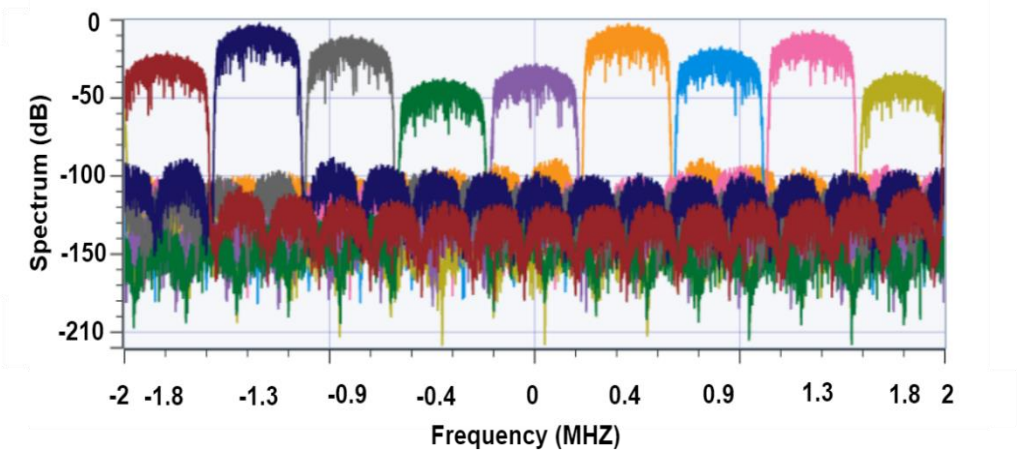

Figure (3.8) Power spectrum of the nine transmitters (unequal power)

According to the semi-deterministic and burst traffic modes, figure (3.9) shows a snapshot of the spectrum of the nine PUs, where it shows that five of the spectrum bands are used by PUs or SUs, and four are empty.

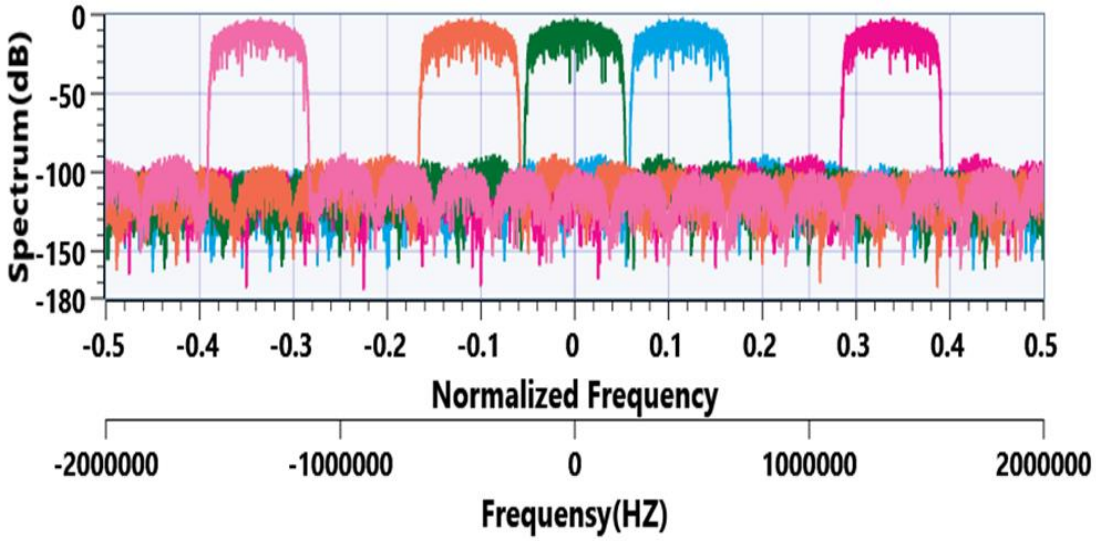

Figure (3.9) Snapshot for the transmitters

D. RF up-converter

The RF up-converter is a stage that is intended to convert the baseband signal to a higher frequency RF signal. This stage will be used in practical implementation, which will be illustrated in chapter four.

Figure (3.10) shows part of the transmission side design.

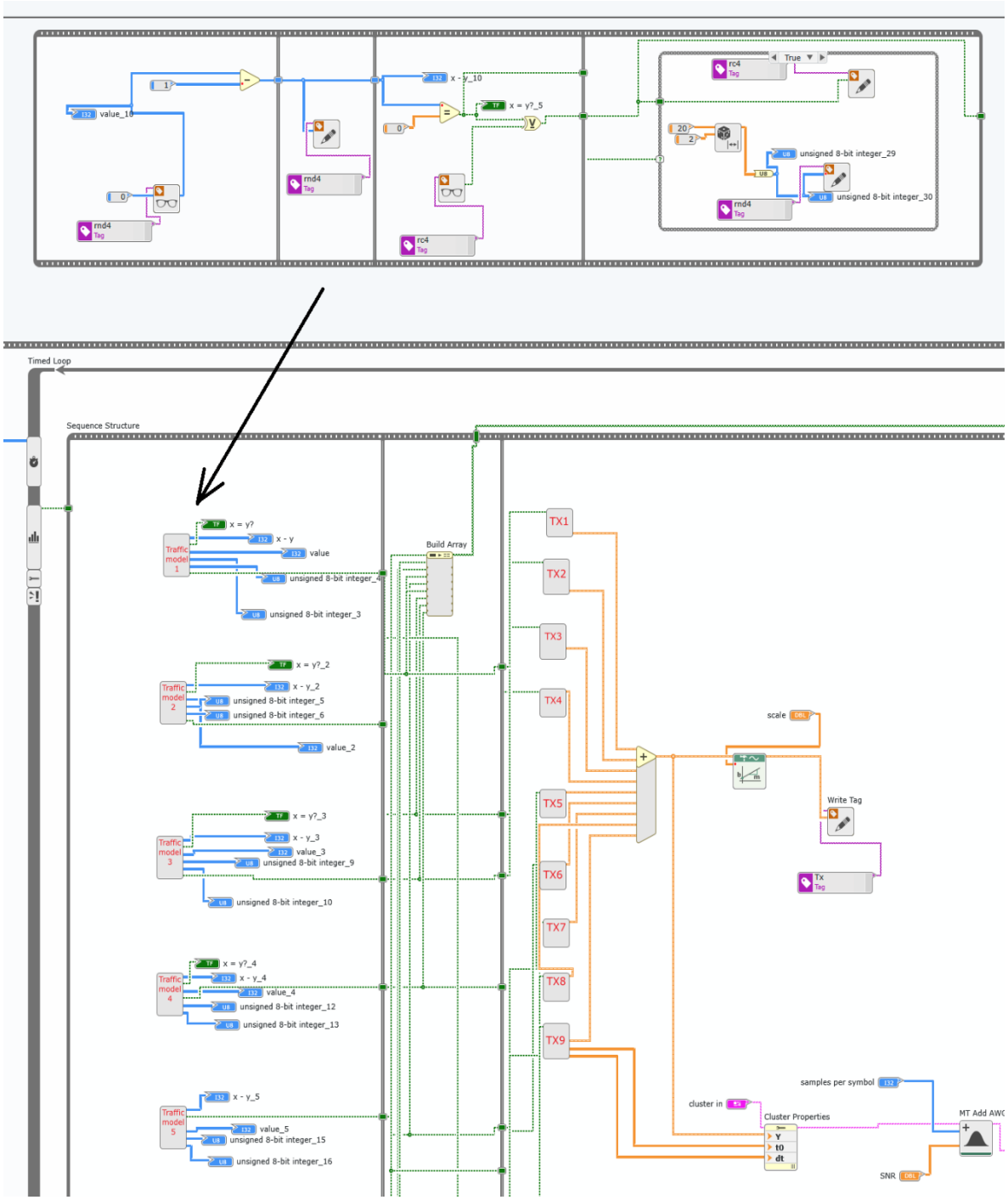

Figure (3.10) part of the transmission side design.

3.4.2 Additive White Gaussian Noise Channel

AWGN is a type of noise that exists in the communication channels generally. The term AWGN originates due to the following reasons:

- **(Additive)** The noise is additive, i.e., the received signal is equal to the transmitted signal plus noise. This gives the most widely used equality in

communication systems. Moreover, this noise is statistically independent of the signal.

- **(White)** Just like the white color which is composed of all frequencies in the visible spectrum, white noise refers to the idea that it has uniform power across the whole frequency band. As a consequence, the Power Spectral Density (PSD) of white noise is constant for the working bandwidth.
- **(Gaussian)** the noise samples have a Gaussian distribution.

3.4.3 Cognitive Receiver Side

The receiver side consists of a down-converter, SS estimation, and channel status estimation, they are illustrated as follows:

A. Down-Converter

The RF down-converter is a stage that is intended to convert the high-frequency RF signal to a lower frequency IF signal. This stage will be used in practical implementation, which will be illustrated in chapter four.

B. Spectrum Sensing Estimation

The SS is the key enabling technology in CR networks. Thus, SS is one of the most important issues in CR networks. The main idea of SS is to provide more chances for a CR user to access the spectrum without causing interference with PUs.

Based on the information provided by the SS process, unlicensed SUs can determine whether there are vacant spectrum holes or not. The PUs have complete control over the assigned frequency band. Unlicensed SUs using CR technology can sense and use spectrum holes when the frequency spectrums are not occupied by PUs. It is important to keep sensing to avoid interference, where SUs must leave the frequency spectrum as soon as the presence of the PU is sensed.

The performance of the ED algorithm is important for determining CR efficiency. The ED algorithm can be implemented in the frequency and time

domains. Theoretically, regardless of whether the implementation of the energy detection algorithm uses the time domain or the frequency domain, the results are the same. The time-domain representation of this method is shown in Figure (3.11).

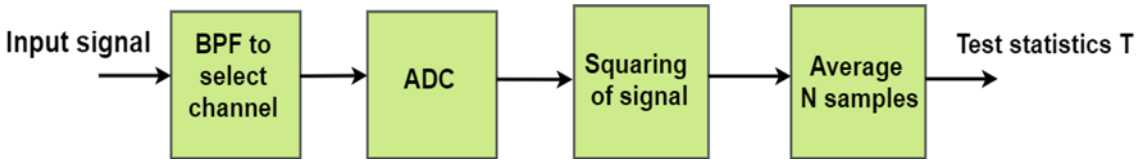

Figure (3.11) Time-domain representation of ED.

In the time domain representation, the received signal passes through the Band Pass Filter (BPF). After the filtering, the signal is converted from analog to digital, followed by a square. Finally, the average is calculated to get the test statistic. The test statistic is compared to a certain threshold, and then a decision is made about whether or not the signal is present or not.

Figure (3.12) illustrates the frequency domain representation of the ED algorithm.

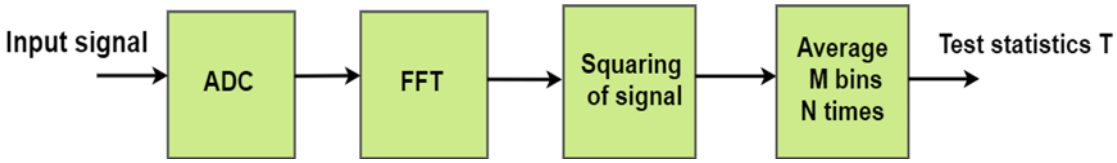

Figure (3.12) Frequency domain representation of ED

In frequency domain representation, first, to sample the received signal, the signal is converted from analog to digital. The Fast Fourier Transform (FFT) is then applied to samples to convert the signal to the frequency domain, and the FFT is squared. After that, the average is calculated. Finally, for decision-making, the test statistic is compared with a specific threshold.

From the time domain representation observation, it is clear that there must be a pre-filter corresponding to the bandwidth of the received signal. The need for a filter makes this representation complex and inflexible compared to frequency domain representation. Also, frequency domain

representation is beneficial for the following reasons: accuracy and ease of measurement, simplification of mathematical analysis, and also, for the frequency domain, visualization tools like spectrum analyzer are commonly used when visualizing electronic signals.

According to the features mentioned above, the frequency domain is used in this work to implement the ED algorithm.

The received signals spectrum from the time domain is converted to the frequency domain using the FFT node in LabVIEW NXG. Figure (3.13) shows the spectrum of the signal received in the frequency domain.

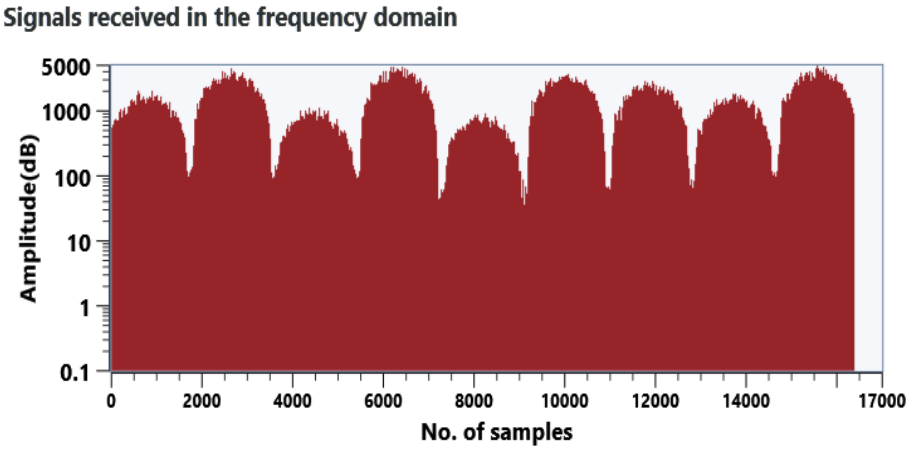

Figure (3.13) Spectrum of the signal received in the frequency domain

Using the array subset function in LabVIEW, each of the nine channels is isolated individually and the energy per channel is calculated according to the equations (3.11, 3.12, 3.13, and 3.14). This energy is then compared to the threshold to determine the presence or absence of PU.

C. Channel Status Estimation

Understanding how SS works will be very useful for a more accurate analysis of CR networks. The SS process can be described as a binary hypothesis that can be defined as follows:

$$y(n) = \begin{cases} w(n) & H_0 \\ s(n) + w(n) & H_1 \end{cases} \qquad (3.6)[50]$$

Where y(n) is the signal received by the cognitive user or SU, s(n) is the transmitted signal of the PU, and w(n) is the AWGN. H_0 is a null hypothesis that refers to the absence of a licensed user signal in a certain spectrum band. On the other hand, H_1 is an alternative hypothesis, which indicates that there exists licensed user signals. There are four possible cases of signal detection:

1. declare H_0 when H_0 is correct ($H_0 \mid H_0$).
2. declare H_1 when H_1 is correct ($H_1 \mid H_1$).
3. declare H_0 when H_1 is correct ($H_0 \mid H_1$).
4. declare H_1 when H_0 is correct ($H_1 \mid H_0$).

Figure (3.14) depicts all four possible cases of signal detection:

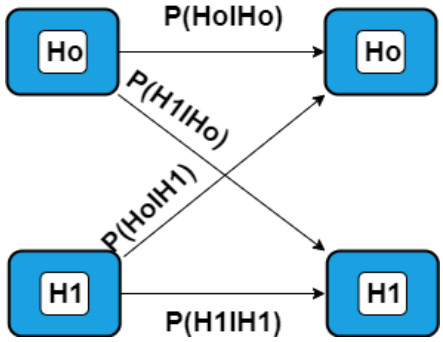

Figure (3.14) Hypothesis tests

Case 3 is known as the missed detection, while case 4 is a false alarm, and cases 1 and 2 are correct detection, which are the most important measures of performance in the SS process.

Assuming the detection metrics and their respective thresholds are denoted as E and λ when a signal is really detected, the P_d can be expressed as follows [51]:

$$P_d = Pr(E > \lambda | H_1) \qquad (3.7)$$

While a false alarm occurs when the spectrum is detected incorrectly as occupied such that:

$$P_{fa} = Pr(E > \lambda | H_0) \qquad (3.8)$$

Consequently, miss detections occur when the spectrum is detected as unoccupied, however, it actually is not, and its P_m is denoted as:

$$P_m = 1 - P_d \qquad (3.9)[51]$$

Figure (3.15) illustrates the receiver side of the system.

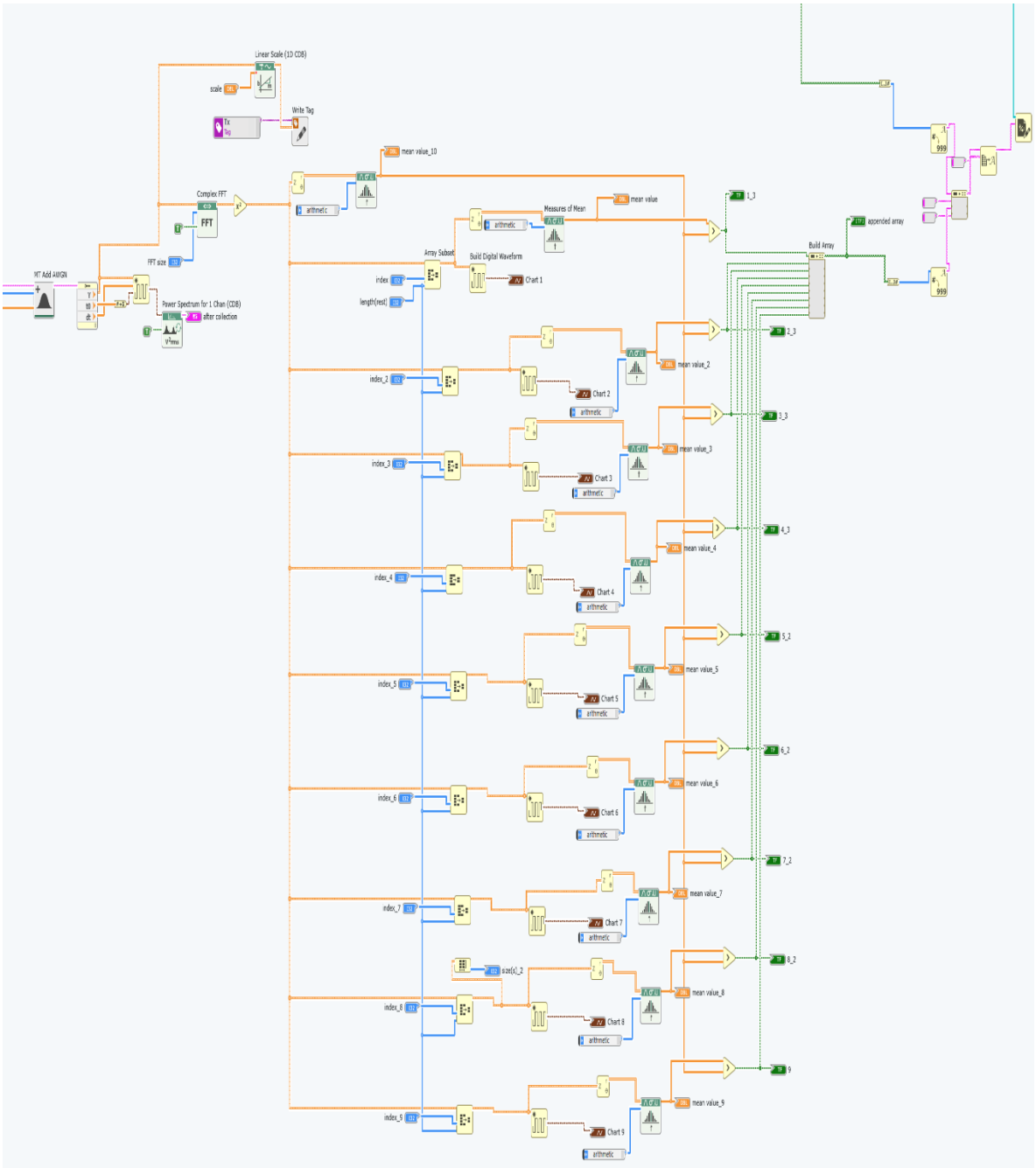

Figure (3.15) Receiver side of the system

3.5 Improved Energy Detection Algorithm

The ED algorithm is classified as the non-cooperative SS method (primary transmitter detection). ED is a common SS technique that is characterized by low implementation complexity and computational. A priori information about the PU signal is not needed for signal detection. In general, in the ED algorithm, the calculation of the energy of the receiving signal gives the test statistic, which is compared to a predetermined threshold. The threshold is determined by the noise energy, and the accuracy of the threshold determination is key to the performance of the energy detector. If the energy of the received signal at CR is greater than the set threshold, the alternate hypothesis H_1 is validated, and the PU is concluded to be present. If the energy is lower, the null hypothesis H_0 is validated, thus signifying the presence of a spectrum hole. Figure (3.16) illustrates a block diagram for an energy detector.

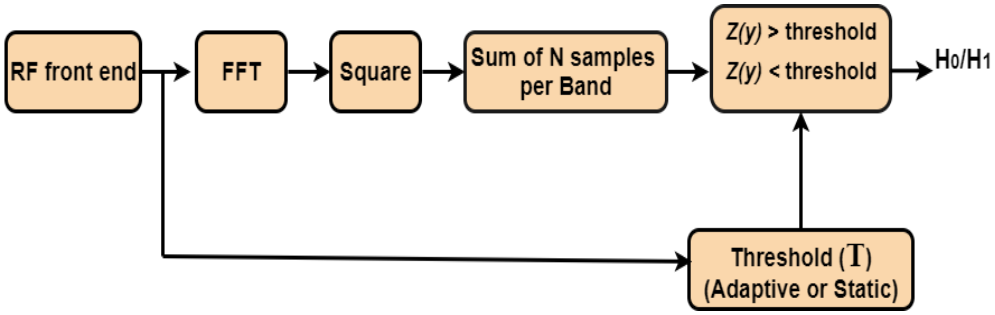

Figure (3.16) Block diagram for energy detector.

The test statistic Z(y) can be computed as [50]:

$$Z(y) = \frac{1}{Ns}\sum_{1}^{Ns} |y[n]|^2 \qquad (3.10)$$

Here, y[n] is the received signal sample, and Ns is the total number of received samples. The computed value of the test statistic Z(y) is then compared with a pre-computed Threshold (T).

The threshold selected to distinguish between the two hypotheses is the decisive factor determining the performance of the ED. Hence, the choice

of the threshold for making the decision has a great impact on the performance of the CR.

3.5.1 Fixed Threshold Technique (The Power of Received Signals is Equal)

For CR, the most appropriate sensing technique is the conventional energy detector. The conventional energy detector uses a fixed threshold value where the fixed threshold value is set above the noise floor to distinguish spectrum preoccupation. Therefore, information on the noise floor level is3. Necessary for the threshold to be determined. Too bad the performance of the conventional energy detector is significantly affected by noise volatility. As a result, there are more false alarms and missed detections. A false alarm occurs when the noise signal is mistakenly identified as the principal signal. Therefore, this results in the underutilization of the spectrum resource due to the missed transmission opportunities.

Moreover, miss detection indicates a circumstance in which the primary signal is incorrectly categorized as a noise signal. This is an extremely undesirable state since it leads to interference with the PU's transmission. Another disadvantage of fixed threshold systems is that the decision threshold is fixed at a fixed level above the noise floor. Therefore, weak primary signals would go undetected if they fell below the detection threshold, and the secondary transmission might cause severe interference to the PU. The fixed threshold is considered impractical in the case of CR sensor networks, where nodes must be completely independent and require no human intervention to function. As a result, when it comes to CR applications, adaptive and autonomous threshold approaches are preferable.

In this study, the ED algorithm was implemented with a fixed threshold where the average energy per available band was calculated and then compared with the threshold to detect the presence or not of PU.

Equation (3.11) shows how the energy for each sub-band is calculated. Figure (3.17) shows how the energy of the spectrum sub-band is calculated.

$$E\ sub = \frac{1}{\text{Sub size}} \sum_{\text{n=start}}^{\text{stop}} |X(n)|^2 \qquad (3.11)$$

$$Sub\ size = \frac{N}{9} \qquad (3.12)$$

$$Start: n = (\text{K} - 1) \times \text{sub size} \qquad (3.13)$$

$$Stop = K \times subsize \qquad (3.14)$$

Where :

Esub: is energy for the sub-band, which is the test statistic that is compared with the fixed threshold.

n: is the sample number

K: is the sub-bands number

$X(n)$: is the magnitude of received signal FFT.

N: is the number of FFT samples.

The fixed threshold (T) value was set at 0.8 of the maximum channel average energy.

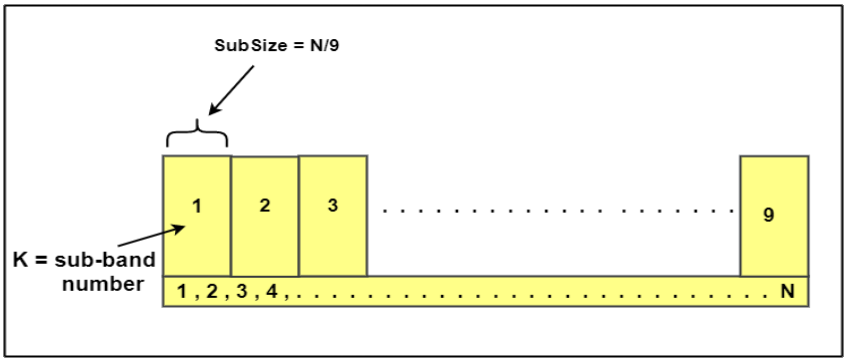

Figure (3.17) sub-band divided

The flow chart of the ED algorithm (fixed threshold) is illustrated in figure (3.18)

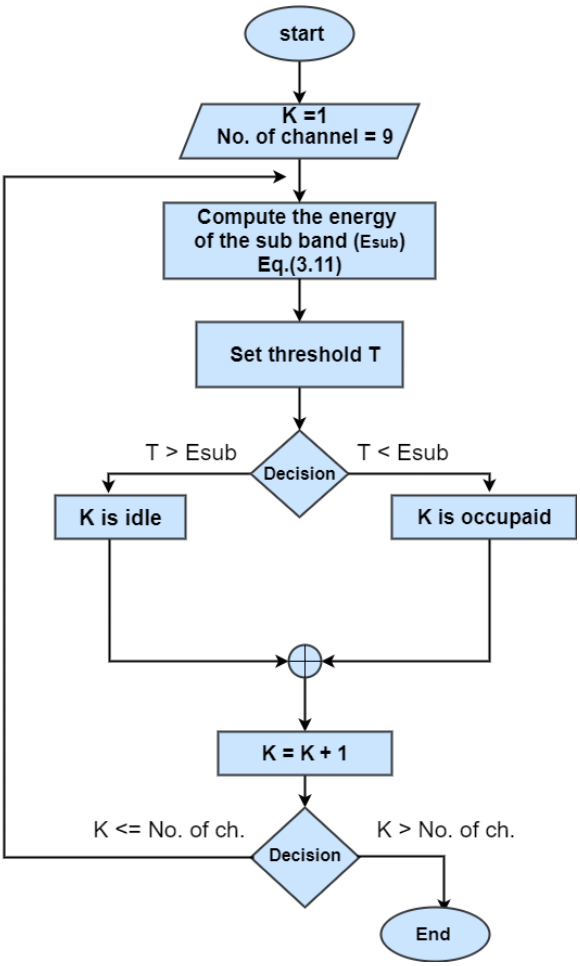

Figure (3.18) ED with a fixed threshold.

3.5.2 Adaptive Threshold Technique (The First Proposed Method -The Power of Received Signals is Equal)

The fixed threshold is considered impractical, especially in the CR system, because of the missed transmission opportunities that lead to the underutilization of spectrum resources. When it comes to CR systems, the adaptive threshold, also called the dynamic threshold, is preferred because of its ability to dynamically modify the threshold level, which increases the dependability of the ED. In this thesis, an adaptive threshold for the ED algorithm is proposed to enhance the reliability and performance of the work.

The proposed adaptive threshold will change adaptively based on the signals received. The adaptive threshold was determined by relying on the average of the total energy of the receiving signals, according to the following equation:

$$ET = \frac{1}{N} \sum_{n=0}^{N} |X(n)|^2 \qquad (3.15)$$

Where ET is the total energy for the received signals, N is the number of FFT samples, n is the sample number, and X(n) is the magnitude of the received signals FFT.

The algorithm has been run on each variation of the SNR value, and accordingly, the threshold value will vary depending on its response to the energy of the receiving signals, which consists of PUs signals with a noise signal. Figure (3.19) illustrates the flow chart of the proposed adaptive threshold algorithm.

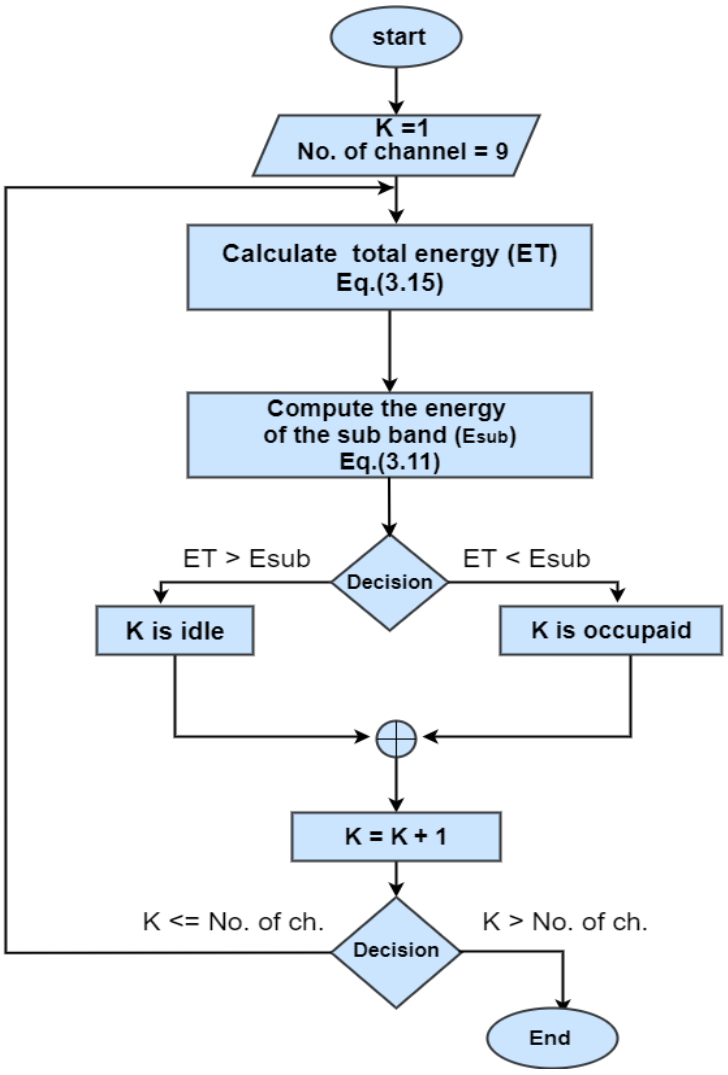

Figure (3.19) Flow chart of the first proposed adaptive threshold algorithm

Table (3.4), presents a comparison of the fixed threshold and the adaptive threshold in terms of performance.

Table (3.4) Fixed and adaptive thresholds comparison

Fixed threshold	Adaptive threshold
• The fixed threshold requires prior knowledge of the bandwidth and the noise level	• Doesn't require prior knowledge of the bandwidth and the noise level.
• Human intervention is necessary to adjust the fixed threshold value.	• There is no need for human intervention to adjust the fixed threshold value.
• The threshold value remains constant doesn't change and is set directly above the noise floor.	• The threshold value is dynamically determined by relying on a certain set of measurements.
• There are more false alarms and missed detection than the adaptive threshold.	• Helps reduce the missed detection and false alarm than the fixed threshold.
• There is a significant degradation in the performance of an algorithm that is based on the fixed threshold when low SNR.	• When compared to fixed threshold approaches, these techniques are more robust to noise uncertainty.

3.5.3 Adaptive Threshold Technique (Second Proposed Method-The Power of Received Signals is Unequal)

When the power of all received signals is unequal, which is the closest to realism, the first proposed method of adaptive threshold (that depends on the average of the total energy of the receiving signals) is inefficient and poorly performed. That is because of the variable power of the signals, the threshold value may be higher than the low-average signals and will therefore not be detected. So an adaptive threshold has been proposed that

depends on taking the average of the Total Energy (ET) of the receiving signal plus the average of energy for the lowest two bands (here, as if the average energy for the two lowest bands represents the noise level). Equation (3.16) illustrates how to calculate the proposed adaptive threshold.

$$T = \frac{ave.ET + ave.lowest\ two\ band}{2} \qquad (3.16)$$

Figure (3.20) illustrates the flow chart of the proposed adaptive threshold algorithm.

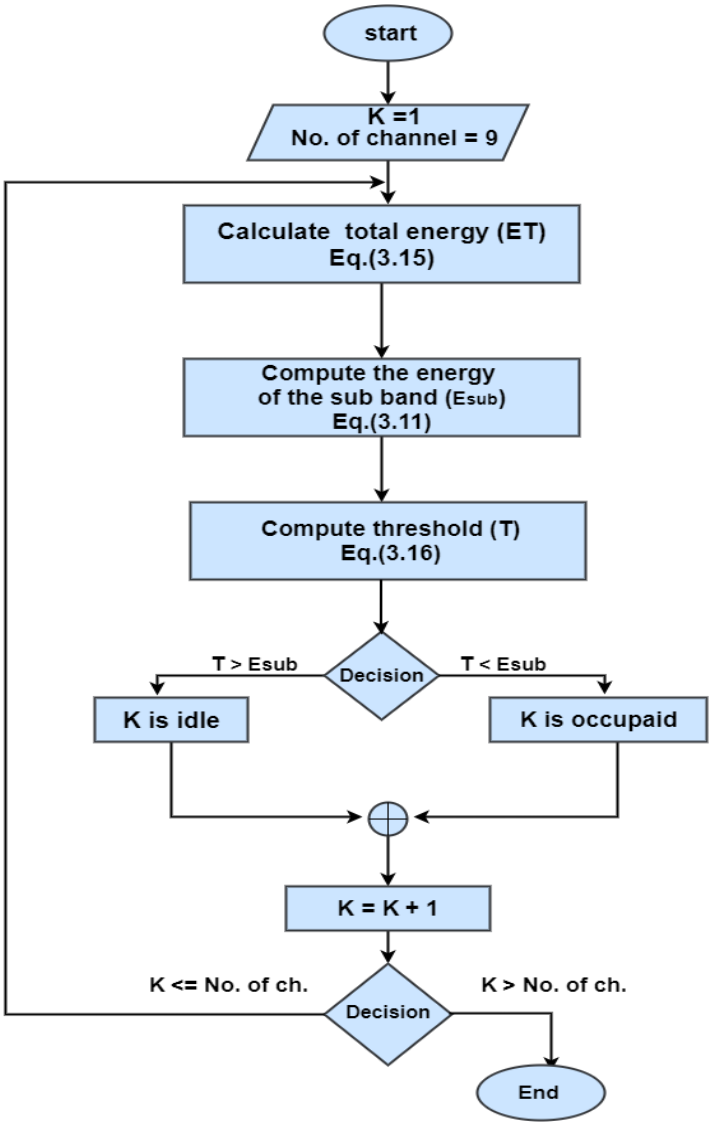

Figure (3.20) Flow chart of the second proposed adaptive threshold algorithm

3.5.4 Adaptive Threshold Technique (Third Proposed Method-The Power of Received Signals is Unequal)

The proposed adaptive threshold approach is based on the average of the lowest and highest energy bands. Equation (3.17) illustrates how to calculate the proposed adaptive threshold.

$$T = \frac{ave.lowest\ two\ bands + ave.highest\ two\ bands}{2} \qquad (3.17)$$

Figure (3.21) illustrates the flow chart of the proposed adaptive threshold algorithm.

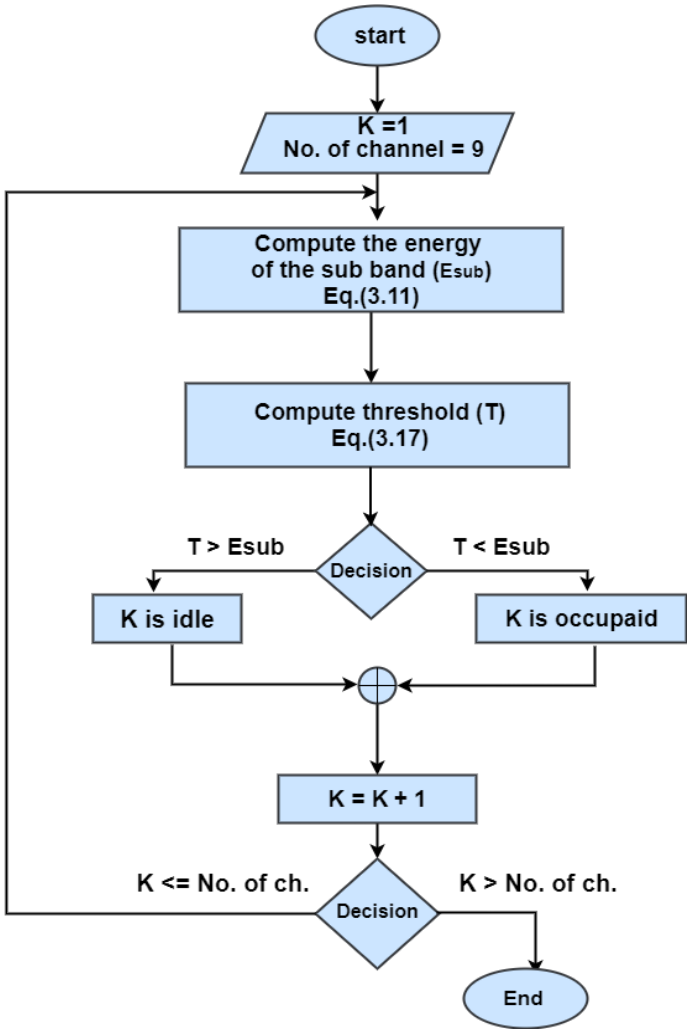

Figure (3.21) Flow chart of the third proposed adaptive threshold algorithm

3.6 Results and Analysis

In this section, the performance of the energy-based SS is evaluated. The metrics used to analyze the performance of the ED algorithm in this work are P_d, P_{fa}, P_m, and P_{te}. The performance of the ED was evaluated over an AWGN channel.

The performance of the ED is described based on the curve of the Receiver Operating Characteristics (ROC). This curve offers a mathematical framework for calculating P_d, P_{fa}, and P_m for the fixed and adaptive threshold technique. The area below the curve denotes accuracy. The performance of the detector improves when the area under the curve becomes closer to one unit square, as shown in figure (3.22).

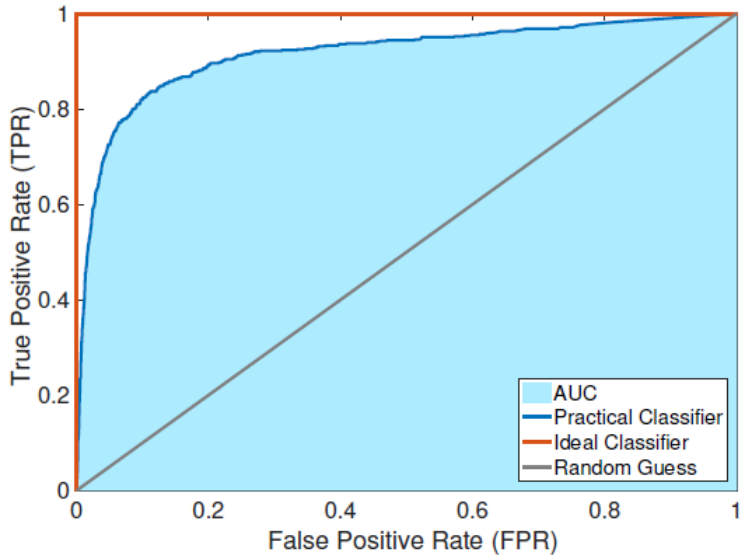

Figure (3.22) Receiver operating characteristic curves and the area under the ROC curve [52].

The following sub-sections explain and analyze the results of SS using the conventional ED and the proposed techniques in both scenarios (first and second).

3.6.1 Fixed and First Adaptive Method Simulation Results (Received Signals Power are Equal)

This sub-section presents the simulation results (for the first and second scenario) of the conventional energy detector and compares them with the first proposed method results of the adaptive threshold. The adaptive threshold was set based on the average of the total energy of the signal that was being received. Here, it has been assumed that the power of all received signals is equal (special case).

3.6.1.1 First Scenario (Semi-Deterministic Traffic Mode)-Special Case

In the first scenario, the performance of the ED algorithm is evaluated when the semi-deterministic traffic mode is adopted for the PUs. The results of the conventional energy detector and the first proposed method are compared when the power of all received signals is equal. Figure (3.23) depicts the relationship between the variance of the P_d and the SNR.

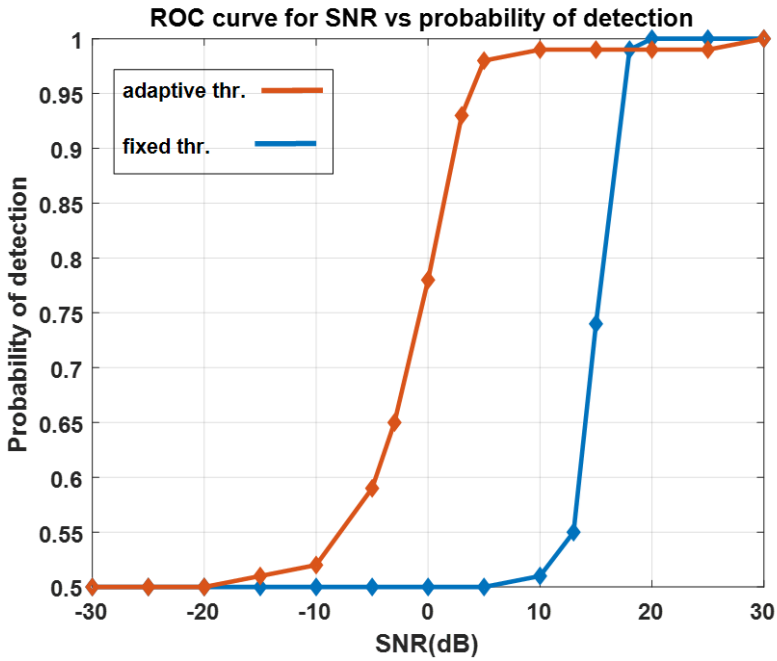

Figure (3.23) P_d vs SNR for fixed and first adaptive threshold (semi-deterministic traffic mode)

According to the results obtained, the fixed threshold results show that there is a significant degradation in its performance at the lower SNR values.

The ED detection probability is stable at 0.5 when SNR = -30dB to SNR = 5dB, then it starts to increase until it gets closer to 1 at SNR = 18dB. At SNR greater than 18 dB, it can be noted that the energy detector has no difficulty in differentiating between the principal signal and the noise signals. However, when SNR is less than 5 dB, the performance of the energy detector degrades significantly. The SNR wall represents the minimum SNR below which a signal cannot be detected; for the fixed threshold The SNR wall is located at 15dB.

The results of the adaptive threshold show that at SNR values larger than 5dB, the ED has little trouble differentiating between the primary and noise signals. The performance of the ED degrades significantly when SNR values fall below -10dB. The SNR wall is located at 0dB when P_d value = 0.77.

For the sake of comparison, it can be seen that the adaptive threshold method outperforms the fixed threshold method in detection probability. For example, at SNR= 0 dB, the probability of detection using the proposed method increased from 0.5 to 0.787.

Another parameter that shows the performance of the ED is the P_{fa}. The false alarm occurs when the spectrum is incorrectly detected as busy. Figure (3.24) illustrates the ROC curve for P_{fa} VS. SNR from -30 dB to 30 dB. For the fixed threshold ROC curve, P_{fa} is high at the lower SNR values, and it starts to decrease at SNR = 15 dB until it reaches zero at 20 dB.

The adaptive threshold results indicate that when the SNR is between 5dB and 30dB, the performance of the ED is better. When comparing the two results of the false alarm, it can be noticed that the adaptive threshold is more efficient than the fixed threshold.

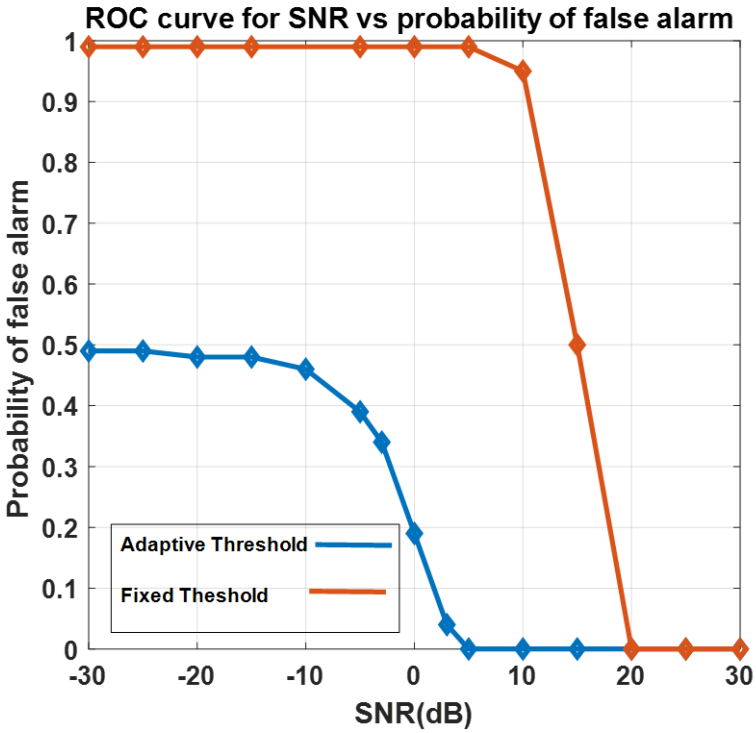

Figure (3.24) P_{fa} vs SNR for fixed and first adaptive threshold (semi-deterministic traffic mode)

It is also feasible to assess the ED in terms of the P_m, as illustrated in figure (3.25). According to the ROC curve, the P_m is high at SNR = -30dB and zero at SNR = 15dB; this is because the SNR is high enough at 15 dB to prevent misdetection. For the sake of comparison between the performances of the two thresholds (fixed and adaptive), the fixed threshold seems to be better than the adaptive threshold, but the reality is not, because, the previous figure, shows that the P_{fa} was 100% at SNR values from -30dB to 5dB. And by the equation of the P_{te}, which represents the sum of the P_{fa} and the P_m, the matter becomes clearer.

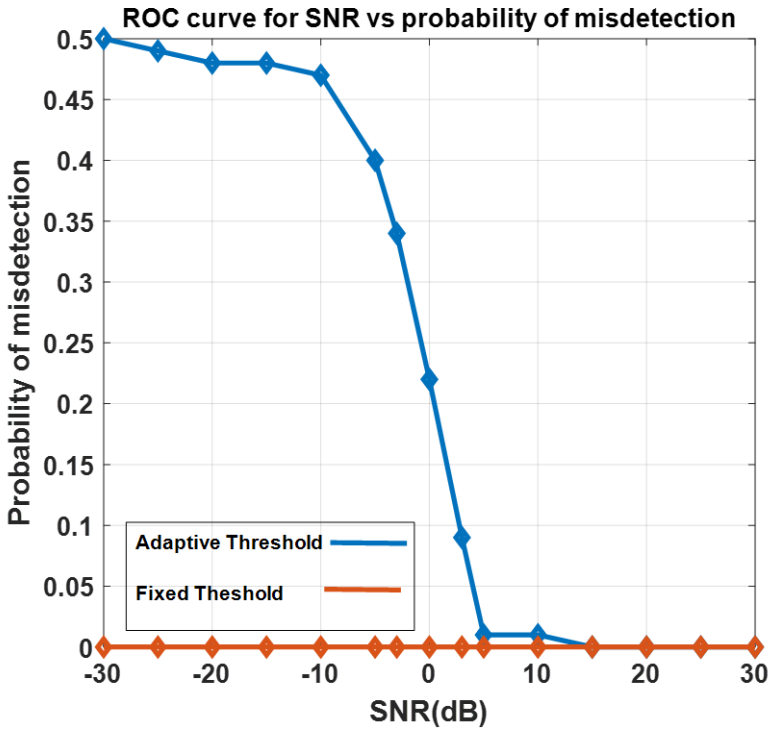

Figure (3.25) P_m vs SNR for fixed and a first adaptive threshold (semi-deterministic traffic mode)

The results of the fixed threshold in figure (3.26) illustrate the P_{te} versus SNR. P_{te} is (P_m) plus (P_{fa}). The results show the highest P_{te} at a low SNR value, which is the worst case, and then it decreases until it reaches zero at 20dB. At SNR values of between 20dB and 30dB, the performance of ED works better. The adaptive threshold results show the highest P_{te} at a low SNR value and then start to decrease until it reaches zero at 15dB. At SNR values of between 5dB and 30dB, the performance of the ED is better. The results show that the adaptive threshold performance is more efficient than a fixed threshold.

$$Pte = Pm + Pf \qquad (3.18)$$

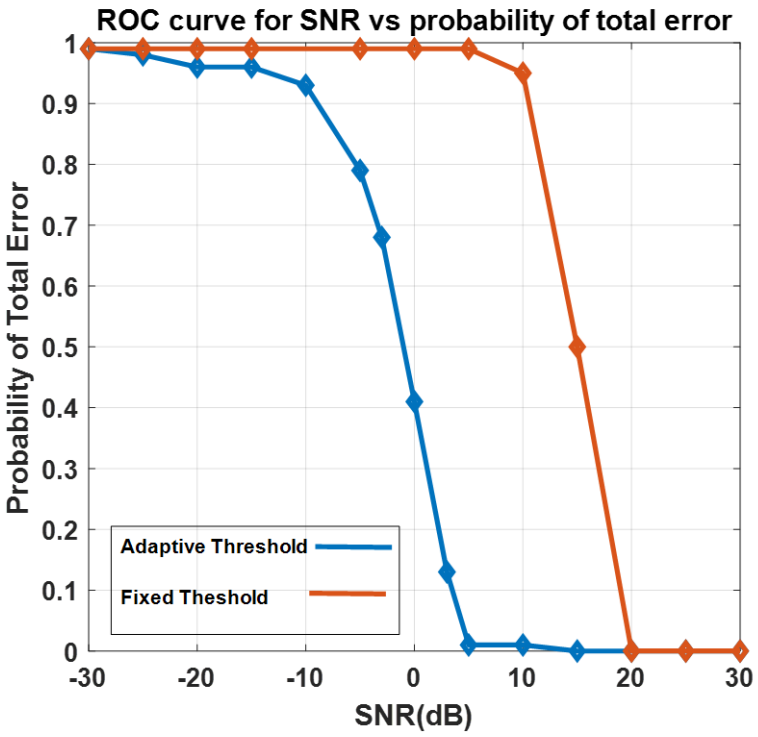

Figure (3.26) P_{te} vs SNR for fixed and first adaptive threshold (semi-deterministic traffic mode)

3.6.1.2 Second Scenario (Burst Traffic Mode)-Special Case

To demonstrate the efficiency and the ability of the system to sense the spectrum, the burst traffic mode for PUs was implemented using the same algorithm and threshold (fixed and first adaptive threshold) techniques.

Figure (3.27) illustrates the relationship between the variance of the P_d and the SNR.

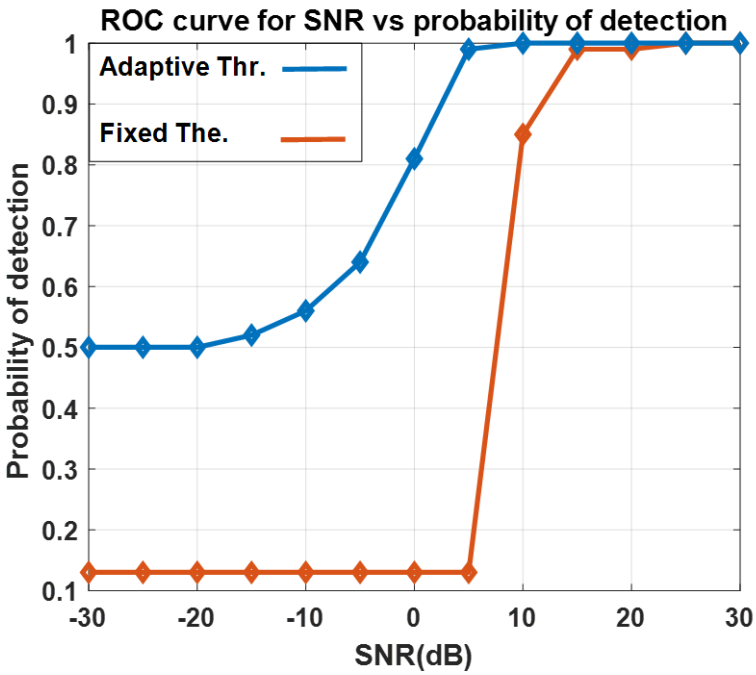

Figure (3.27) P_d vs SNR for fixed and first adaptive threshold (burst traffic mode)

When assessing the performance of the ED algorithm at fixed threshold utilization, it was observed that the curve did not start at 0.5 because the burst traffic mode follows the Poisson distribution. In addition, the threshold value is constant. In this scenario, the fixed threshold value was set at 0.8 of the maximum channel average energy. According to the results, at lower SNR values, the performance of the ED degrades. At SNR values larger than 15dB, the ED has little trouble differentiating between the primary and noise signals. The performance of the ED degrades significantly when SNR values fall below 5dB.

The results of the adaptive threshold show that the P_d = 1 at SNR = 5dB. The SNR wall is located at 0dB when P_d value = 0.818. The utilization of the adaptive threshold improves the performance of the ED algorithm in terms of P_d in comparison to the fixed threshold.

Figure (3.28) illustrates the ROC curve for P_{fa} versus SNR. For the fixed threshold ROC curve, P_{fa} is high at the low SNR values but starts to decrease at SNR = 10dB until it reaches zero at SNR = 15dB.

At SNR values of between 5 and 30dB, the ED performance using the adaptive threshold is better. When comparing the performance of the two thresholds, it can be seen that the adaptive threshold is a more efficient approach than the fixed approach.

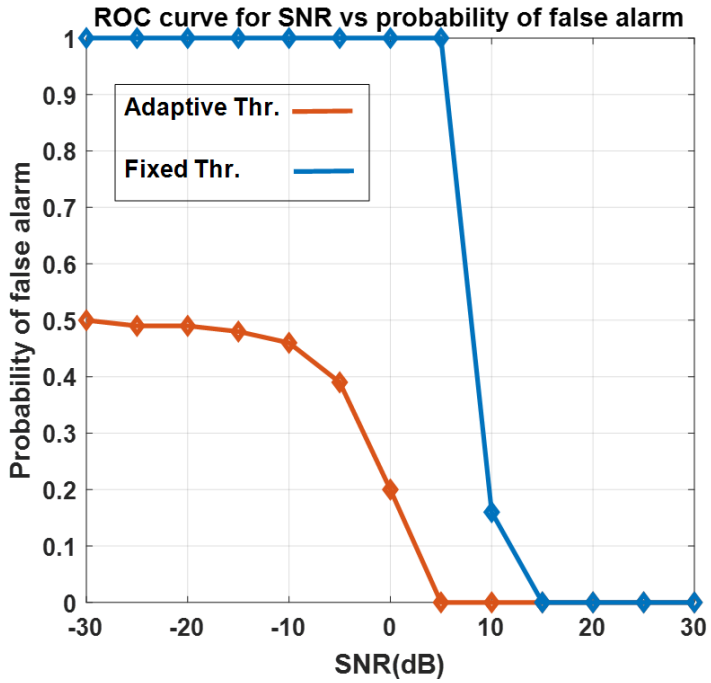

Figure (3.28) P_{fa} vs SNR for fixed and first adaptive threshold (burst traffic mode)

According to the ROC curve using adaptive threshold, the $P_m$is high at SNR = -30dB and zero at SNR = 0dB as shown in figure (3.29).

By comparing the results, the fixed threshold seems to be better than the adaptive threshold. This is not the case in reality, as the previous figure shows that the P_{fa} was 100% at SNR values from -30dB to 5dB.

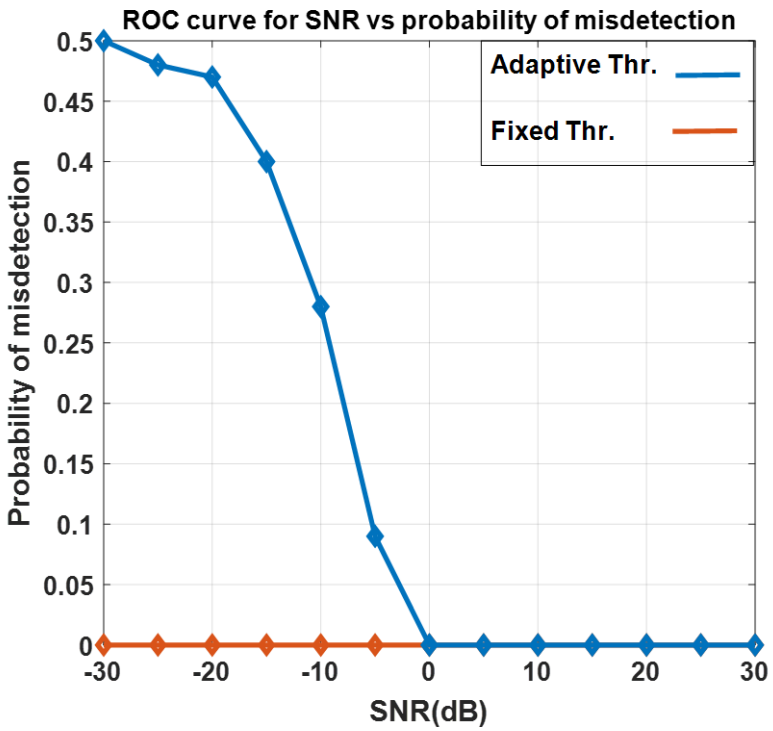

Figure (3.29) P_m vs SNR for fixed and first adaptive threshold (burst traffic mode)

The fixed threshold results shown in figure (3.30) illustrate the P_{te} versus SNR. The results show the highest P_{te} at low SNR values, which is the worst case, and then it starts to decrease until it reaches zero at SNR = 15dB. At SNR values of between 15dB and 30dB, the performance of the ED works better. For the adaptive threshold, the results show the highest P_{te} at the lower SNR values and then start to decrease until it reaches zero at SNR = 5dB. At SNR values of between 5dB and 30dB, the performance of the ED is better. The results show that adaptive threshold performance is a more efficient approach than a fixed threshold approach.

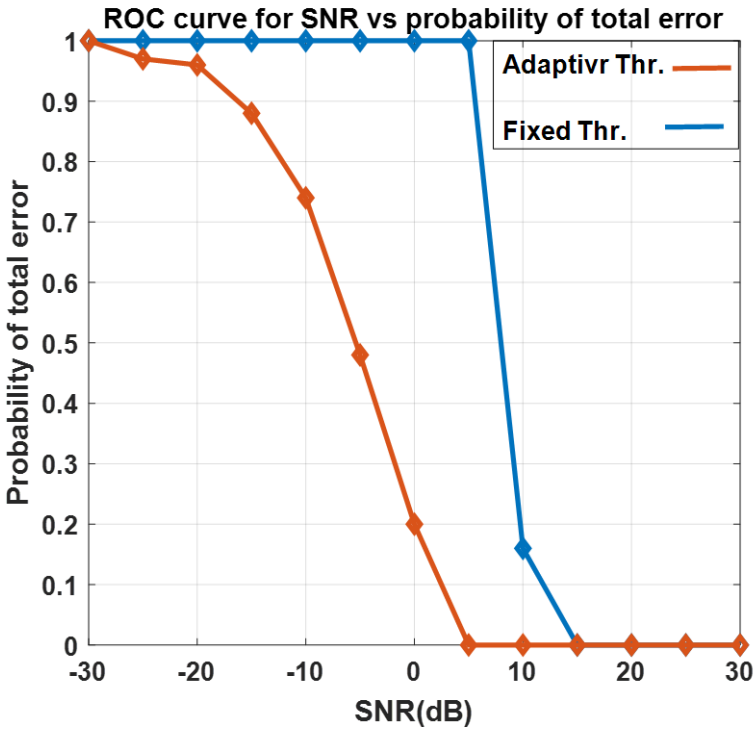

Figure (3.30) P_{te} vs SNR for fixed and first adaptive threshold (burst traffic mode)

3.6.2 Second and Third Adaptive Thresholds Simulation Results (The Power of Received Signals is Unequal)

This sub-section presents the simulation results for the second and third adaptive thresholds (when the power of all received signals is unequal -general case) for the ED algorithm. The comparison between the performance of each threshold in both scenarios (semi-deterministic and burst traffic mode) is also introduced.

3.6.2.1 First Scenario (Semi-Deterministic Traffic Mode)-General Case

This sub-section presents the results for the performance of the second and third suggested adaptive thresholds where the semi-deterministic mode is adopted for the PUs.

Figure (3.31) illustrates the relationship between the P_d and the SNR.

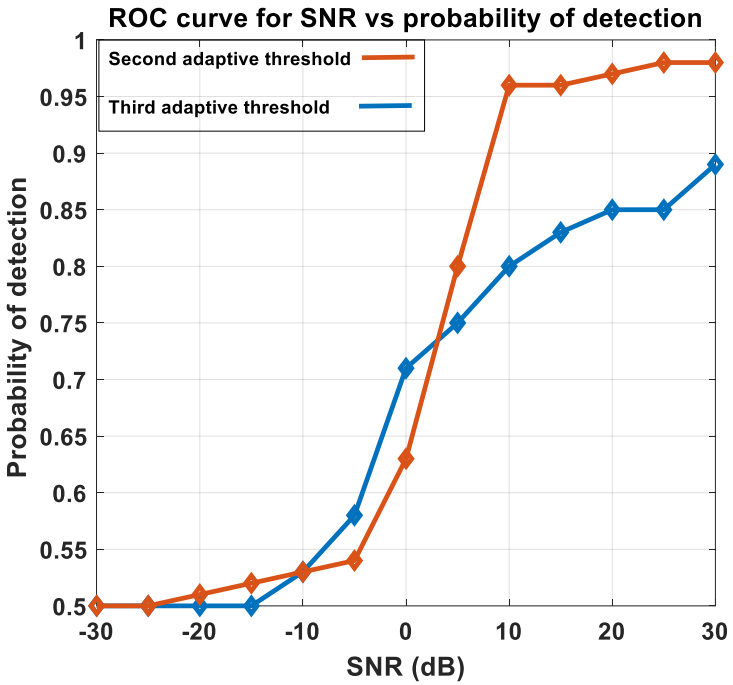

Figure (3.31) P_d vs SNR for 2nd. and 3th. Suggested adaptive threshold (semi-deterministic traffic mode)

According to the results shown, the performance of the second adaptive threshold, which was calculated according to equation (3.16), outperformed the third adaptive threshold, calculated according to equation (3.17). In the second adaptive threshold, the results show that the curve doesn't reach 100% at high SNR values. This is because the power of all received signals is unequal and, thus, part of the received power may have very little value. This means it will be within the noise.

In figure (3.31), the performance of the third adaptive threshold is less efficient than the second threshold. For the second and third thresholds, the SNR wall is located at 5dB.

The P_{fa} is shown in figure (3.32), which announces that the spectrum is busy by PU in case the spectrum is actually empty.

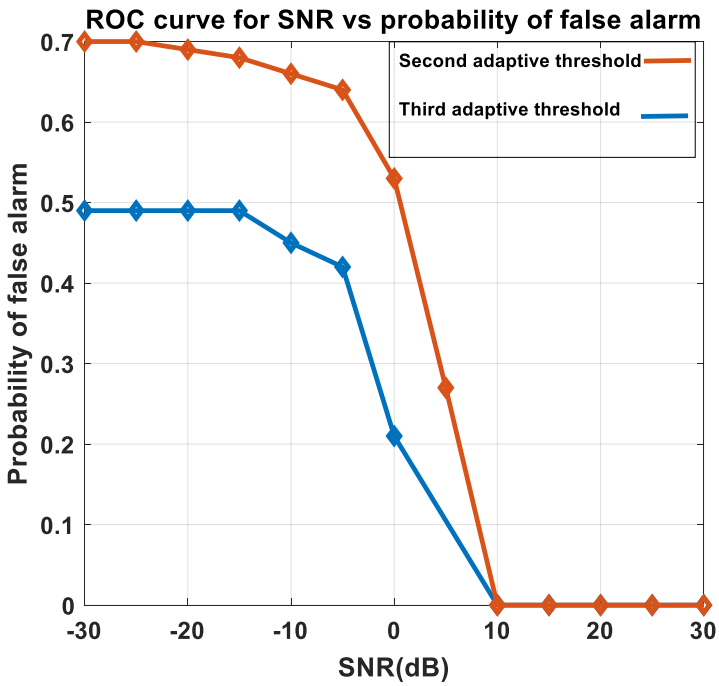

Figure (3.32) P_{fa} vs SNR for 2nd. and 3th. Suggested adaptive threshold (semi-deterministic traffic mode)

The results show that P_{fa} is high at the second adaptive threshold, and this leads to a loss in the use and exploitation of the spectrum compared to the performance of the third adaptive threshold. The performance of both thresholds at SNR values from 10dB to 30dB is more efficient.

Figure (3.33) illustrates the P_m. It means that the sensor's decision about the PU signal is absent while it is present. In this case, if the spectrum is used, it will lead to interference between the PUs and SUs. Results show that the performance of the third adaptive threshold is deteriorating even if the SNR is high. The second adaptive threshold is better than the third adaptive at SNR values from 5dB to 30dB.

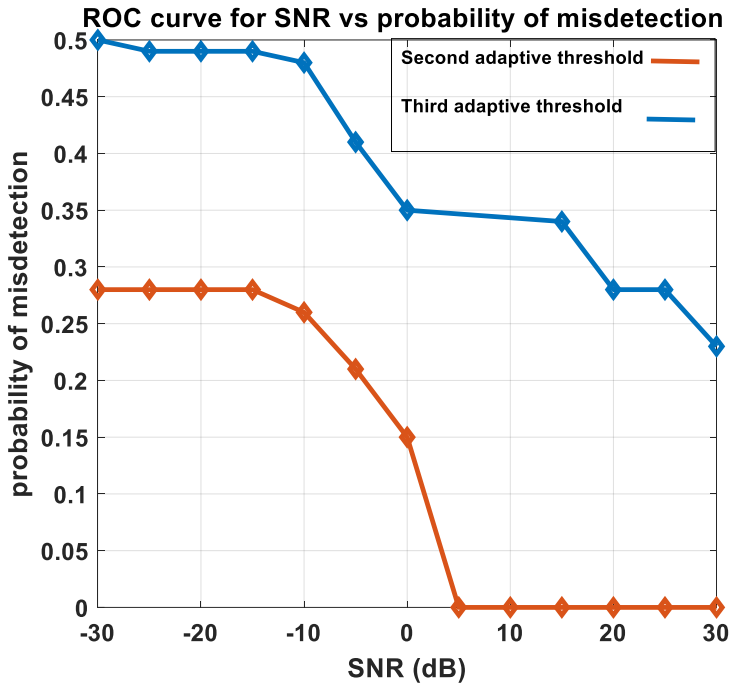

Figure (3.33) P_m vs SNR for 2nd. and 3th. Suggested adaptive threshold (semi-deterministic traffic mode)

The P_{te} is shown in figure (3.34). The second adaptive threshold result shows that the P_{te} is high at lower SNR values. It then starts to decrease until it reaches zero at SNR = 10dB, and after this value, the performance of this threshold gets better and improves.

For the sake of comparison between the second and third adaptive thresholds, the second method is better.

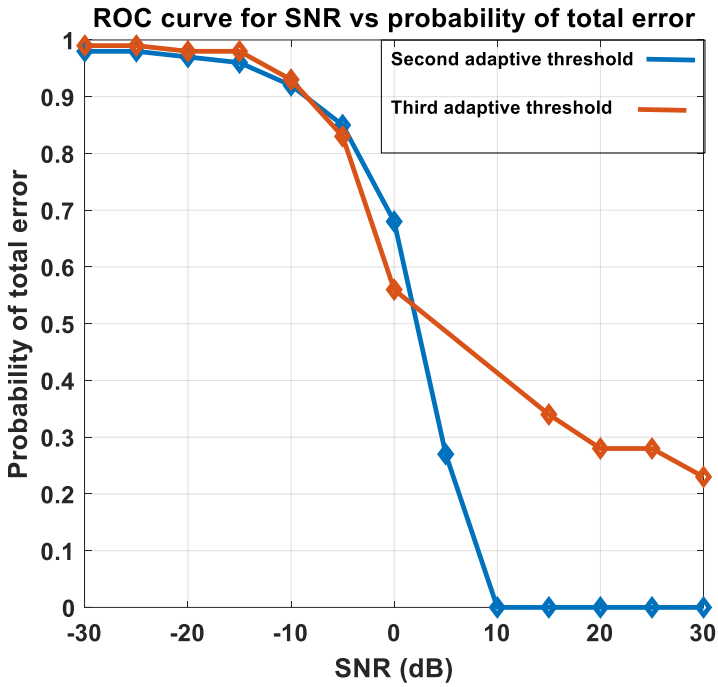

Figure (3.34) P_{te} vs SNR for 2nd and 3rd. Suggested adaptive threshold (semi-deterministic traffic mode)

3.6.2.2 Second Scenario (Burst Traffic Mode)-General Case

In this sub-section, the performance of the second and third suggested adaptive thresholds is assessed where the burst traffic mode is adopted for the PUs. The relationship between P_d and SNR is shown in figure (3.35), which shows the comparison between both adaptive thresholds. The results show that the third threshold outperforms the second threshold. For the second and third thresholds, the SNR wall is located at 5dB and -5dB, respectively.

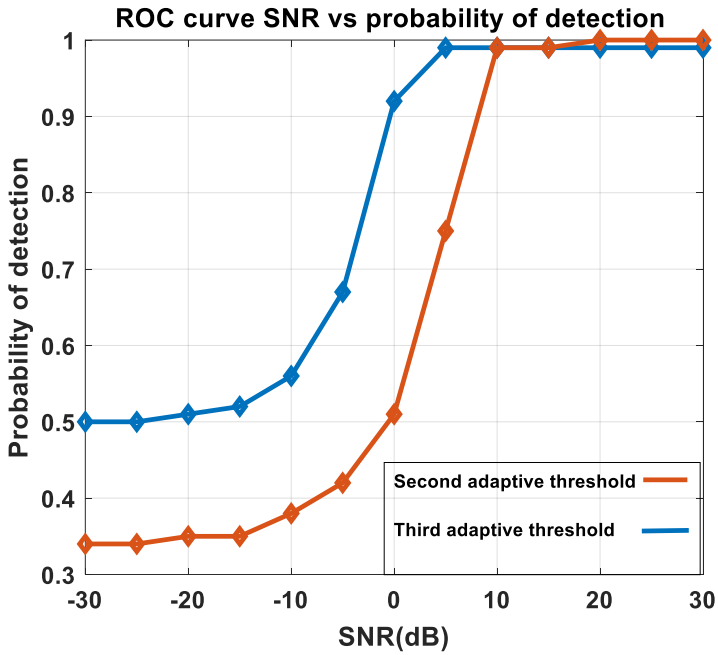

Figure (3.35) P_d vs SNR for 2nd. and 3th. Suggested adaptive threshold (burst traffic mode)

In this scenario, it is clear that the second and third proposed adaptive threshold performs better than the first scenario where the P_d is closer to 100% when the value of SNR is high. This is because, in the burst traffic mode, there will be little interference between channels. In the semi-deterministic traffic mode, the probability of interference between channels will be high.

Figure (3.36) illustrates the ROC curve for P_{fa} versus SNR. For the second adaptive threshold ROC curve, P_{fa} is high at the lower SNR values and starts to decrease until it reaches zero at SNR = 10dB.

The results of the third adaptive threshold show that when the SNR is between values of 0dB and 30dB, the performance of the ED is better. By comparing the results in terms of P_{fa}, the performance of the third threshold is better.

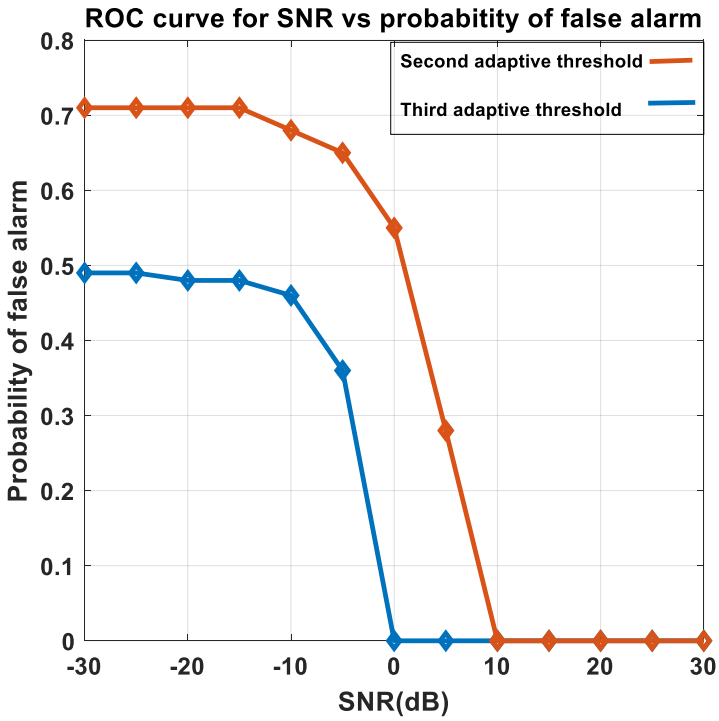

Figure (3.36) P_{fa} vs SNR for 2nd. and 3th. Suggested adaptive threshold (burst traffic mode)

In figure (3.37), for the second adaptive threshold, the ROC curve for the P_m is depicted in the graph. The probability of misdetection is high at SNR = -30dB and zero at SNR = -5dB. At SNR between values of -5dB and 30dB, the performance of the second adaptive threshold is better.

In figure (3.37), the performance of the third adaptive threshold for P_m is very bad at low SNR values when compared to the second threshold. The performance of the third adaptive threshold becomes more efficient at SNR = 0dB and beyond. In addition, the second adaptive threshold is better in terms of P_m than the third.

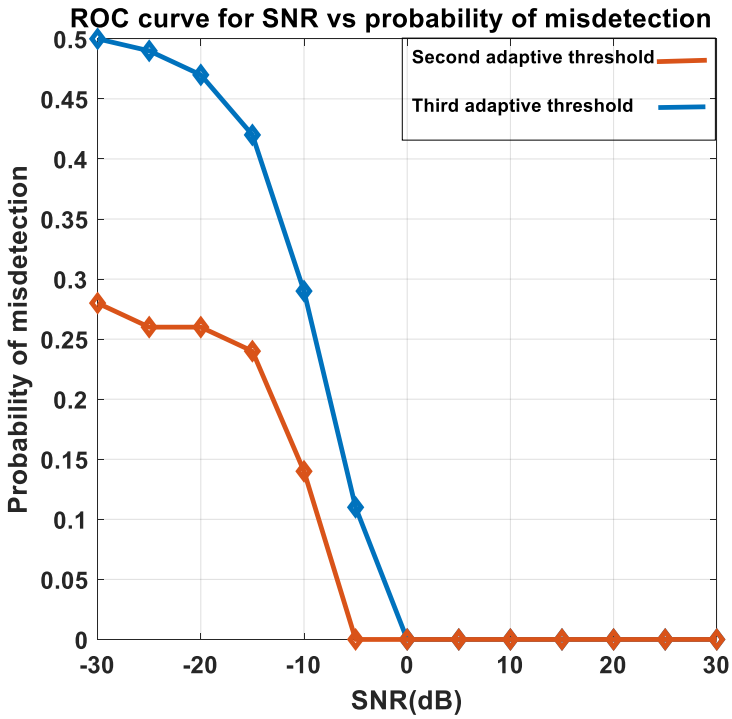

Figure (3.37) P_m vs SNR for 2nd. and 3th. Suggested adaptive threshold (burst traffic mode)

Figure (3.38) illustrates the P_{te} versus SNR for the second adaptive threshold results. The results show the highest P_{te} at lower SNR, which is the worst case, and then decrease until it reaches zero at SNR = 10dB. At SNR values of between 10dB and 30dB, the threshold performance is better. The third adaptive threshold results show the highest P_{te} at low SNR values and then decrease until it reaches zero at SNR = 0dB. The threshold's performance is best when the SNR is between 0dB and 30dB. The results show that the third adaptive threshold performance for P_{te} is more efficient than the second threshold.

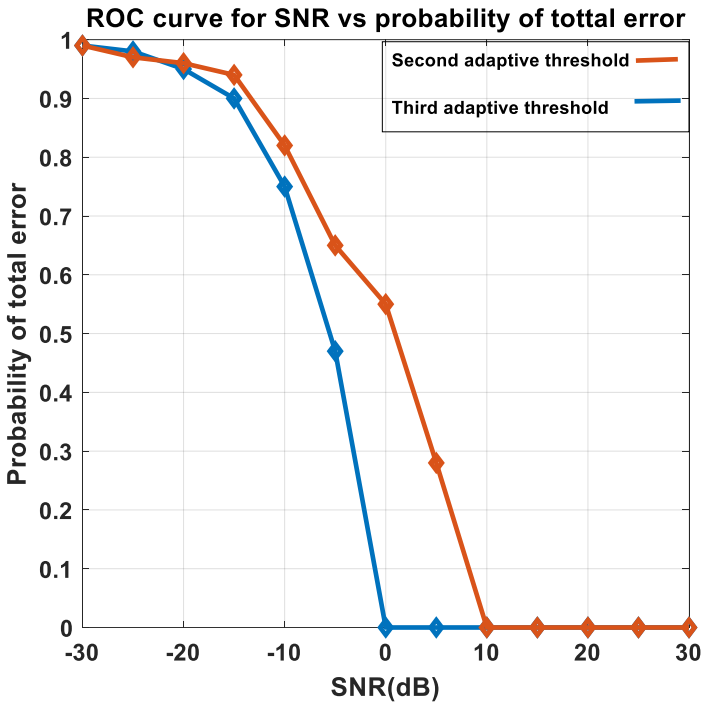

Figure (3.38) P_{te} vs SNR for 2nd. and 3th. Suggested adaptive threshold (burst traffic mode)

3.6.2.3 Performance Comparison of First Method with Some Relevant Works

Table (3.5) illustrates the performance comparison between the first proposed in this thesis and some relevant works in terms of algorithm type, P_d , and P_{fa}.

Table (3.5) Comparison the performance of the first proposed in this thesis to some relevant works.

Reference	Used algorithm type	Main remarks	SNR range (dB)	P_d		P_{fa}	
[6]	RDM	The comparison is made with the wireless microphone signal with a sample size = 2 and L=smoothing factor.	-30 to 10	SNR = -30	0.98	SNR = -30	0.1
				SNR = 0	1	SNR = 0	0.1
[8]	• MME • EME • cyclostationary	The comparison is made with the cyclostationary, which provided the best performance. When using the 8PSK signal as PU and NS=512, FFT=2048.	-18 to 0	SNR = -18	0.15	SNR= -18	0.08
				SNR= -6	1	SNR= -6	0.08
[9]	• Matched filter • ED • cyclostationary	When information is available about the PU signal, the MF technique is applied. If no information is available about the PU, the ED and Eigenvalue are applied.	-20 to 30	SNR= -14	0.3	SNR= -14	0.1
				SNR= -14	0.3	SNR= -14	0.1
[10]	ED	This algorithm is dependent on the adaptive threshold; when the spectrum utilization is P (H1) = 0.5, it means that SUs are using half of the available channels.	-25 to -10	SNR= -25	0.55	SNR= -25	----
				SNR= -10	1	SNR= -10	----
Proposed thesis designs	ED	The adaptive threshold was set based on the average of the total energy of the signal that was being received.	-30 to 30	SNR= 0	0.77	SNR = 0	0.2
				SNR= 30	1	SNR =30	0

CHAPTER FOUR
PRACTICAL IMPLEMENTATION OF ENERGY DETECTION ALGORITHMS USING SOFTWARE-DEFINED RADIO

4.1 Introduction

This chapter presents the general concept and basic structure of SDR, the most important features and challenges of this radio, as well as an explanation of one of the USRP hardware products of SDR. Also in this chapter, practical implementation of the proposed SS system is performed using USRP with the help of the LabVIEW NXG simulator.

4.2 Software-Defined Radios Fundamentals

Over the last several decades, telecommunications have been constantly evolving. The usage of digital technology is one of the most important technological advances. Digital communication technologies have proven their efficiency and introduced a new component in the signal transmitting and receiving chain, the digital processor. The flexibility of a programmable system is provided by this device to modern radio equipment. A communication system's behavior may now be changed easily by modifying its software. This resulted in the development of a new radio model known as SDR. In this new architecture, the responsibility of configuring radio behavior is delegated to software, leaving just the RF front-end implementation to the hardware. As a result, the radio is no longer a static unit defined by its circuits but rather a dynamic device capable of changing its operational properties, like modulation, bandwidth, coding rate, etc. [53].

SDR was proposed by Joseph Mitola. SDR replaces traditional hardware components with software modules for programmability [54].

The term SDR is defined as *"radio in which the radio frequency (RF) operating parameters including, but not limited to, frequency range, modulation type, or output power can be set or altered by software, and/or the technique by which this is achieved"*. In collaboration with IEEE working group P1900.1, the SDR Forum, currently known as the Wireless Innovation Forum, has created a definition of SDR: *"Radio in which some or all of the physical layer functions are software-defined"* [55].

The main backbone of CR systems is SDR technology. This radio may be dynamically changed to provide flexible communication across a broad range of communication protocols. The SDR device is a programmable terminal that is software-based and designed using programmable components like Field-Programmable Gate Arrays (FPGAs), smart antennas, Digital Signal Processors (DSP), reconfigurable amplifiers, accurate and band. Advanced (Analogue-to-Digital Converter / Digital-to-Analogue Converter) ADC/DAC, multiband RF circuits, and other programmable components [56].

4.2.1 SDR Main Functions

1- Wireless data transfers have been supported by SDR across a variety of frequency spectrums utilized by various wireless access systems, like the ISM band, TV band, and cellular

2- Multistandard support: Different standards have been supported by SDR like Wideband Code Division Multiple Access (WCDMA), Worldwide Interoperability for Microwave Access (WiMAX), Global System for Mobile (GSM), WiFi, and Code Division Multiple Access (CDMA) 2000. Moreover, different air interfaces within the same standard like IEEE 802.11a, 802.11b, 802.11g, or 802.11n in the WiFi standard can be supported by SDR.

3- Multiservice support: Multiple types of services have been supported by SDR, like broadband wireless Internet access or cellular telephony.

4- Multichannel support: SDR has been able to operate on many frequency bands at the same time (i.e. transmit and receive) [35].

4.2.2 Architecture Overview of the Software Defined Radio

A typical SDR transceiver consists of the following components: antenna, analog RF front end, digital front end, and signal processing as illustrated in Figures 4.1 (a) and (b).

1- **Antenna:** SDR platforms usually employ several antennas to cover a wide range of frequency bands. Antennas are often described as "smart" or "intelligent" because of their capacity to choose a frequency range and interference cancellation or their ability to adapt to mobile tracking.

2- **RF Front End**: RF circuitry is used for transmitting and receiving signals at different frequencies. Switching signals to and from the Intermediate Frequency (IF) is another function of the RF circuitry. Based on the direction of the signal (i.e., Tx or Rx), the operation will be divided into two sections:

   - During the transmission route, the DAC converts digital samples into analog signals, which are then sent to the RF Front End. This analog signal is combined with a predetermined RF frequency, modulated, and sent.
   - In the receiving route, the antenna receives the RF signal. To ensure optimal signal power transmission, the antenna input is connected to the RF Front End through matching circuitry. It then goes via a Low Noise Amplifier (LNA), which is located near the antenna, to amplify poor signals and reduce noise. This amplified signal is fed into the mixer, with a signal from the Local Oscillator (LO), to be down-converted to the IF.

3- **Analog-to-Digital and Digital-to-Analog Conversion:** As indicated in the preceding section, the DAC is responsible for generating the analog signal that will be transferred from the digital samples. The ADC is

located on the receiver side and is an important component in radio receivers. The ADC converts a continuous-time signal into a discrete-time signal.

4- **Digital Front End:** The digital front end of an SDR transceiver performs the following tasks:
   - On the transmitting side, the Digital Up Converter (DUC) converts the above-mentioned baseband signal to IF (Figure 4.1 (a)). The digital IF samples are then converted to an analog IF signal by the DAC connected to the DUC. After that, the analog IF signal is converted to RF frequencies by the RF up-converter.
   - The ADC transforms the IF signal into digital samples on the receiving side (Figure 4.1(b)). These samples are then passed into the Digital Down Converter (DDC). The DDC consists of a numerically controlled oscillator and a digital mixer. The baseband digital signal is extracted from the ADC by DDC and sent to a high-speed digital signal processing block after being processed by the Digital Front End.
5- **Signal Processing:** This block performs signal processing actions such as modulation/demodulation, interleaving/deinterleaving, scrambling/descrambling, and encoding/decoding [57].

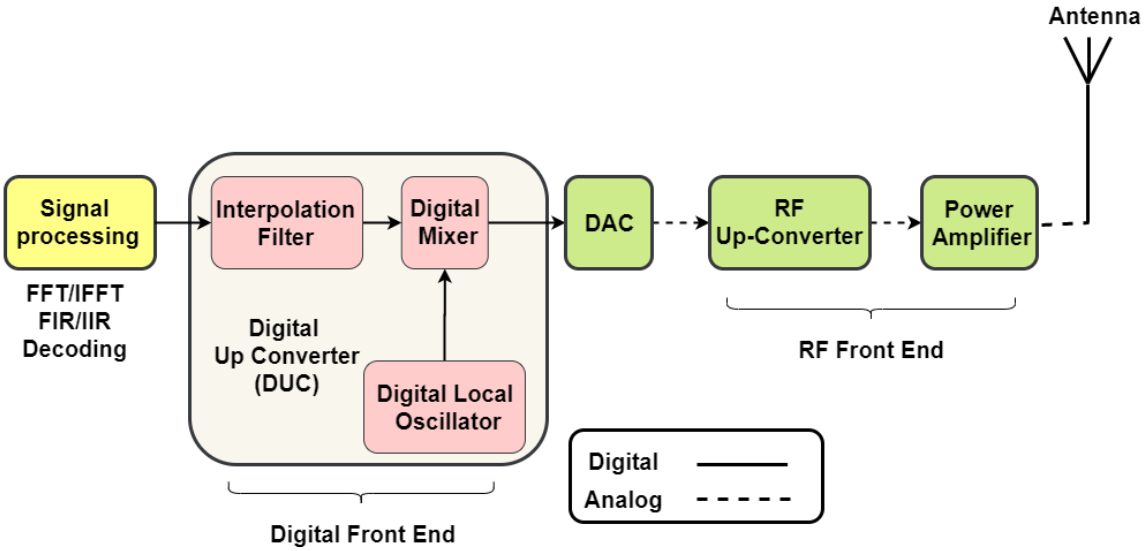

(a) Transmitter

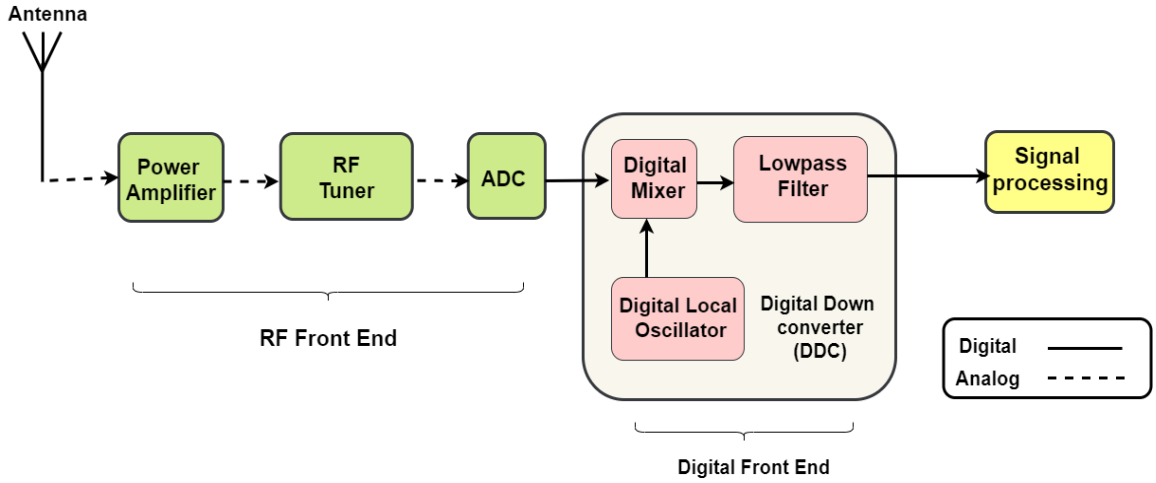

(b) Receiver

Figure (4.1) SDR architecture. Sub-figure (a) SDR transmitter block diagram, and sub-figure (b) SDR receiver block diagram [57].

4.2.3 SDR Benefits

1- Seamless ubiquitous communication; It is feasible by picking the wireless network that is best suited to the area and needs of the user.

2- Re-configurability; capable of changing all of its radio parameters in accordance with internal and external policies.

3- Interoperability; capable of exploring and communicating with many wireless networks.

4- Providing the necessary service quality while improving the service economy based on data rate and cost [56].

4.2.4 SDR Challenges

1- Cost: the biggest challenge to the spread of SDR use is cost. SDR is generally more complex than single-function radio systems, so it is more expensive.

2- High power consumption: the second challenge facing the SDR is the high power consumption of devices using this technology. There are two reasons that contribute to the power consumption of the SDR: the large bandwidth of these systems and the increased complexity of the DSP unit.

3- Complexity: another challenge facing the SDR is the additional complexity that this type of system requires. The complexity case has at least three components:

a- Increase the cost and time of implementation of SDR.

b- Complex specifications and requirements, where SDR is designed to support specific basic waveforms, also support some waveforms that are expected to emerge in the future.

c- Increase risk where there are at least two sources of risk to consider.

- Inability to complete designs on time and within budget due to the unpredictability of SDR project timelines.
- Inability to thoroughly test the radio in all of the supported and anticipated modes [58].

4.3 Universal Software Radio Peripheral

USRP is a product developed under the concept of SDR by Ettus Research, a subsidiary of National Instruments (NI) [59].

The USRP offers one-of-a-kind possibilities for research and development in the wireless sector. It allows for the creation of a communication system on a software level from the lower to the higher levels by enabling the user to select the data scheme, symbol rate, modulation, coding scheme, packet size, antenna configuration, frequency, and error correction scheme, etc. The

user defines all of these system parameters using the software. LabVIEW, MATrix LABoratory (MATLAB), GNU Radio, and other software platforms operate on a computer linked to the USRP through a Gigabit Ethernet (GigE) interface. These drivers translate computer code into machine language and make it accessible to the USRP through an Ethernet wire. When used as a transmitter, the USRP hardware is an interface that can take baseband signals and output an RF signal or vice versa when used as a receiver [60].

4.4 USRP X310 Device

The Ettus Research USRP X310 is a high-performance, scalable SDR platform for building and deploying next-generation wireless communications systems. The hardware architecture combines two extended-bandwidth daughterboard slots covering DC–6 GHz with up to 160 MHz of baseband bandwidth, multiple high-speed interface options (dual 10 GigE, dual 1 GigE, Peripheral Component Interconnect Express (PCIe)), and a large user-programmable Kintex-7 FPGA [61].

4.4.1 Key Features of the USRP X310

1- Kintex-7 XC7K410T FPGA from Xilinx
2- 16 bit 800 MS/s DAC
3- 14 bit 200 MS/s ADC
4- When used with an appropriate daughterboard, the frequency range is from DC to 6 GHz.
5- Up to 160MHz of bandwidth per channel is enabled.
6- Two slots for wide-bandwidth RF daughterboard.
7- Optional GPSDO.
8- Multiple high-speed interfaces (Dual 1G, Dual 10G, PCIe Express, Express Card) [62].

4.4.2 USRP Interfaces and Connectivity

In this sub-section, the interfaces and connectivity for the X310 are illustrated where the details of both the front and rear panels of the X310 are presented.

A- USRP X310 front panel

Figure (4.2) represents a detailed view of the front and back panels of the USRP X310. The front panel consists of:

1- JTAG: USB for the on-board USB-JTAG programmer.

2- RF A set.

- TX/RX LED: indicates that data is flowing on the TX/RX channel of daughterboard A.
- RX2 LED: indicates that data is flowing on the RX2 channel of daughterboard A.

3- REF: It refers to a locked external reference clock.

4- PPS: refers to a valid PPS signal with pulses once per second.

5- AUX I/O: Front panel GPIO connector.

6- GPS: refers to that GPS reference is locked.

7- LINK: refers to the computer being connected to the device.

8- RF B set.

- TX/RX LED: indicates that data is flowing on the TX/RX channel of daughterboard B.
- RX2 LED: indicates that data is flowing on the RX2 channel of daughterboard B.

9- PWR: Power switch [62].

(a)

(b)

Figure (4.2) USRP detailed view: (a) Front panel (b) Back panel.

B- USRP X310 back panel

The Rear Panel consists of:

1- PWR: Adapter for the power supply of the USRP-X Series.

2- 1G/10G ETH: SFP+ Ethernet interface ports

3- REF OUT: The exported reference clock's output port.

4- REF IN: Input for the reference clock.

5- PCIe x4: adapter for wired PCI express link.

6- PPS/TRIG OUT: The PPS signal's output port.

7- PPS/TRIG IN: The PPS signal's input port.

8- GPS: GPS antenna connection [62].

4.5 System Structure in Practical Implementation

The USRP offers a combination of NI’s software and hardware that provides the functionality and flexibility for physical layer design. All system settings, such as modulation scheme, data, frequency, antenna configuration, etc., are software-defined by the user. The software platform, such as GNU Radio, MATLAB, LabVIEW, etc., operates on a computer that is linked to the USRP through a GigE port or other interfaces. In this study, LabVIEW has been used to control the USRP X310 hardware, where the

USRP connects to the host Personal Computer (PC) through an Ethernet cable, as shown in Figure (4.3).

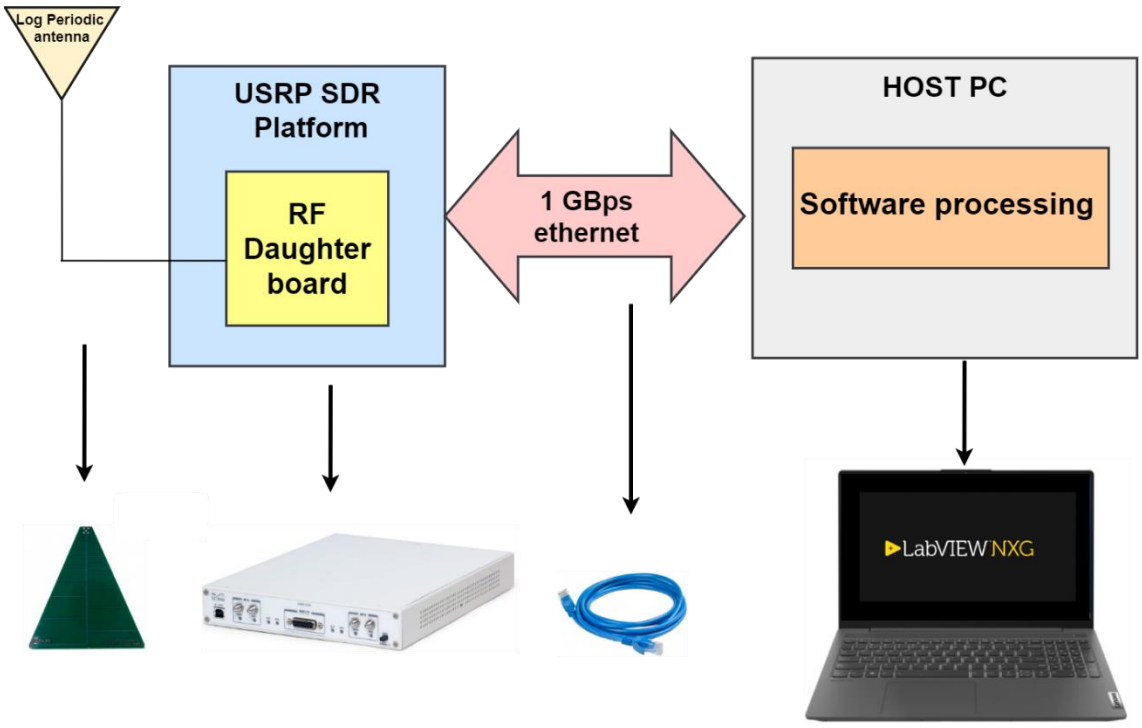

Figure (4.3) Practical implementation structure

This study used an Ettus USRP X310 radio, When USRP works as a transmitter, the main role of the URSP platform is to convert the digital baseband signal received from the computer via the 1 GigE port (the baseband In-phase and Quadrature components (IQ) signal samples) to an analog signal in the RF stage. This process is realized in two steps. The first step is converting the digital signal to the digital IF domain through the DUC this stage is achieved through the motherboard, which is the basis of the USRP platform. After that, the signal is processed on the daughter-board, which is responsible for transforming the digital IF signal to its analog form in the RF band (The daughter-boards are the physical radio front-ends); finally, the analog signal is mixed to the required carrier frequency, and then

the signal is radiated by the RF antenna. Figure 4.4 depicts the Motherboard and Daughterboard in the USRP X310.

When USRP works as a receiver, the analog signal is acquired from the selected RX port. The received RF signal is converted to IF, then converted to the baseband IQ signal. Finally, the baseband IQ signal is transmitted to the PC via a 1GigE port for further processing.

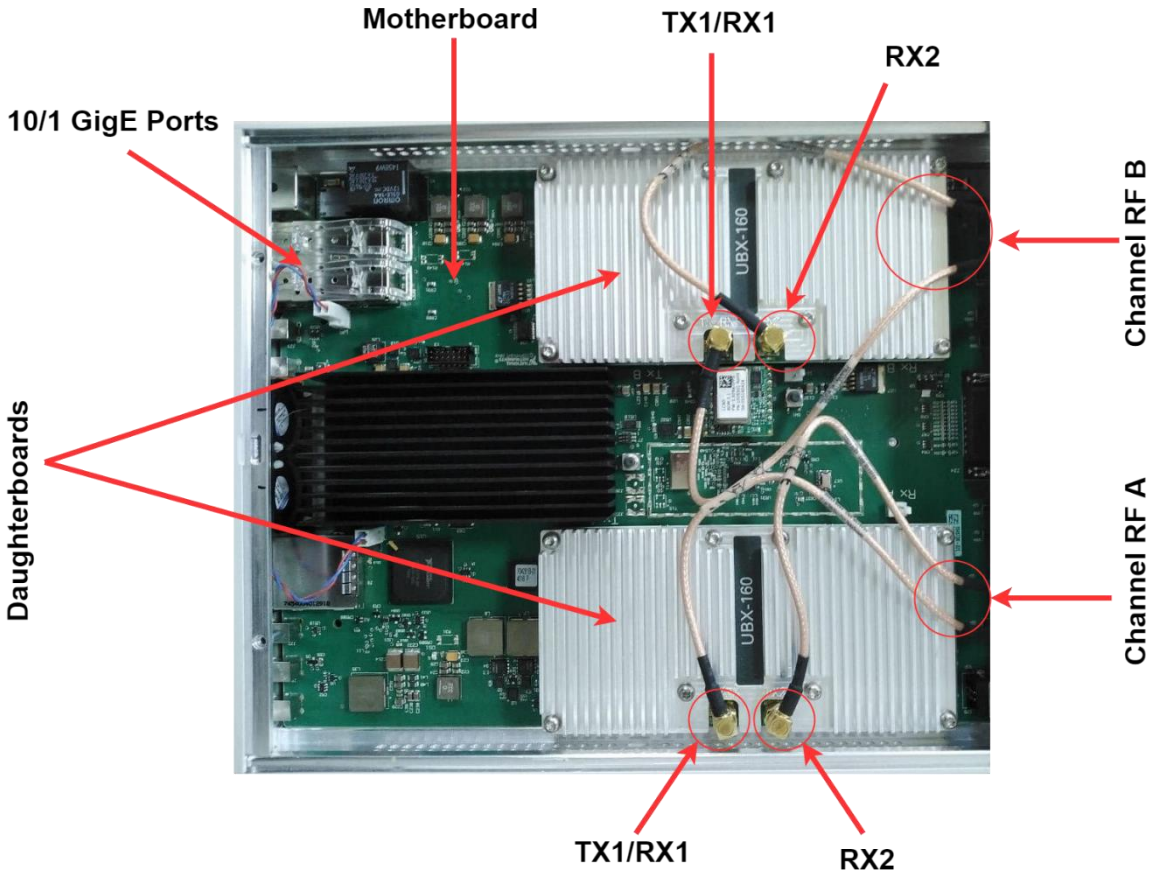

Figure (4.4) USRP X310 components

4.6 USRP Configuration in LabVIEW NXG

LabVIEW offers the concept of Virtual Instruments (VIs). In LabVIEW, every program appears as a VI. LabVIEW includes a block diagram and a front panel. The front panel of a VI has the same function as the actual instrument's front panel; designers can add inputs like connections, switches, numeric inputs, etc., in addition to indicators such as

graphs. The actual programming is done in the block diagram. When creating a designer interface element in the front panel, a corresponding icon is also created in the block diagram. The project is done by connecting the icons together to form a block diagram of the specific project. In addition, NI provides a large number of built-in functions and toolkits that may be used for a variety of applications and are highly efficient to use when programming, the basic control of USRP is simple through built-in functions available in LabVIEW, as shown in figure (4.5). This control can be divided into the following steps:

1- Configuration of the USRP parameters according to the designer's demands, like carrier frequency, gain, active antenna, IQ sampling rate, and so on.
2- Starting read (receiver) or write (transmitter) processes to receive or send data depending on the parameters chosen in the first step. Loops are often used in this stage to constantly receive or transmit.
3- The USRP connection must be closed when the transmitting and/or receiving has been completed.

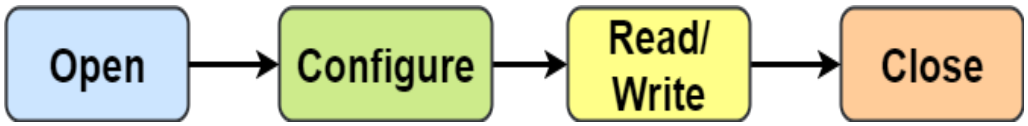

Figure (4.5) Basic steps of controlling USRP by LabVIEW NXG

In LabVIEW, there are eight built-in functions for controlling USRP, which are split into three groups according to the steps indicated above. Figure (4.6) depicts the eight most frequently utilized NI USRP functions. The five specified functions in the leftmost column are used to configure and start the USRP. The two functions in the middle read and write data from and to the USRP. At the end of the process, the functions in the right-most column are used to close the connection between the PC and the USRP.

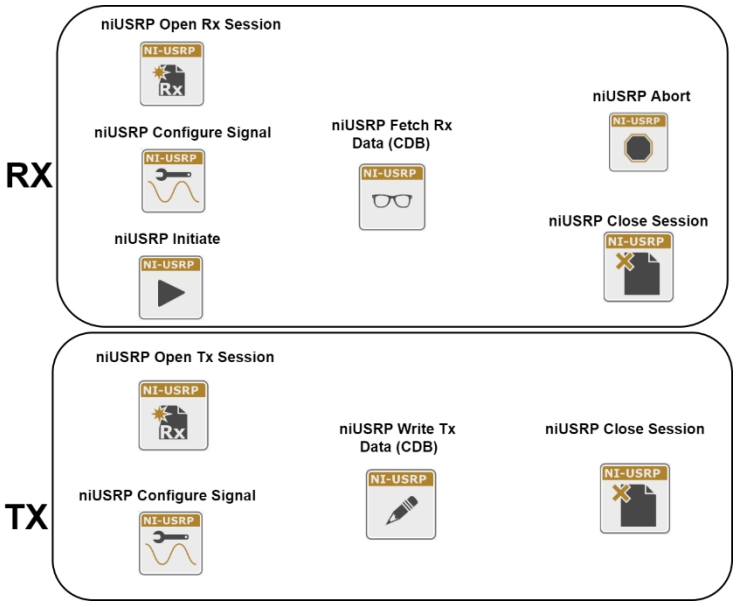

Figure (4.6) eight most frequently utilized NI USRP functions

4.7 Spectrum Sensing Algorithm Practical Implementation

This section shows how the proposed SS system is implemented in real-time, based on the first scenario when the traffic mode for the PU is semi-deterministic, (mentioned in chapter 3, sub-section 3.4.1)

The transmitted signals of the nine channels are modulated with QAM. These signals are transmitted and received to/from the communication channel via the same USRP chain. The center frequency of the transmitted signals is set at 915 MHz. Using the LabVIEW NXG software platform's graphical programming environment and the USRP X310, it is easy to make the transmitter and receiver chains. The implementation requires the following equipment:

1- Single USRP X310 SDR platform.
2- Personal Computer (Laptop).
3- Two Antennas (log-periodic operate from 850 MHz to 6500 MHz).
4- Spectrum Analyzer device.
5- GigE and Sub Miniature version A (SMA) cables.

4.7.1 Practical Implementation Procedures

In this study, practical implementation depends on the same specifications that were presented in the simulation part in chapter three. The following steps illustrate the practical implementation of the spectrum sensing system based on the energy detection algorithm.

1. In the first step, signals to be transmitted are prepared (QAM modulated signals), where the transmitted signals' data (on the transmission side) is written in a (TX) Tag (a Tag can store a single value of any data type that represents the state of a process), as shown in figure (4.7).

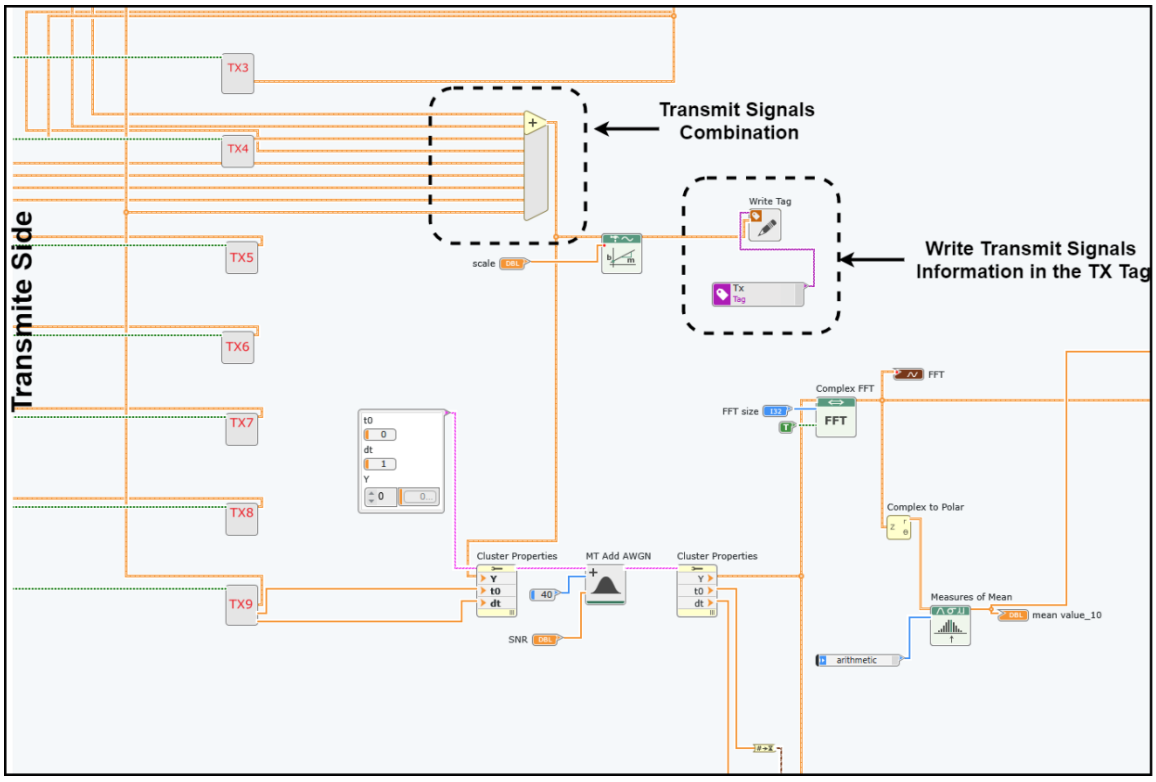

Figure (4.7) Transmit side block diagram

2. A new VI is created to prepare the signals for transmission to the USRP device. In this code, the IQ signals are read from the TX Tag, then the data is written to the specified channel using the (niUSRP write TX) node. The IQ signals are sent to the USRP via Ethernet. Figure (4.8) shows the preparation of transmission signals.

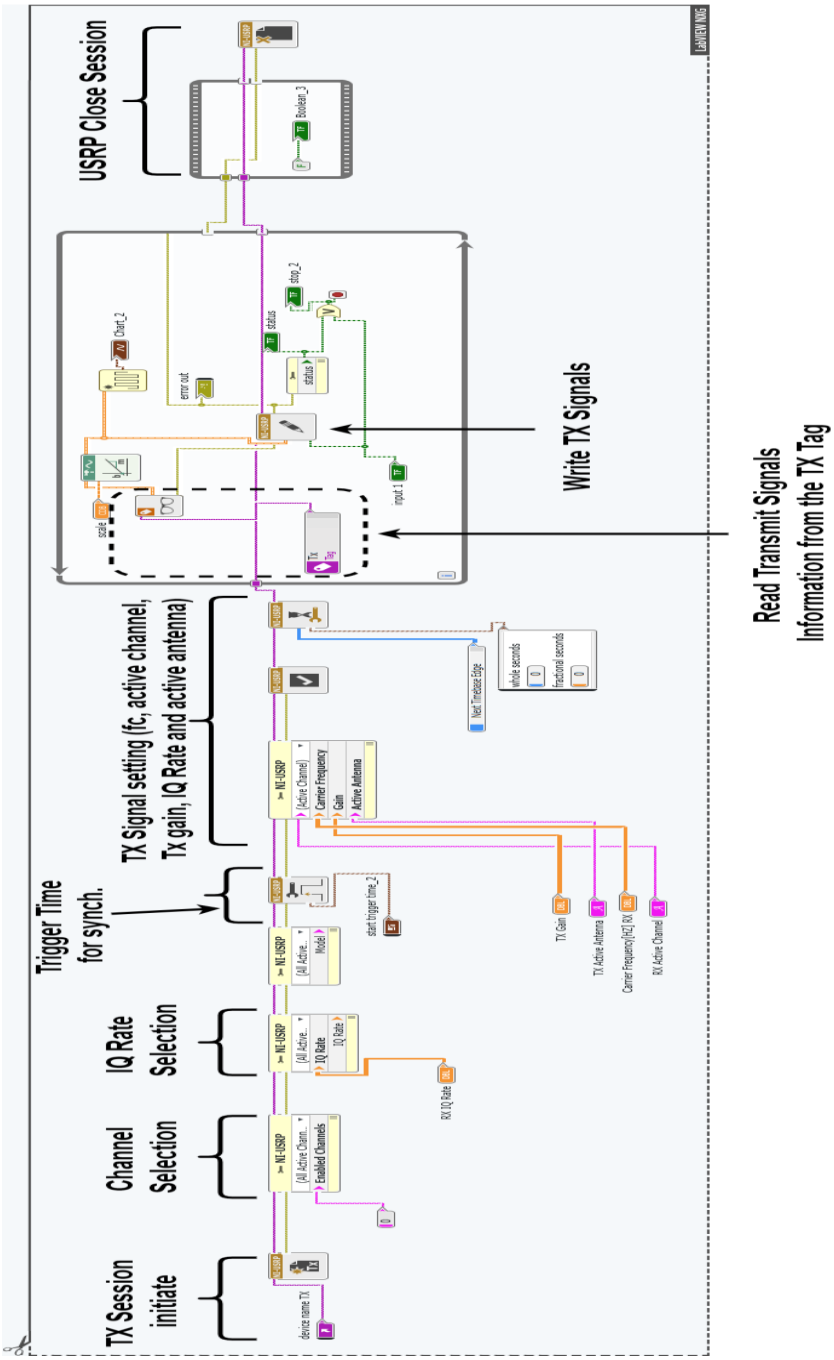

Figure (4.8) LabVIEW NXG transmission signals configuration diagram

3- Transmitting and receiving parameters are configured as in figure (4.9)

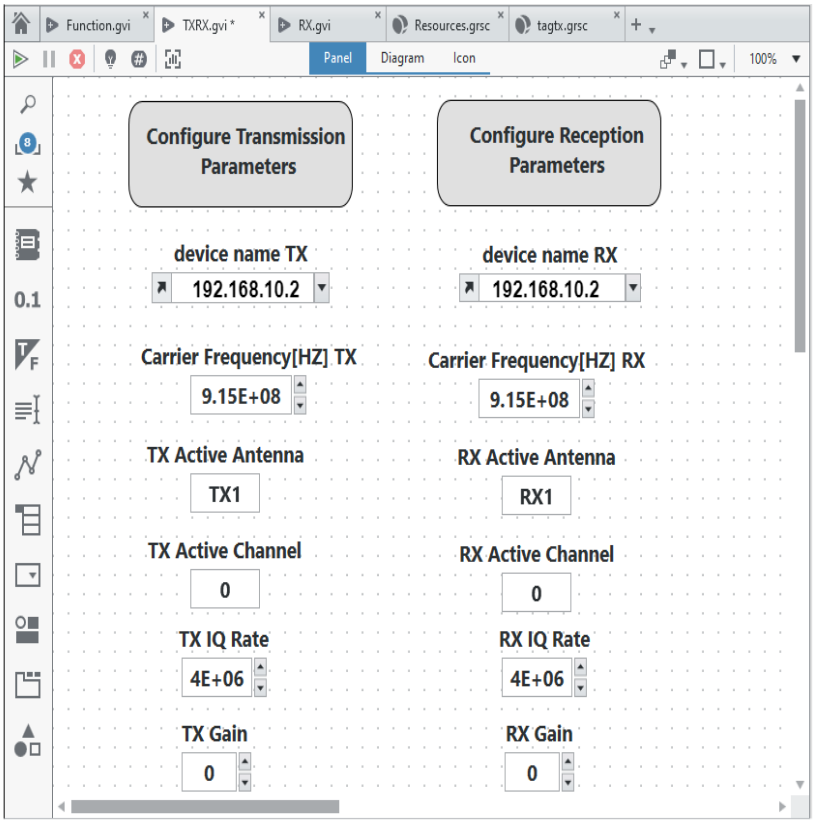

Figure (4.9) Setting parameters for USRP

4- The IQ signals are transmitted using a USRP device via the (TX1) channel and broadcast by the antenna.

5- The signals are received on the same USRP device via the (RX1) channel and then transferred to the computer via the Ethernet cable.

6- A new code is created to prepare the signals for receipt from the USRP. In this code, the received signals' data is written in the RX Tag as shown in figure (4.10).

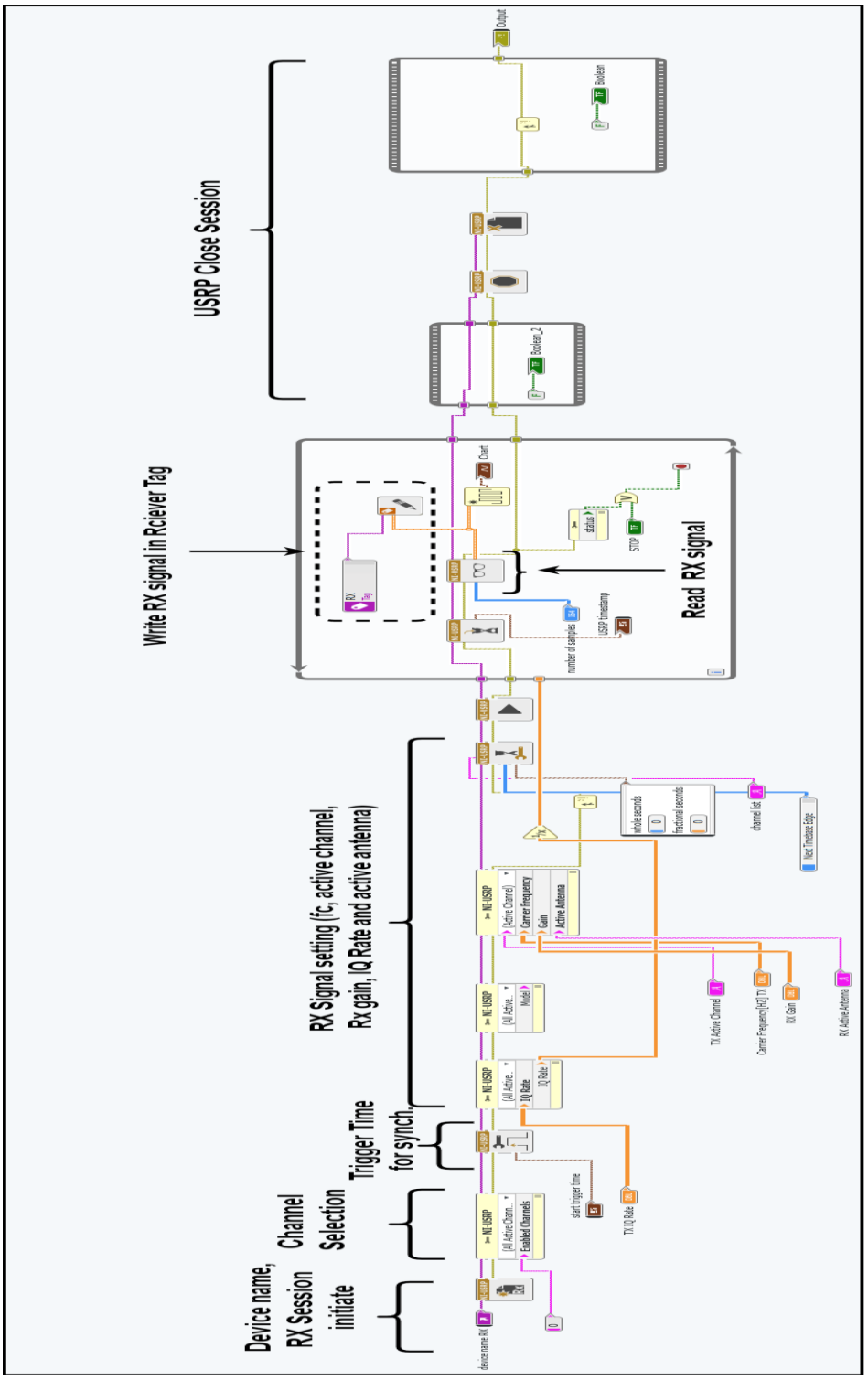

Figure (4.10) Configuration of receive signals in LabVIEW NXG

7- In the same project in LabVIEW, the last IV is created to present the entire receiving procedure by reading the received signals' data from the RX Tag. The ED algorithm is then implemented to sense the spectrum and detect the

presence or absence of the signals. Finally, the received and transmitted signals' data is stored in a text file to evaluate the performance of the algorithm as shown in figure (4.11). Using a code in MATLAB, the data is processed and the results are obtained.

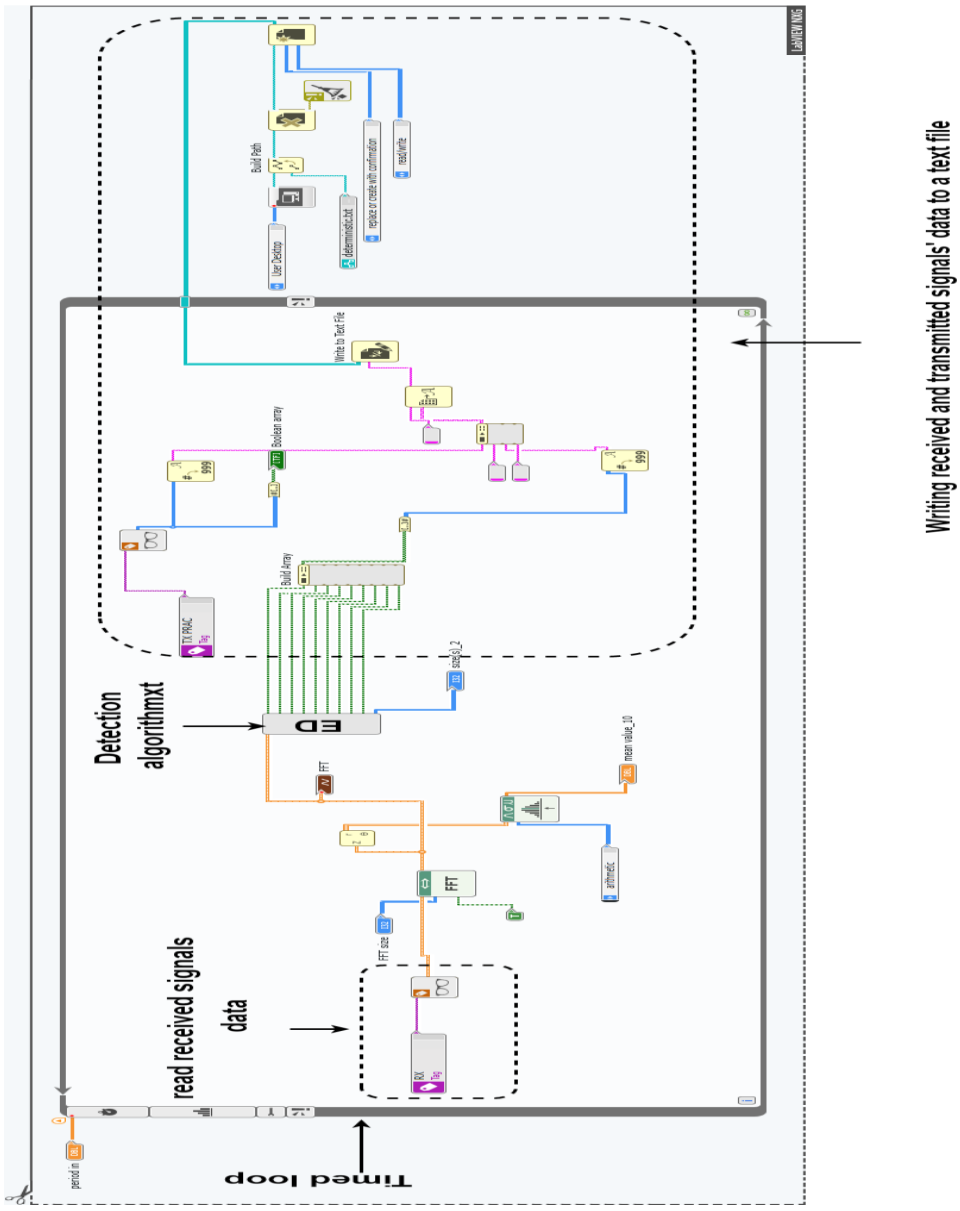

Figure (4.11) LabVIEW NXG diagram of the detection algorithm

Figure (4.12) shows the laboratory testbed setup of the real-time ED for the first scenario (semi-deterministic traffic mode of the PU signal). The PC is connected to the USRP (transceiver) using a 1 GigE cable with Registered Jack-45 (RJ-45) connectors as well as a Log-periodic antenna.

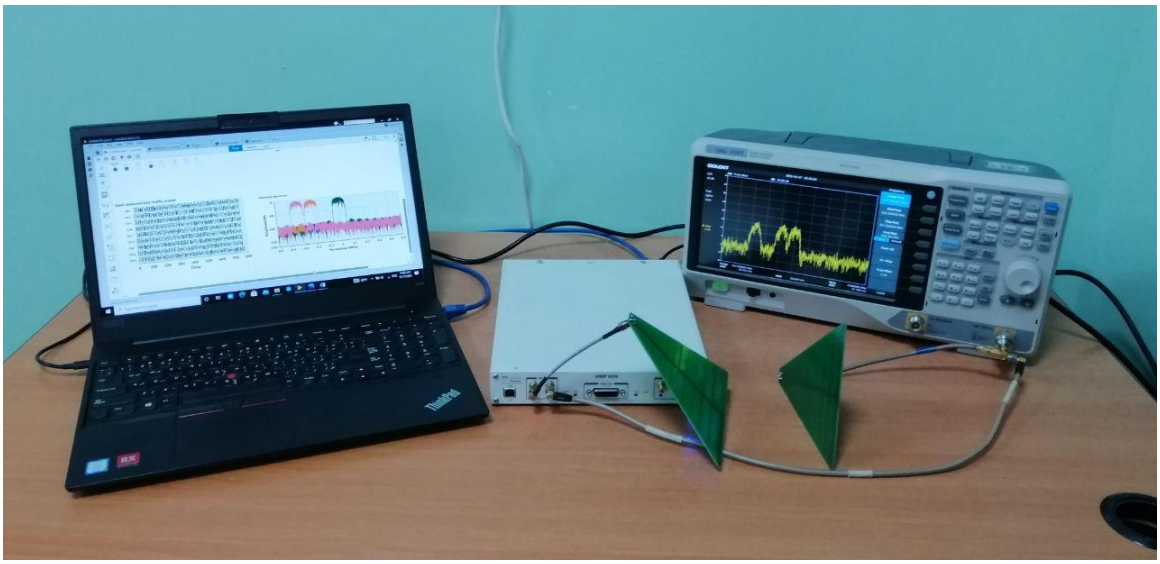

Figure (4.12) laboratory testbed for the first scenario (semi-deterministic traffic mode of the PU signal)

The effect of SNR on the signals' spectrum can be observed at 915MHz using a Siglent SSA3032X spectrum analyzer. Figure (4.13) shows the signals received at SNR = 30dB, where through the spectrum sensing process based on the ED algorithm, five busy channels were detected, as well as four idle channels that SUs exploit opportunistically. Figure (4.14) also shows the signal received at SNR = 20dB.

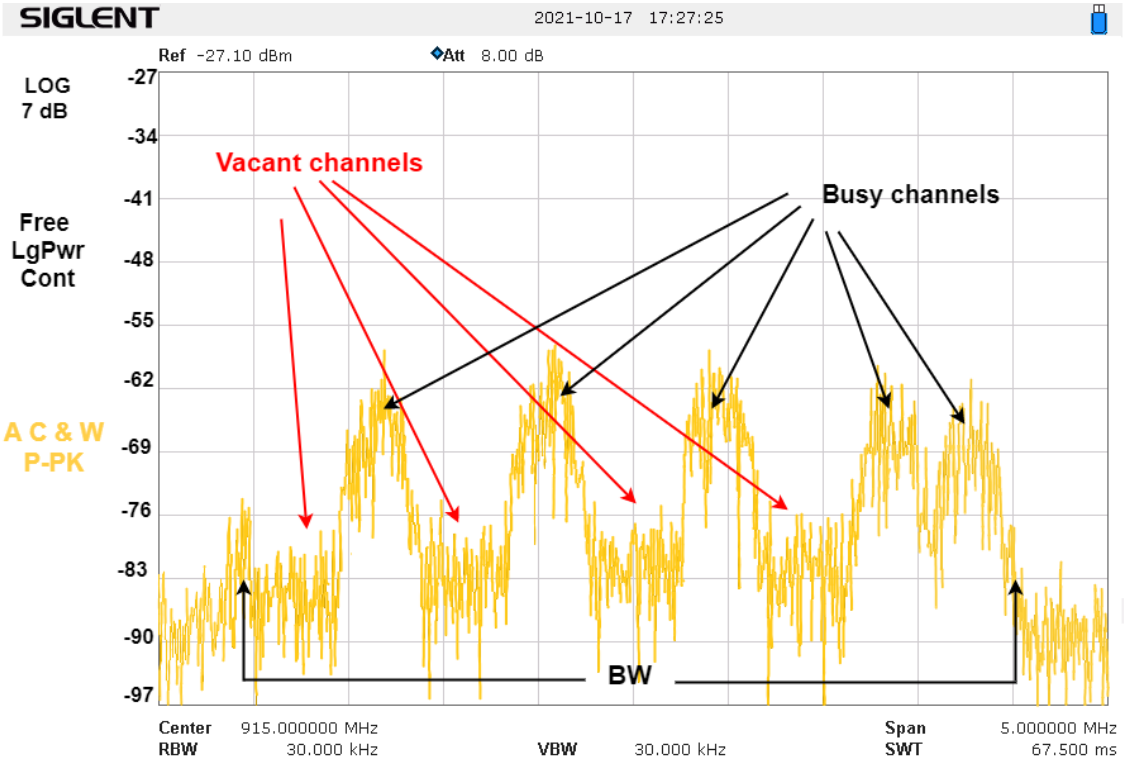

Figure (4.13) Spectrum of received signals at SNR = 30dB

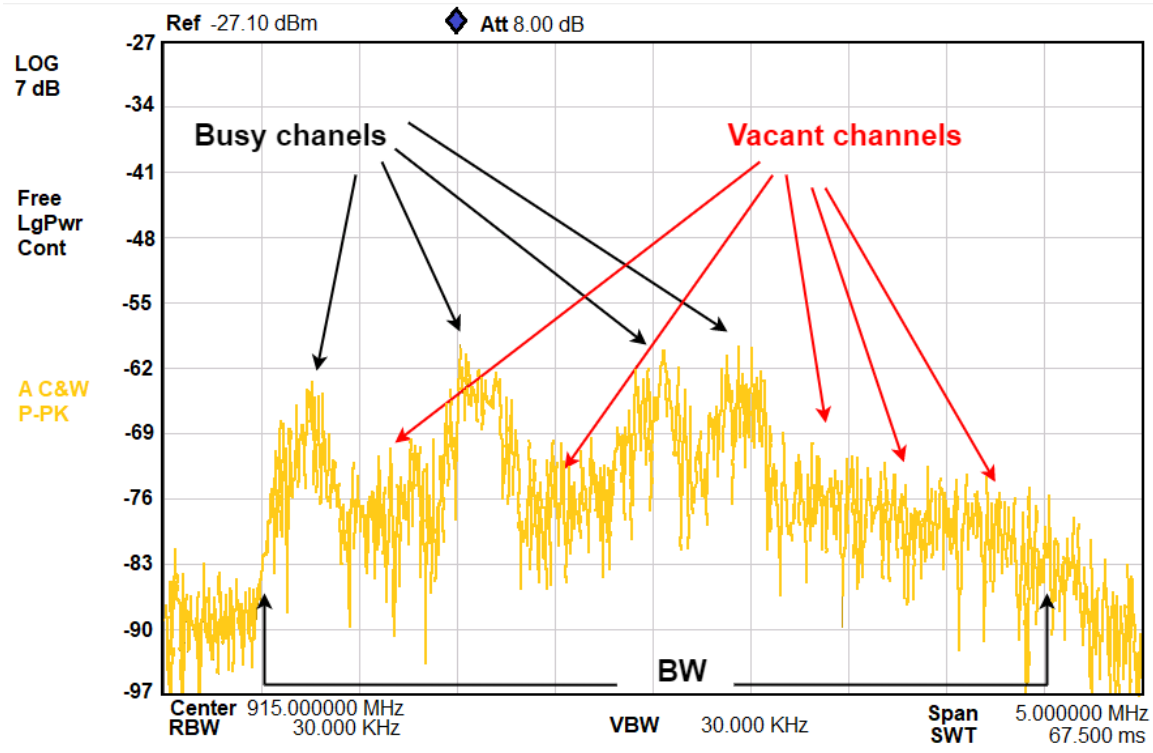

Figure (4.14) Spectrum of received signals at SNR = 20dB

Figure (4.15) illustrates a summary of the transmitting and receiving processes using the USRP device.

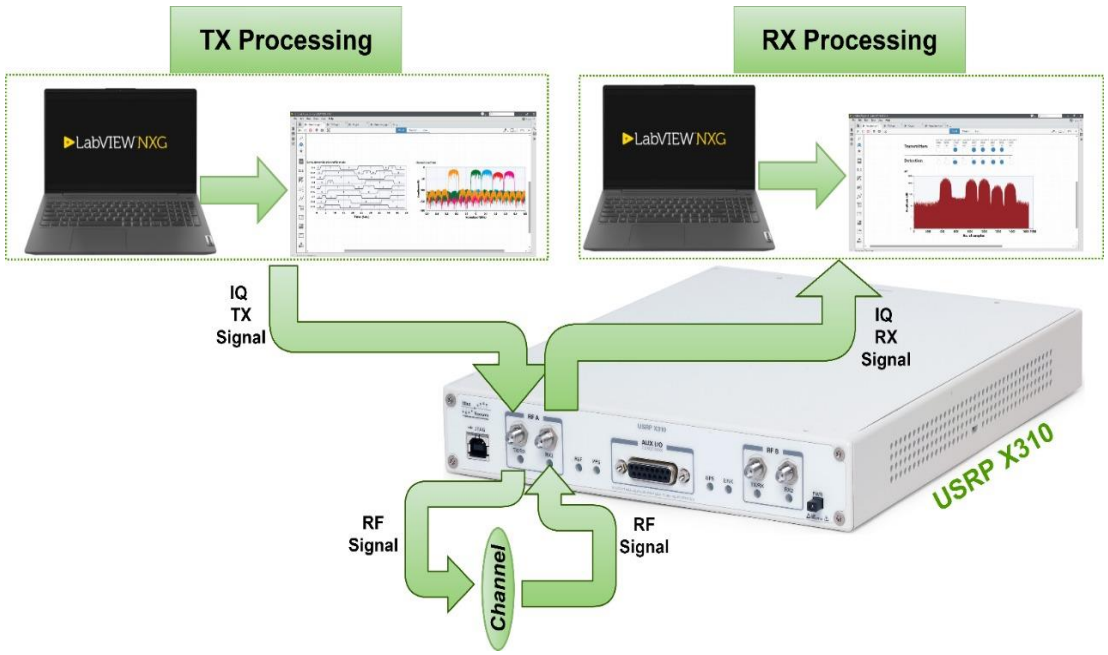

Figure (4.15) Transmit/Receive process summary for spectrum sensing.

4.7.2 Practical Results and Analysis

This sub-section describes the practical implementation of energy detector-based sensing using the USRP X310 and an average of 1000 realizations.

In this implementation, the effect of different SNR values on (P_d, P_{fa}, and P_m) have been tested, varying the SNR value from -30 dB to 30 dB with a step of 5dB. Each measurement result is the average value of 1000 measurement results for the same SNR value. The results of the first scenario of the three proposed adaptive thresholds techniques are presented.

4.7.2.1 First Proposed Adaptive Threshold (The Power of Received Signals is Equal)

In the first proposed adaptive threshold, the adaptive threshold was set based on the average of the total energy of the signal that was being received. Figure (4.16) illustrates the LabVIEW NXG simulation and USRP

implementation of the P_d versus SNR for the first scenario (the PUs traffic mode is semi-deterministic).

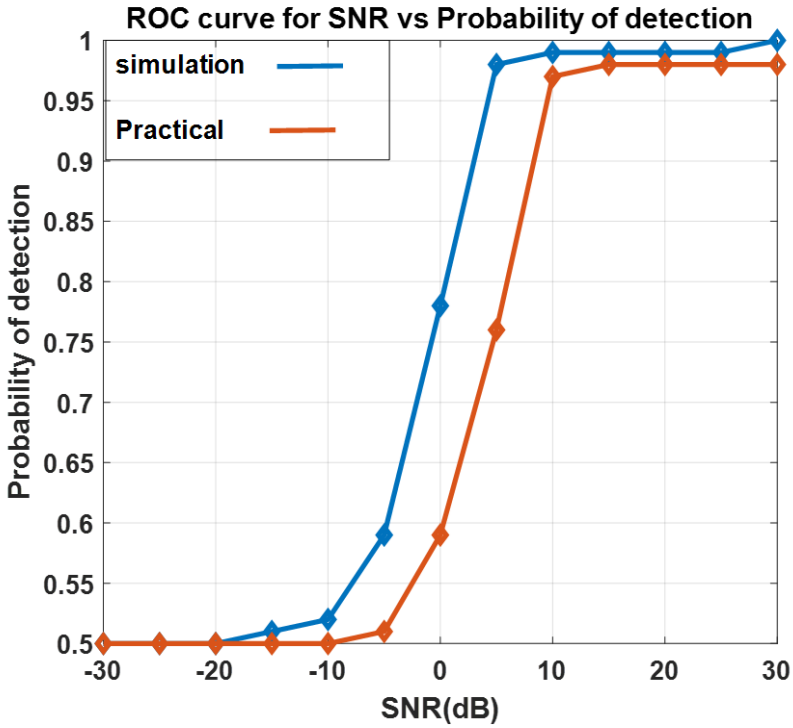

Figure (4.16) P_d vs SNR for the first adaptive threshold

By comparing Labview simulation and USRP implementation, there is a difference between them. This is a difference because the signal, when sent through the communication channel, suffers from distortion due to the many phenomena facing wireless signals, such as absorption, multipath, and scattering. In addition, thermal noise from the USRP hardware also contributed to this difference.

Practical results show that energy detector performance is good at high SNR values, and performance declines at SNR values of less than -5 dB. In the simulation results, at SNR values greater than 5dB, the ED has little trouble differentiating between the noise and primary signals. The performance of the ED degrades significantly when SNR values fall below -10dB.

Figure (4.17) illustrates the simulation and USRP implementation of the P_{fa} vs SNR.

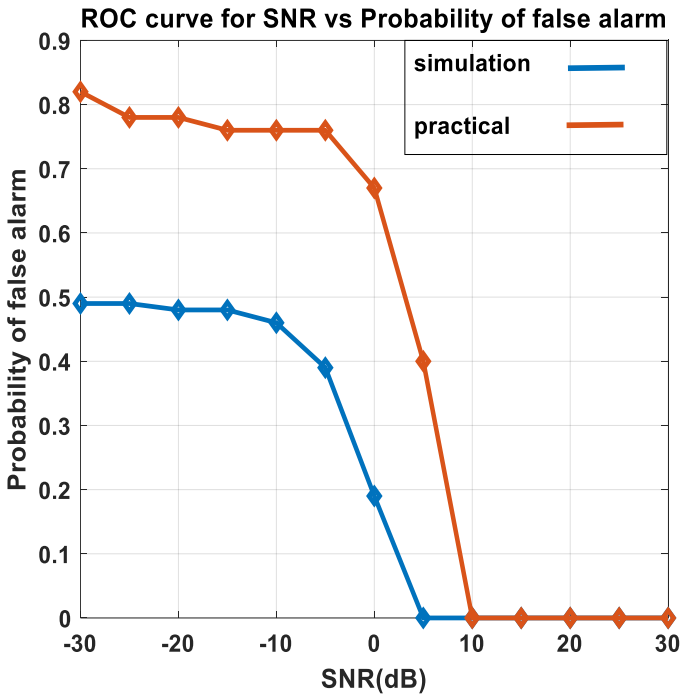

Figure (4.17) P_{fa} vs SNR for the first adaptive threshold

In the simulation result, when the SNR is between values of 5dB and 30dB, the performance of the ED works better. The results of practical implementation show that P_{fa} is high at the low SNR values but starts to decrease until it reaches zero at 10dB. It can be seen that practical results are worse than simulation results due to the loss caused by practical implementation.

Figure (4.18) depicts the P_m. The results show that the P_m is high at low SNR values but starts to decrease at high SNR values until it reaches zero at 5dB in both results. It can be seen that simulation results are worse than practical results.

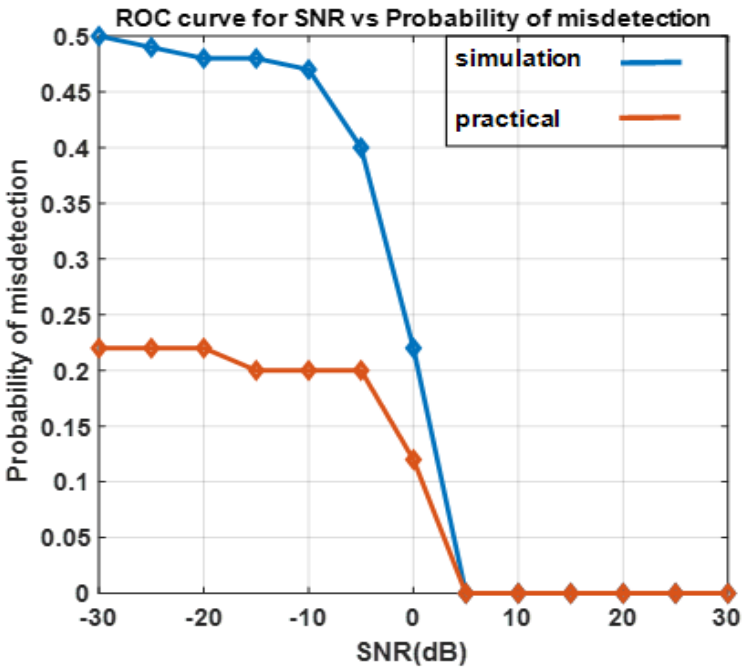

Figure (4.18) P_m vs SNR for the first adaptive threshold

As seen in Figure (4.19), both the implementation and the simulation results show that the total error probability is high when the SNR is low. It then starts to decrease as the SNR increases until it reaches zero at SNR = 5dB in simulation and SNR=10dB in practical implementation. As seen in Figure (4.19), the performance of the LabVIEW simulation is better than the practical implementation.

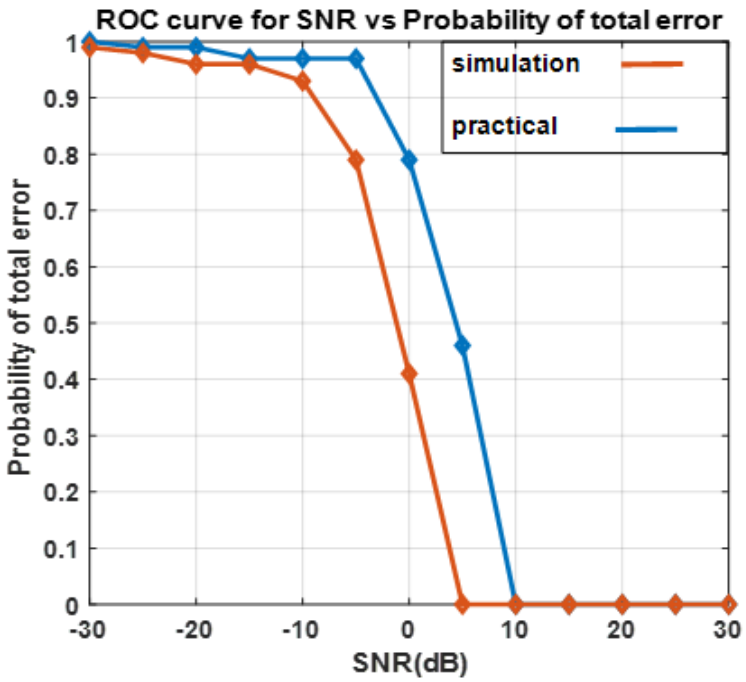

Figure (4.19) P_{te} vs SNR for the first adaptive threshold

4.7.2.2 Second Proposed Adaptive Threshold (The Power of Received Signals is Unequal)

In the second proposed adaptive threshold, when the threshold relies on taking the average of the total energy ET of the receiving signals plus the average of energy for the lowest two bands, the results in figure (4.20) show P_d vs SNR for simulation and practical implementation. As seen in this figure the measurement results of the practical implementation are similar compared to the simulation results.

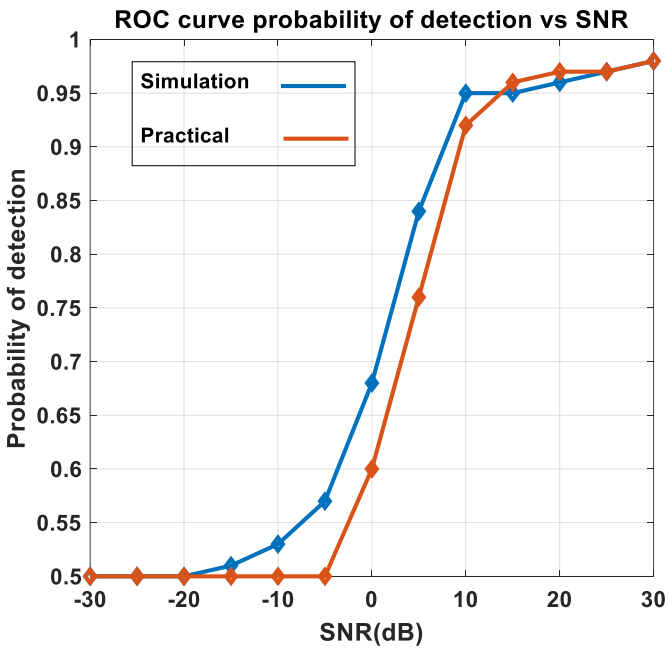

Figure (4.20) P_d vs SNR for the second adaptive threshold

Figure (4.21) shows that the P_{fa} in simulation and practical implementation improves at SNR = 10dB and beyond. The measurement results of the implementation are similar compared to the simulation results.

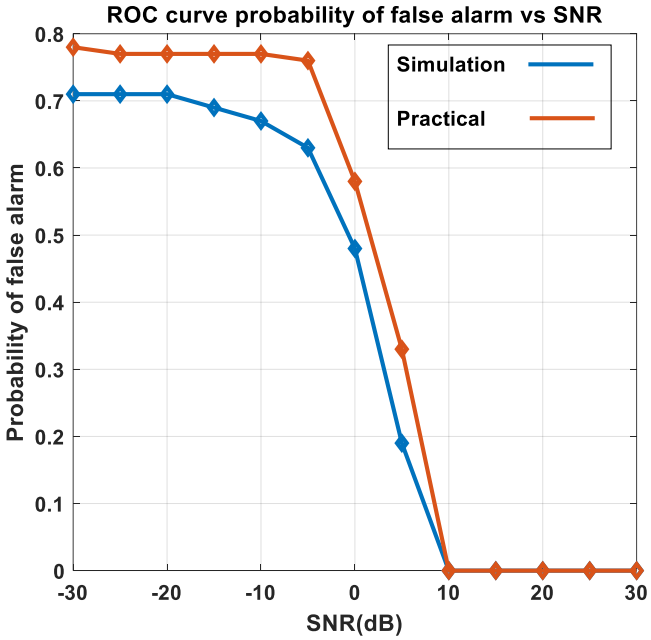

Figure (4.21) P_{fa} vs SNR for second adaptive threshold

Figure (4.22) illustrates the P_m, which declares that the spectrum is not busy but is busy in fact. The figure shows that practical results are better compared to the simulation at SNR values from -30dB to -5dB, but the simulation results are better than the practical results at SNR values from -5dB to 10dB.

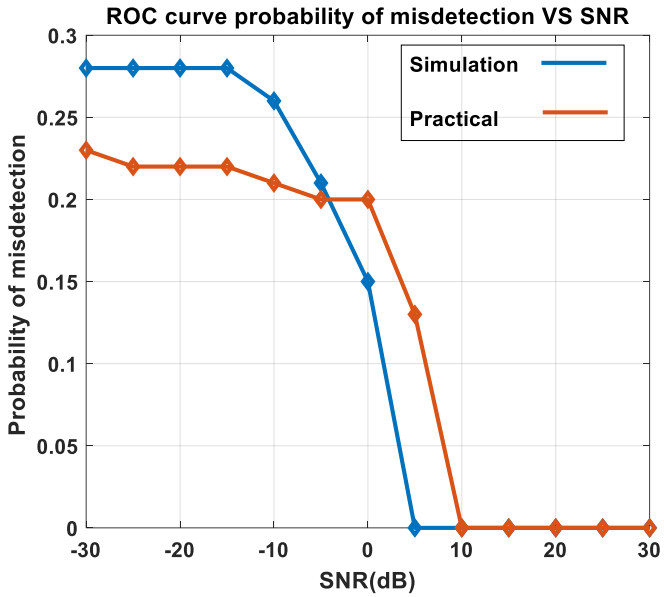

Figure (4.22) P_m vs SNR for the second adaptive threshold

Figure (4.23) illustrates the P_{te}vs SNR. Both the practical implementation and the simulation results show the highest P_{te} when the SNR is low, which is the worst case, and then decreases as the SNR increases until it reaches zero at 10dB. When the SNR is between 10dB and 30dB, the performance of the threshold works better.

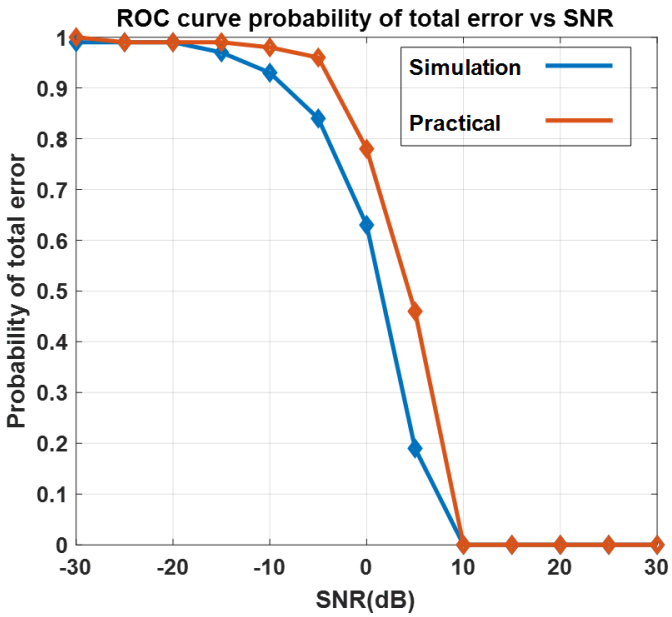

Figure (4.23) P_{te} vs SNR for the second adaptive threshold

4.7.2.3 Third Proposed Adaptive Threshold (The Power of Received Signals is Unequal)

In the third proposed adaptive threshold, when the threshold relies on the average of the lowest and the highest energy bands, figure (4.24) shows the simulation and practical implementation of the P_d vs SNR. As shown in this figure, USRP implementations are closer to LabVIEW simulations.

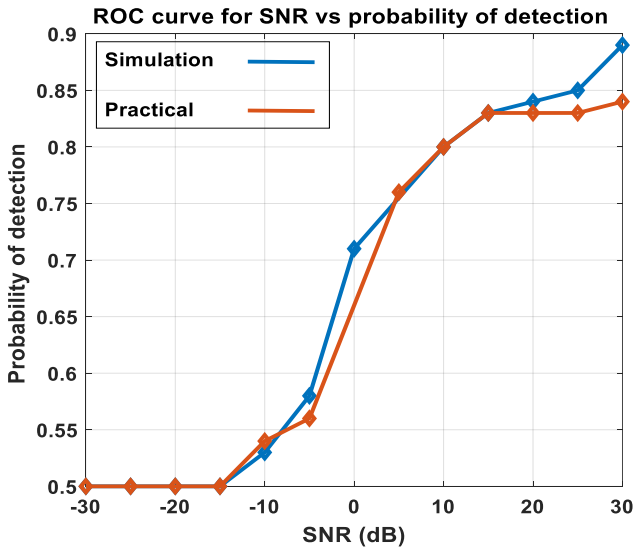

Figure (4.24) P_d vs SNR for third adaptive threshold

Figure (4.25) illustrates the P_{fa}vs SNR. As shown in this figure, the simulation results are better compared to the practical at SNR values from -30dB to -5dB. In both the practical implementation and the simulation results, performance improves at SNR = 10dB and beyond.

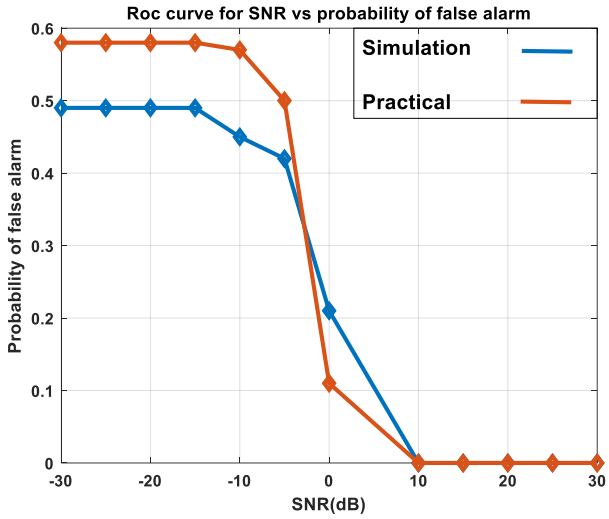

Figure (4.25) P_{fa} vs SNR for the third adaptive threshold

Figure (4.26) illustrates the P_m, The results show that the P_m is high at low SNR values but starts to decrease at high SNR values.

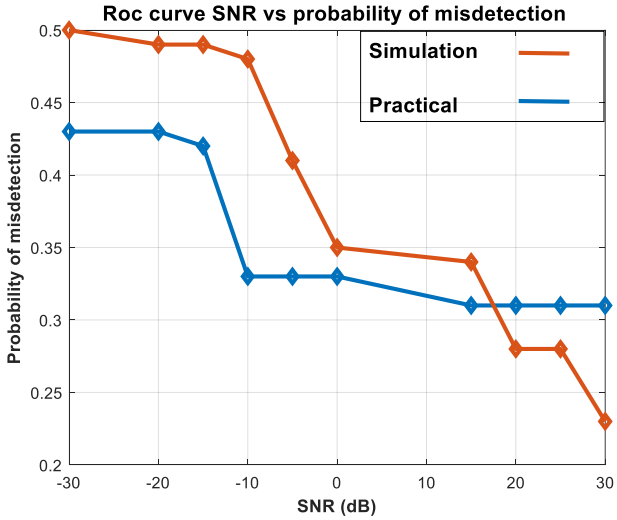

Figure (4.26) P_m vs SNR for the third adaptive threshold

Figure (4.27) illustrates the P_{te} vs SNR. In both simulation and practical implementation results, the third adaptive threshold shows that the total error probability is high when the SNR is low, and it starts to decrease when the SNR increases. As shown in this figure, USRP implementations are closer to LabVIEW simulations.

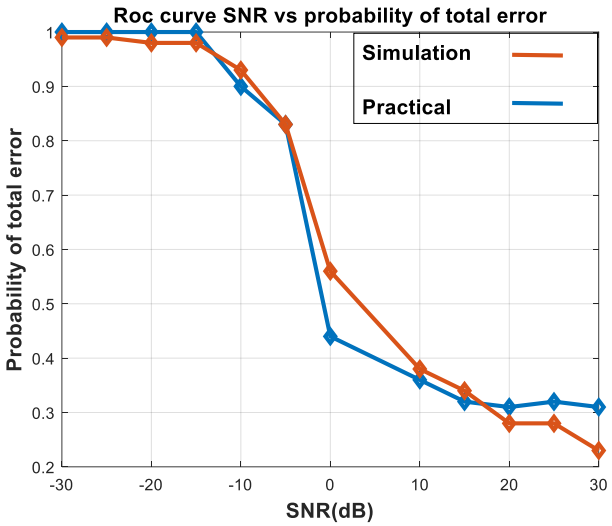

Figure (4.27) P_{te} vs SNR for the third adaptive threshold

CHAPTER FIVE

CONCLUSIONS AND FUTURE WORK

5.1 Conclusion

This thesis deals with the problem of limited spectrum resources, which is one of the challenges facing UDN technology in 5G. CR technology represents the solution to the issue of inefficient use of the spectrum. SS algorithms are the effective key to CR performance. Hence the need to evaluate the performance of SS algorithms. This study focused on evaluating the performance of the energy detector-based SS technique using simulations with the LabVIEW NXG software. Since the performance of the ED depends on the accuracy of the threshold, this thesis presented a study of the fixed threshold technique as well as three proposed methods for the adaptive threshold to improve the performance. The real-time system was realized on an SDR platform, built using USRP X310 kits from Ettus Research, with the energy sensor implemented on a personal computer using LabVIEW NXG. The conclusions are presented as follows:

1- In the special case, when the received signals power are equal.

A. In the first scenario, the semi-deterministic traffic mode has been adopted for the PUs. The ED algorithm was introduced using a fixed threshold and the first proposed adaptive threshold (that depends on the average of the total energy of the receiving signals). Although the fixed threshold approaches are relatively simple to apply, the fixed threshold is prone to error due to the fluctuating nature of noise signals. The results showed that the adaptive threshold outperformed the fixed threshold, where the detection process begins with small SNR values compared to the fixed threshold.

   In the fixed threshold, the P_d value was 0.5 at SNR = -30 dB, then it started to increase until it got closer to 1 at SNR = 18dB, while in the first

adaptive method, the P_d value was 0.51 at SNR = -30dB and continuously increased until it got close to 1 at SNR = 5dB.

B. In the second scenario, the burst traffic mode has been adopted for PUs to demonstrate the algorithm's efficiency and ability to sense the spectrum. The same algorithm and thresholds used in the first scenario were reused for the second scenario. The results showed good performance of the adaptive threshold compared to the fixed threshold.

In the fixed threshold, the P_d value was 0.13 at SNR = -30 dB and went up to 1 at SNR = 15dB, while in the first adaptive method, the P_d value was 0.5 at SNR = -30dB and increased to 1 at SNR = 5dB.

In both semi-deterministic and burst traffic modes, it is not recommended to use the fixed threshold, especially when the SNR is lower, but the adaptive threshold is recommended.

2- In the general case, when the power of all received signals is unequal.

A. In the first scenario, two adaptive threshold methods have been proposed (the second and third adaptive thresholds). The second adaptive threshold depends on taking the average of the total energy of the receiving signal plus the average of the energy for the lowest two bands, while the third adaptive threshold depends on the average of the lowest and highest energy bands. The results showed that the second proposed threshold in signal detection performed better than the third proposed threshold. In the second adaptive method, the P_d value was 0.5 at SNR = -30 and went up to 0.97 at SNR = 30dB. While in the third adaptive method, the P_d value was 0.5 at SNR = -30dB and increased to 0.89 at SNR = 30dB.

In the semi-deterministic traffic mode, it is recommended to use the second adaptive method instead of the third adaptive method, especially when SNR > 10dB.

B. In the second scenario, the third proposed threshold outperformed the second proposed threshold. Where in the second adaptive method, the P_d

value was 0.34 at SNR = -30dB and increased to 0.99 at SNR = 10dB. While in the third adaptive method, the P_d value was 0.5 at SNR = -30dB and increased to 0.99 at SNR = 5dB. In the burst traffic mode, it is not recommended to use the second adaptive threshold, especially when SNR is lower, but the third adaptive threshold is recommended.

3- The semi-deterministic traffic mode has been practically implemented using SDR. The obtained practical performance is worse than that obtained in the simulations. This was attributed to the fact that the transmitted signals were affected by more than propagation factors in the channel. In addition, thermal noise from the USRP hardware also contributed to this disparity.

   In the first adaptive method, the P_d value was 0.50 at SNR = -30dB and continuously increased until it got close to 0.97 at SNR = 15dB, while in the second adaptive method, the P_d value was 0.5 at SNR = -30 and went up to 0.97 at SNR = 30dB, and in the third adaptive method, the P_d value was 0.5 at SNR = -30dB and increased to 0.84 at SNR = 30dB.

4- In general, the study showed the impact of SNR on signal detection, where the higher the SNR, the greater the probability of detecting the signal.

5.2 Future Work

1. Implementing the proposed SS system in the LabVIEW NXG simulator on the FPGA of the USRP for faster transmission (offloading).
2. Using other types of channels and noise, for example, (Rayleigh, fading colored noise, etc.).
3. Applying parallel or sequential multistage SS algorithms in order to enhance the performance and overcome the limitations of conventional SS techniques.
4. Applying the cooperative SS technique (more than one detector to check the spectrum and share information among CR users) because the SS of individual nodes cannot achieve high detection accuracy.

5. Applying the ED algorithm using other types of adaptive thresholds.

REFERENCES

[1] S. Ahmadi, 5G NR architecture, technology, implementation, and operation of 3GPP new radio standards, 1st ed., Academic Press-Elsevier, 2019, doi:10.1016/B978-0-08-102267-2.00001-4.

[2] X. Ge et al., "5G Ultra-Dense Cellular Networks," IEEE Wireless Communications, vol. 23, no. 1, pp. 72-79, February 2016, doi: 10.1109/MWC.2016.7422408.

[3] J. An et al., "Achieving Sustainable Ultra-Dense Heterogeneous Networks for 5G," IEEE Communications Magazine, vol. 55, no. 12, pp. 84-90, Dec. 2017, doi: 10.1109/MCOM.2017.1700410.

[4] A. Ivanov et al., "Framework for Implementation of Cognitive Radio Based Ultra-Dense Networks," 2019 2nd International Conference on Telecommunications and Signal Processing (TSP), 2019, pp. 481-486, doi: 10.1109/TSP.2019.8769067.

[5] F. Hu, B. Chen and K. Zhu, "Full Spectrum Sharing in Cognitive Radio Networks Toward 5G: A Survey," IEEE Access, vol. 6, pp. 15754-15776, 2018, doi: 10.1109/ACCESS.2018.2802450.

[6] R. Ujjinimatad, and S. R. Patil, "Sensing algorithm for cognitive radio networks based on random data matrix," International Journal of Computer Applications, vol. 62, no. 3, pp. (2013), Jan. 2013.

[7] Y. Zhao et al., "Wavelet transform for spectrum sensing in Cognitive Radio networks," 2014 International Conference on Audio, Language and Image Processing, 2014, pp. 565-569, doi: 10.1109/ICALIP.2014.7009857.

[8] A. Nafkha et al., "Cyclostationarity-based versus eigenvalues-based algorithms for spectrum sensing in cognitive radio systems: Experimental evaluation using GNU radio and USRP," 2015 IEEE 11th International Conference on Wireless and Mobile Computing,

Networking and Communications (WiMob), 2015, pp. 310-315, doi: 10.1109/WiMOB.2015.7347977.

[9] S. Lavanya, B. Sindhuja and M. A. Bhagyaveni, "Implementation of an adaptive spectrum sensing technique in cognitive radio networks," 2015 International Conference on Computing and Communications Technologies (ICCCT), 2015, pp. 344-349, doi: 10.1109/ICCCT2.2015.7292773.

[10] L. K. Mathew, S. Sharma and P. Verma, "An Adaptive Algorithm for Energy Detection in Cognitive Radio Networks," 2015 Second International Conference on Advances in Computing and Communication Engineering, 2015, pp. 104-107, doi: 10.1109/ICACCE.2015.47.

[11] M. Sardana and A. Vohra, "Analysis of different Spectrum Sensing techniques," 2017 International Conference on Computer, Communications and Electronics (Comptelix), 2017, pp. 422-425, doi: 10.1109/COMPTELIX.2017.8004006.

[12] F. Wasonga, T. O. Olwal and A. M. Abu-Mahfouz, "Efficient Two Stage Spectrum Sensing for Cognitive Radios," 2018 IEEE 27th International Symposium on Industrial Electronics (ISIE), 2018, pp. 1308-1313, doi: 10.1109/ISIE.2018.8433776.

[13] V. S. Muradi et al., "Spectrum sensing in cognitive radio using Labview and NI USRP," 2018 2nd International Conference on Inventive Systems and Control (ICISC), 2018, pp. 1316-1319, doi: 10.1109/ICISC.2018.8399019.

[14] R. M. Elshishtawy et al., "Implementation of Multi-Channel Energy Detection Spectrum Sensing Technique in Cognitive Radio Networks Using LabVIEW on USRP-2942R," 2019 15th International

Computer Engineering Conference (ICENCO), 2019, pp. 1-6, doi: 10.1109/ICENCO48310.2019.9027423.

[15] M. Saber et al., "Spectrum sensing for smart embedded devices in cognitive networks using machine learning algorithms," Procedia Computer Science, vol. 176, pp. 2404-2413, October 2020, doi: 10.1016/j.procs.2020.09.311.

[16] D. N. Reddy, and Y. Ravinder, "Spectrum Sensing in Non-Gaussian Noise," Indian Journal of Science and Technology, vol. 14, no. 32, pp. 2596-2606. Sep. 2021, doi: 10.17485/IJST/v14i32.1034.

[17] A. Brito, P. Sebastião and F. J. Velez, "Hybrid Matched Filter Detection Spectrum Sensing," IEEE Access, vol. 9, pp. 165504-165516, 2021, doi: 10.1109/ACCESS.2021.3134796.

[18] C. Cox, An Introduction to 5G: The New Radio, 5G Network and Beyond, 1st ed., Cambridge, UK. Wiley & Sons Ltd, 2021, doi:10.1002/9781119602682.

[19] A. A. Ateya et al., "Study of 5G Services Standardization: Specifications and Requirements," 2018 10th International Congress on Ultra Modern Telecommunications and Control Systems and Workshops (ICUMT), 2018, pp. 1-6, doi: 10.1109/ICUMT.2018.8631201.

[20] B. U. Kazi and G. A. Wainer, "Next generation wireless cellular networks: ultra-dense multi-tier and multi-cell cooperation perspective," Wireless Networks, vol. 25 , no. 4, pp. 2041-64, May 2018, doi: 10.1007/s11276-018-1796-y.

[21] S. K. Ghosh and S. C. Ghosh, "A predictive handoff mechanism for 5G ultra dense networks," 2017 IEEE 16th International Symposium on Network Computing and Applications (NCA), 2017, pp. 1-5, doi: 10.1109/NCA.2017.8171395.

[22] T. Q. Duong, X. Chu, H. A. Suraweera Eds., Ultra-dense Networks for 5G and Beyond Modelling, Analysis, and Applications, 1st ed., Chennai, India, John Wiley & Sons, 2019, doi: 10.1002/9781119473756.

[23] H. Cho, D. Kim, and J. Lee, “3D-Based BaseStation Deployment in Ultra-dense Nwtwork,” in: Ultra-dense Networks Principles and Applications, H. Zhang, J. Lee, T.Q.S.Quek, C-Lini Ed.,1st ed., Cambridge, New York, Cambridge University Press, 2020, Ch.7, Sec. 7.1, doi: 10.1017/9781108671323.

[24] A. A. Ajani, V. K. Oduol, and Z. K. Adeyemo, " GPON and V-band mmWave in green backhaul solution for 5G ultra-dense network," International Journal of Electrical and Computer Engineering, vol. 11, no. 1, pp. 390-401, February 2021, doi: 10.11591/ijece.v11i1.

[25] G. Chopra, R. K. Jha, and S. Jain, "A Survey on Ultra-Dense Network and Emerging Technologies: Security Challenges and Possible Solutions," Journal of Network and Computer Applications, vol. 95, pp. 54-78, Oct. 2017, doi:10.1016/j.jnca.2017.07.007.

[26] M. A. Adedoyin and O. E. Falowo, "Combination of Ultra-Dense Networks and Other 5G Enabling Technologies: A Survey," IEEE Access, vol. 8, pp. 22893-22932, 2020, doi: 10.1109/ACCESS.2020.2969980.

[27] W. Yu et al., "Ultra-Dense Networks: Survey of State of the Art and Future Directions," 2016 25th International Conference on Computer Communication and Networks (ICCCN), 2016, pp. 1-10, doi: 10.1109/ICCCN.2016.7568592.

[28] Nokia white paper, "Ultra Dense Network (UDN) White Paper," June 2016, [Online] Availabe: http://resources.alcatel-lucent.com/asset/200295, (accessed Feb. 11, 2022).

[29] A. H. Jafari et al, "Small cell backhaul: challenges and prospective solutions," EURASIP Journal on Wireless Communications and Networking, no. 1, pp. 1-18, Dec. 2015, doi:10.1186/s13638-015-0426-y

[30] N. Sharma, and K. Kumar, "Resource allocation trends for ultra dense networks in 5G and beyond networks: A classification and comprehensive survey." Physical Communication, vol. 48, pp. 101415, Oct. 2021, doi:10.1016/j.phycom.2021.101415.

[31] R. Mahajan, and D. Bagai, "Cognitive radio technology: introduction and its applications," International Journal of Engineering Research and Development, vol. 12, no.9, pp.17-24. Sep. 2016.

[32] N. Swetha, P. N. Sastry and Y. R. Rao, "Analysis of Spectrum Sensing Based on Energy Detection Method in Cognitive Radio Networks," 2014 International Conference on IT Convergence and Security (ICITCS), 2014, pp. 1-4, doi: 10.1109/ICITCS.2014.7021738.

[33] P. T. V. Bhuvaneswari, "Spectrum Sensing in Cognitive Radio Networks: A Survey," in: Introduction to Cognitive Radio Networks and Applications, G. Tomar, A. Bagwari, and J. Kanti Ed. 1st ed., New York, CRC Press, 2017, Ch. 5, Sec. 5.1.1, doi: 10.1201/9781315367545.

[34] W. Ahmed, M. Faulkner and J. Gao, "Opportunistic Spectrum Access in Cognitive Radio Network," in: Foundation of cognitive radio systems, S. Cheng Ed., Rijeka, Croatia, In Tech , 2012, Ch. 9, Sec. 1, doi:10.5772/1104.

[35] E. Hossain, D. Niyato, and Z. Han, Dynamic Spectrum Access and Management in Cognitive Radio Networks, 1st ed., New York, NY, United States, Cambridge University Press, 2009. doi:10.1017/CBO9780511609909.

[36] R. Kaur, A. S. Buttar and J. Anand, "Spectrum Sharing Schemes in Cognitive Radio Network: A Survey," 2018 Second International Conference on Electronics, Communication and Aerospace Technology (ICECA), 2018, pp. 1279-1284, doi: 10.1109/ICECA.2018.8474662.

[37] A. Briones-Reyes et al., "Mathematical evaluation of spectrum sharing in cognitive radio networks for 5G systems using Markov processes," Computer Networks, vol. 182, pp. 107521, Dec. 2020, doi:10.1016/j.comnet.2020.107521.

[38] I. Christian et al., "Spectrum mobility in cognitive radio networks," IEEE Communications Magazine, vol. 50, no. 6, pp. 114-121, June 2012, doi: 10.1109/MCOM.2012.6211495.

[39] S. Atapattu, C. Tellambura, and H. Jiang, Energy Detection for Spectrum Sensing in Cognitive Radio, NewYork, NY, USA, Springer , 2014, doi: 10.1007/978-1-4939-0494-5.

[40] A. A. Khan, M. H. Rehmani and A. Rachedi, "Cognitive-Radio-Based Internet of Things: Applications, Architectures, Spectrum Related Functionalities, and Future Research Directions," in IEEE Wireless Communications, vol. 24, no. 3, pp. 17-25, June 2017, doi: 10.1109/MWC.2017.1600404.

[41] A. Ali and W. Hamouda, "Advances on Spectrum Sensing for Cognitive Radio Networks: Theory and Applications," IEEE Communications Surveys & Tutorials, vol. 19, no. 2, pp. 1277-1304, Secondquarter 2017, doi: 10.1109/COMST.2016.2631080.

[42] H. Hu, “Cyclostationary Approach to Signal Detection and Classification in CognitiveRadio Systems,” in: Cognitive radio systems, W. Wang Ed., 1st ed., China, In-Tech, 2009. Ch.5, Sec. 2.

[43] G. Zhao, W.Zhang, and S. Li, Advanced Sensing Techniques for Cognitive Radio, 1st ed., Springer, 2017, doi:10.1007/978-3-319-42784-3.

[44] L. Khalid and A. Anpalagan, " Principles and Challenges of Cooperative Spectrum Sensing in Cognitive Radio Networks," in: Handbook of Cognitive Radio, W. Zhang Ed., 1st ed., Singapore, Springer, May 2017, pp. 1-28, doi.org/10.1007/978-981-10-1389-8-1-1.

[45] J. Hemanth, and V. E. Balas, Biologically Rationalized Computing Techniques For Image Processing Applications, 1st ed., Cham, Switzerland, Springer International Publishing AG, 2018, doi: 10.1007/978-3-319-61316-1.

[46] D.D. Gutierrez, Machine Learning and Data Science: An Introduction to Statistical Learning Methods with R, 1st ed. Technics Publications, 2015.

[47] NI-National Instruments, https://www.ni.com/en-lb.html (accessed Feb. 2, 2022).

[48] J. M. Patton & F. Can, “Determining translation invariant characteristics of James Joyce’s Dubliners,” in: Quantitative methods in corpus-based translation studies: A practical guide to descriptive translation research, M. P. Oakes, M. Ji Ed., 2012, doi:10.1075/scl.51.

[49] S. L. Mirtaheri, and L. Grandinetti, "Dynamic load balancing in distributed exascale computing systems," Cluster Computing, vol. 20, no. 4, pp. 3677-3689, May 2017, doi:10.1007/s10586-017-0902-8.

[50] M. S. Falih, and H. N. Abdullah, "Cooperative Spectrum Sensing Method Using Sub-band Decomposition with DCT for Cognitive Radio System," International Conference on Applied Computing to Support Industry: Innovation and Technology, 2020, pp. 465–475, doi:10.1007/978-3-030-38752-5_36.

[51] N. M. Anas, H. Mohamad and M. Tahir, "Cognitive Radio test bed experimentation using USRP and Matlab®/Simulink®," 2012 International Symposium on Computer Applications and Industrial Electronics (ISCAIE), 2012, pp. 229-232, doi: 10.1109/ISCAIE.2012.6482102.

[52] H. Chen, D. S. Boning, "Machine Learning Approaches for IC Manufacturing Yield Enhancement," In: Machine Learning in VLSI Computer-Aided Design, I. M. Elfadel, D. S. Boning, X. Li Ed., 1st ed., Springer, Cham, Jan. 2019, ch. 6, sec. 6.3.2, pp. 157-199, doi:10.1007/978-3-030-04666-8.

[53] A. L. Garcia Reis et al., "Introduction to the Software-defined Radio Approach," IEEE Latin America Transactions, vol. 10, no. 1, pp. 1156-1161, Jan. 2012, doi: 10.1109/TLA.2012.6142453.

[54] F. h. Tseng et al., "Ultra-dense small cell planning using cognitive radio network toward 5G," IEEE Wireless Communications, vol. 22, no. 6, pp. 76-83, December 2015, doi: 10.1109/MWC.2015.7368827.

[55] G. Baldini et al., "Security Aspects in Software Defined Radio and Cognitive Radio Networks: A Survey and A Way Ahead," IEEE Communications Surveys & Tutorials, vol. 14, no. 2, pp. 355-379, Second Quarter 2012, doi: 10.1109/SURV.2011.032511.00097.

[56] O. Adigun, M. Pirmoradian and C. Politis, “Cognitive Radio for 5G Wireless Networks,” in: Fundamentals of 5G mobile networks, J. Rodriguez Ed. 1st ed., John Wiley & Sons Ltd, 2015. Ch.6, Sec. 6.7.1 doi: 10.1002/9781118867464.

[57] R. Akeela, and B. Dezfouli, "Software-defined Radios: Architecture, state-of-the-art, and challenges," Computer Communications, vol. 128, pp. 106-125, April 2018, doi: 10.1016/j.comcom.2018.07.012.

[58] E. Grayver, Implementing software defined radio, 2012th ed., New York, USA, Springer, 2013, doi:10.1007/978-1-4419-9332-8.

[59] F. B. Serkin and N. A. Vazhenin, "USRP platform for communication systems research," 2013 15th International Conference on Transparent Optical Networks (ICTON), 2013, pp. 1-4, doi: 10.1109/ICTON.2013.6602738.

[60] A. Hussain, B. Por Einarsson and P. -S. Kildal, "MIMO OTA Testing of Communication System Using SDRs in Reverberation Chamber [Measurements Corner]," IEEE Antennas and Propagation Magazine, vol. 57, no. 2, pp. 44-53, April 2015, doi: 10.1109/MAP.2015.2419992.

[61] Products, Ettus Research, https://www.ettus.com/all-products/x310-kit/ (accessed Feb. 15, 2022).

[62] X300/X310, Ettus Research, https://kb.ettus.com/X300/X310 (accessed Fed. 23, 2022).

PUBLISHING

[1] Dia M. Ali and Marwa Y. Abdulla, “Energy Detection Based Multi-bands Spectrum Sensing using Adaptive Threshold,” Muthanna International Conference on Engineering Science and Technology-(MICEST-2022), Al-Muthanna, Iraq. (Accepted).

[2] Marwa Y. Abdallah and Dia M. Ali, “Evaluating the Practical Performance of Energy Detector Based Spectrum Sensing for Cognitive Radio,” 2nd International Conference on Engineering and Advance Technology (ICEAT 2022), 2022. (Accepted).

الخلاصة

لتلبية الزيادة في الخدمات والتطبيقات اللاسلكية للجيل الخامس (5G) ، تطورت الشبكة فائقة الكثافة (UDN) مؤخرًا كواحدة من تقنيات التمكين الرئيسية لأنظمة 5G المستقبلية.

في UDN ، يتم نشر عدد كبير من الخلايا الصغيرة (SCs) مقارنة بعدد المستخدمين النشطين. ستزيد كثافة SCs من مشكلة ندرة الطيف. تم اقتراح الراديو المعرفي (CR) كحل لمشكلة موارد الطيف المحدودة من خلال استغلال الطيف غير المستخدم المخصص للمستخدمين الأساسيين (PUs). يمكّن هذا النهج المستخدم الثانوي (SU) من استخدام الطيف عندما لا يستخدمه PU ، ويجب أن يحدث هذا دون التداخل مع PU. يعد استشعار الطيف (SS) أحد أهم الوظائف في CR.

في هذا العمل ، تم اقتراح نموذج لنظام SS لأداء عملية الاستشعار. تم الاعتماد على خوارزمية الكشف عن الطاقة (ED) ، ولتعزيز الأداء ، تم اقتراح ثلاث عتبات تكيفية باستخدام برنامج LabVIEW NXG Simulink . لتمثيل أوضاع حركة المرور الخاصة بـ Pus، تم اعتماد سيناريوهين. كان السيناريو الأول في شكل أسلوب الحركة شبه الحتمي ، والثاني هو أسلوب حركة الرشقة.

تمت مقارنة نتائج محاكاة كاشف الطاقة التقليدي (العتبة الثابتة) بالطريقة المقترحة الأولى (التي تعتمد على متوسط الطاقة الإجمالية لإشارات الاستقبال) عندما تكون قدرة جميع الاشارات المستقبلة متساوية (حالة خاصة). بالمقارنة مع الحد الثابت ، أدت الطريقة الأولى المقترحة إلى تحسين أداء الكشف مقارنة بالحد الثابت في كلا السيناريوهين. في الحالة العامة حيث تعتمد إشارات القدرة المستقبلة على المسافة بين PUs، تم تطبيق العتبات التكيفية المقترحة الثانية والثالثة. تعتمد العتبة التكيفية الثانية على أخذ متوسط الطاقة الإجمالية لإشارات الاستقبال بالإضافة إلى متوسط الطاقة لأدنى نطاقين ، بينما تعتمد العتبة التكيفية الثالثة على متوسط نطاقي الطاقة الأدنى والأعلى. أظهرت نتائج المحاكاة أن الطريقة الثانية المقترحة كان أداؤها أفضل من الطريقة الثالثة في السيناريو الأول ، بينما تفوقت العتبة الثالثة المقترحة على العتبة الثانية المقترحة في السيناريو الثاني.

لتوفير تقييم أداء موثوق لنظام SS ، تم تنفيذ خوارزمية ED باستخدام Universal Software Radio Peripheral (USRP) X310 ، أحد منتجات تكنولوجيا أجهزة الراديو المعرّف بالبرمجيات (SDR). باتباع نفس نموذج المحاكاة لنظام SS ، تم تنفيذ الاختبار للسيناريو الأول. تظهر النتائج العملية أن ED حقق أداءً جيدًا وكان أقرب إلى أداء المحاكاة.

وزارة التعليم العالي والبحث العلمي
جامعة نينوى
كلية هندسة الالكترونيات
قسم هندسة الاتصالات

حل الراديو ألإدراكي لاتصالات الجيل الخامس فائقة الكثافة

رسالة تقدمت بها

مروة يونس عبد الله

إلى
مجلس كلية هندسة الالكترونيات
جامعة نينوى
كجزء من متطلبات نيل شهادة الماجستير
في
هندسة الاتصالات

بإشراف

أ.م.د. ضياء محمد علي

1443 هـ **2022 م**

وزارة التعليم العالي والبحث العلمي
جامعة نينوى
كلية هندسة الالكترونيات
قسم هندسة الاتصالات

حل الراديو ألإدراكي لاتصالات الجيل الخامس فائقة الكثافة

مروة يونس عبد الله

رسالة ماجستيرعلوم في هندسة الاتصالات

بإشراف

أ.م.د. ضياء محمد علي

1443 هـ

2022 م